FEA-BASED METHOD TO PREDICT DYNAMIC TEST FAILURES OF INDUSTRIAL RUBBER CASTOR WHEELS

Ampitiyawaththe Vishvajith Wijayasundara

(128413 C)

Dissertation submitted in partial fulfillment of the requirements for the Master of Engineering in Manufacturing Systems Engineering

Department of Mechanical Engineering

University of Moratuwa

Sri Lanka

November 2016

Declaration

I declare that this is my own work and this thesis/dissertation does not incorporate without acknowledgement any material previously submitted for a Degree or Diploma in any other University or institute of higher learning and to the best of my knowledge and belief it does not contain any material previously published or written by another person except where the acknowledgement is made in the text.

Also, I hereby grant to University of Moratuwa the non-exclusive right to reproduce and distribute my dissertation in whole or in part in print, electronic or other medium. I retain the right to use this content in whole or part in future works (such as articles or books)

Signature: Date:

A.V.Wijayasundara (128413c)

The above candidate has carried out research for the Masters Dissertation under my supervision.

Signature of the supervisor: Date:

Dr. H.K.G Punchihewa

Signature of the supervisor: Date :

Mr. R.K.P.S Ranaweera

Acknowledgment

I would first like to thank my research supervisors Dr. H.K.G Punchihewa and Mr. R.K.P.S Ranaweera at department of Mechanical Engineering in university of moratuwa Sri Lanka for their continuous guidance and support provided during this work.

I would like to thank all other staff of department of Mechanical Engineering in university of moratuwa Sri Lanka for sharing valuable knowledge with me and for the guidance given for this work.

I'm very grateful for Elastomeric Engineering Co.Ltd located at NO. 51/54, IDB Industrial Estate, Horana, Sri Lanka for providing me opportunity and resources to carry out this research work.

I would like to thank Mr. S.Ranathunga, General Manager, Elastomeric Engineering Co.Ltd. and other staff members at organization for the valuable support and information given during the work to make this a success.

Abstract

Castor wheels are used in various applications including industries, hospitals, offices, shopping trollies, air ports and other material handling applications. These applications demand different properties from castor wheels, such as dynamic load capacity, high speed capability, and capability to operate in hot and cold environments. Design of a castor wheel plays a major role to fulfill those various demands while being competitive in the market. Dynamic test of castor wheel is one of the main tests done on new castor wheel designs to evaluate its performance for an application. Due to manual trial and error practice used to test new designs in dynamic test, wheel development cost and lead time for deliver new castor wheel designs for new customer requirements is high. In order to evaluate wheel designs in early stages of development in dynamic test performance, Finite element model was developed to check castor wheel dynamic performance using combination of finite element analysis (FEA) techniques and raw material testing.

Initially six samples of castor wheels were selected and dynamic test was carried out on them at various loads to evaluate temperature development inside the wheel and failure modes. Two sets of raw material testing, namely uniaxial tensile test and dynamic mechanical analyze test (DMA), were done on rubber and plastic materials which are used to make castor wheels. One wheel was selected as a case study to develop FEA model. As first step, 3D static loading simulation was done for the selected wheel. Total energy rate was defined for wheel in dynamic motion by data from static test using equations. 2D axisymmetric FEA model was developed as next step to evaluate temperature development of the castor wheel. Calculated energy rate was distributed among rubber elements as heat sources combining with DMA results to predict temperature inside the 2D profile using transient heat. Wheel failure analysis was carried out by combining predicted temperature profile and static loading case with temperature dependent properties of materials used. It was defined as a good design if castor wheel shows higher safety factor in failure simulation. From the case study, step-by-step method was developed to simulated castor wheel designs and evaluated failure. Four castor wheels were simulated according to developed model and predicted temperatures were compared with actual dynamic test temperature to validate the proposed model which showed good match with practical data. As future work, advanced failure analysis of caster wheels can be proposed, which should be carried out considering material chemistry and behavioral changes of materials with heat and fatigue loads.

Table of Contents

List of Figures

List of Tables

1. Introduction

1.1. Background

Castor wheels are mainly used as a tool that makes object movement easy. They are un-driven wheels which are designed to be mounted to a bottom of a larger object so that object can be moved easily. They can be found in various applications around the world such as in Industrial applications, shopping trollies, office chairs, air ports, hospitals and other various material handling equipment. These various applications demand various performance and properties from castor wheels. High capacity heavy duty castors are used in many industrial applications for continuous use under heavy loads such as platform trucks, industrial carts, and automated material handling lines. Castor wheels used in air ports are designed to withstand heavy dynamic and impact loads. Furniture castors are treated as light load castors but still should consider time to time extreme loading conditions and environmental conditions which may occur in practical application. Castor wheels used in hospitals are premium castors which gives comfortable ride and low noise in applications. Some castor wheels are designed to conduct electricity while moving the object fitted.

To cater all these application demands, castor wheels are available in various sizes and designs. Castor wheels are made from various materials such as Rubber, Polyurethane, Nylon, Aluminum and Stainless steel for various types of applications in various types of designs.

Figure 1.1: Castor wheels mounted in industrial trolley
Source: https://www.exportersindia.com/punamenterprises-163389.htm

A castor wheel is defined as “small wheel on a swivel, attached under a piece of furniture or other heavy object to make it easier to move” [1] . These wheels are made from various materials using moulding, forming, matching and assembling methods to form the final castor wheel.

Figure 1.2 : Assembled castor wheel with swivel fork
Source: https://www.tente.com/us-us/

Forks are made from steel or aluminum most of the time with bearings for make it easy to rotate. In general, wheel part can be divided in to three main parts named as outer ring, center part and bearing. Outer ring which is in contact with the floor, manufactured in flexible material like rubber, polyurethane or thermoplastic rubber to get comfort and smooth running of the wheel. Most of the time outer ring is made from moulding method such as compression moulding or injection moulding according to material. Polypropylene is used as center material for light duty Castor Wheels. Nylon, Steel, cast iron or Aluminum is used as center material for heavy duty wheels for different applications. Various methods such as forging, casting, injection moulding and machining are used to make center part according to material used. Summary of general material used to make castor wheels are given on Figure 1.3 both roller type and ball type bearings are used in castor wheels according to applications.

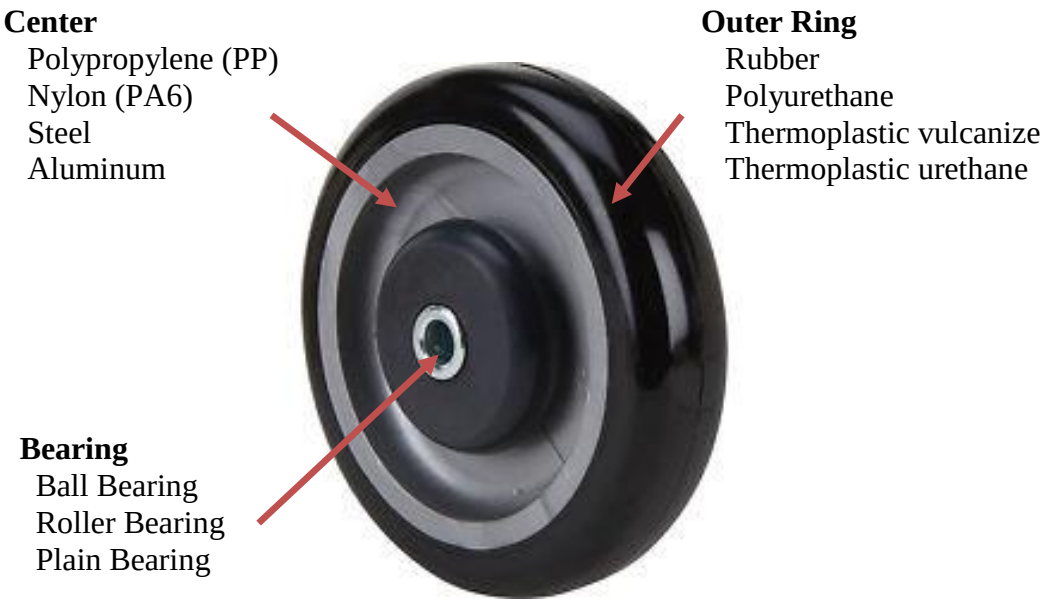

Figure 1.3 : Main parts of a castor wheel and materials

Source: https://www.tente.com/us-us/

1.2. Motivation

Rubber industry started in Sri Lanka 1876 with planting of rubber trees in Henerathgoda Botanical Gardens- Colombo. Now a days Sri Lanka is one of reputed supplier of rubber value-added products for the world market. Sri Lanka Rubber product industry is composed of about 4,530 manufacturing organizations of small, medium, and large-scale industries. Main products manufactured and exported from Sri Lanka are rubber solid tyres, pneumatic tyres, rubber gloves, rubber mats, rubber castor wheels and rubber bands which brings in foreign currency to Sri Lanka. In 2014 rubber finished products industry earned an export income of US$ 889 Million and provided direct and indirect employment opportunities to over 300,000 persons [2]. When considered about competition in world market, other Asian countries such as china, India, Thailand, Indonesia, Malaysia, Vietnam are main competitors for Sri Lankan rubber products.

Castor wheels which are made from rubber material are one of those value-added rubber products which accounted for about US$ 50 Million in year 2014. Several

castor wheel manufactures are located in Sri Lanka who mainly make rubber castor wheels. Sri Lankan made rubber castor wheels are very popular in the world market for their high quality, smooth and reliable operations. These are mostly used in various applications mainly including heavy and light duty industrial applications all around the world [2], [3].

Castor wheel market is very competitive with lots of wheel suppliers around the world including mentioned china, India, Thailand, Indonesia, Malaysia, Vietnam countries. To gain new market share and maintain existing market level, castor wheel manufacturers are always searching ways to minimize their costs and improve performance of their castor wheels. Customers are looking to develop customized castor wheels for their own applications with better performance and minimum cost. In average five to ten new inquiries about castor wheel new developments are given to one castor wheel manufacturer per month which suggest this industry is very dynamic industry. Most of inquiries are new applications in new material handling developments, new machines, high or low temperature applications, premium applications such as hospitals, sports items with new improvements. Lots of developments happening in material handling, castor forks, breaks in castors, automated vehicles, air ports, hospital equipment which constantly demands new castor wheel designs. To develop castor wheels low cost and to deliver intended application, castor wheels must be designed and developed in optimized manner. Lots of designs considerations and options are considered when designing a new design for a castor wheel. Lack of proper standardized method to evaluate designs of castor wheels in design stage was main problem in Sri Lankan castor wheel industry. Most companies do a sample production and do physical testing to evaluate design performance of various proposal designs which consumes time and cost.

In this research work focus is to develop a model to determine performance of a castor wheel design in early design stage so designers can do better designs by evaluating several design options and select best option before going in to sample trial and error stage.

1.3. Problem Definition

When new castor wheel designs are done, it is necessary to evaluate wheel performance under defined conditions to qualify the new design for a given application. Even in day to day productions randomly castor wheels are tested to evaluate performance of castor wheel and ensure quality of supply by castor wheel manufacturers. To evaluate the performance of the castor wheels, standard test methods are developed by international bodies [4], [5], [6]. New designs of castor wheels are tested under defined international test method by manufacture to ensure its performance in the application. For castor wheel testing, wheels are categorized as,

- Furniture Chair Casters
- Industrial Casters
- Institutional and Medical Equipment Casters

In this study standard used to test industrial castors wheels below 4 km/h was considered to test wheel designs [6]. Several tests are listed under industrial castor wheels, tests which are related to wheel part can be categorized as Static tests and dynamic tests of castor wheels.

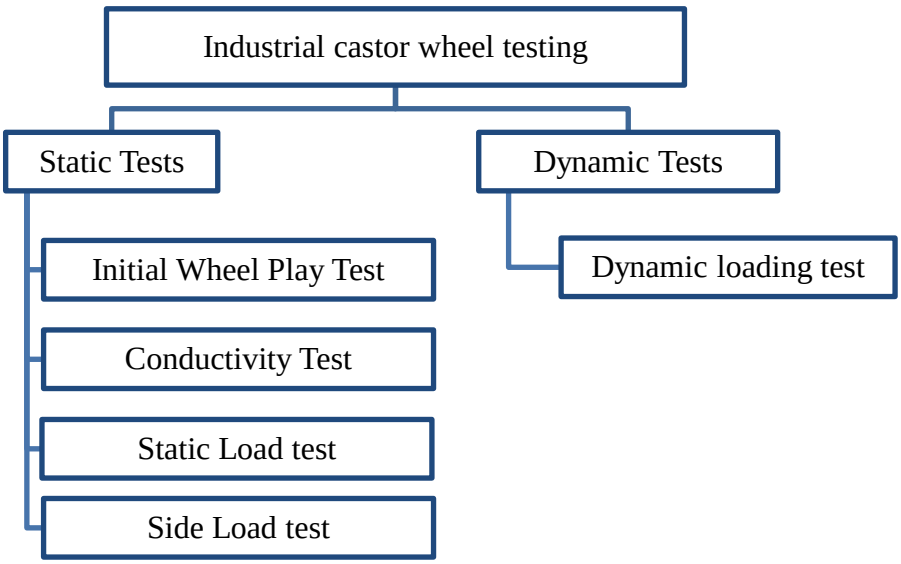

Figure 1.4 : Tests conducted for industrial castors

Static tests can be performed by available simple simulations methods or raw material testing methods. But performance evaluation of a new castor wheel design in dynamic test is hard task for simple simulation and material testing. There is no proper defined simulation method to evaluate castor wheel performance under dynamic load application, because it involves complex parameters like material analyze, viscoelastic hysteresis energy, heat buildup in the rubber wheel and material property variations due to temperature [7], [8] .

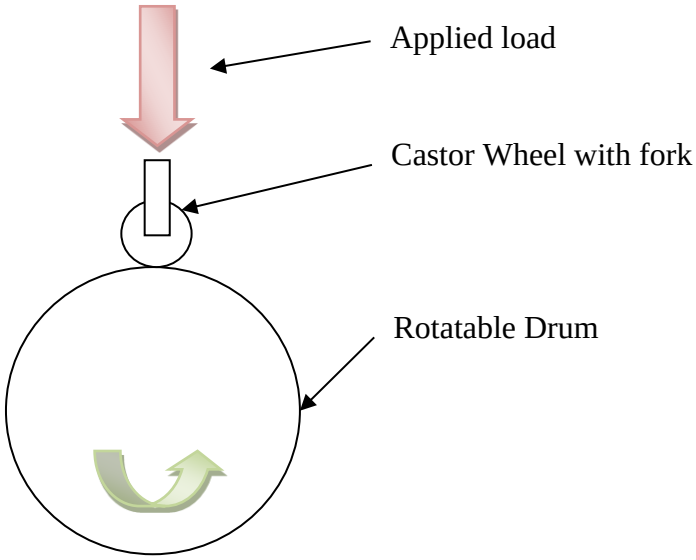

Figure 1.5 : Castor wheel dynamic test apparatus

In the dynamic test castor wheel is mounted on to a rotatable drum and a defined load is applied to the wheel. Then drum is rotated to a given speed for a given defined time period making the wheel to rotate with the load. Castor wheel should pass this test without any failures. Pass criteria for the wheel is defined as “No permanent deformation should happen in castor wheel which adversely affects performance” [6]. This Standard castor wheel test method is given under international standard. If a wheel passed this test it is accepted that wheel will perform in the real-world application.

During the dynamic test, it was observed that most of the wheels were failed at the center part of the castor wheel. When wheel is rotated, given location of rubber

outer ring is continuously loaded and unloaded resulting heat buildup inside the rubber which is commonly known as hysteresis heat buildup [9]. Then this heat is also absorbed by the center part of the castor wheel resulting to reduce its capability to hold against applied load. Then with time it was observed that center part was melted and resulted to failure.

Evaluation of dynamic test performance of a new castor wheel in design stage is important to develop optimized designs with lowest materials for a given application. Optimized design will result in low cost high performance wheel which will generate new markets for castor wheel manufacturers. When considered about material consumption also its always ecofriendly to develop products with minimum weight.

In average five to ten new inquiries are received by manufactures per month to develop castor wheels for various applications. As first step a basic design of castor wheel is done or existing wheel design is used for initial costing. Optimization of wheel design is not considered in this step hence most of times higher price is offered to customer than actually required. Because of that higher risk is there to lose business to another competitor. Two to three days are spent on this for costing.

If customer is positive next step is to develop sample wheels for customer approval which is done by trial and error method. Several moulds will be developed and various material trials will be done on this moulds also to identify best design. These additional trials consume additional development time and approximately 70% of total development cost. If trials are not successful or any improvements are needed, another mould should be developed and trials should be repeated until satisfactory results are obtained in product testing such as dynamic test and others. In average castor wheel development time can range from 1.5 to 3 months' time based on number of trials. Development cost is high due to additional mould and materials physical trials. Because of this method very few design options can be considered in development also which limit the opportunity to develop best design for a given application.

Requirement is to develop a finite element simulation method to simulate castor wheel dynamic test conditions in design stage and evaluate various designs. Through

this simulation model wheel manufacturing companies are able develop new castor wheel designs in optimized manner to a given application with less cost and lead time. Only wheels made from rubber outer rings and plastic centers (PP and PA6) will be studied in this research work since these wheels are the main products which are manufactured in Sri Lanka.

Aim of this research is to develop a finite element model to evaluate castor wheel designs for failures in dynamic testing. Objectives are to,

- Identify of parameters to be used in finite element model
- Develop finite element model to evaluate castor failures in dynamic test
- Validate the developed finite element model

As summary of this research which was done to achieve above aim and objectives, initially detailed literature review was carried out as described in chapter 2. From evaluated literature, Identification of parameters to be used in finite element model was carried out. 3rd chapter gives step by step description about development methodology followed in this research. 4th chapter of this report elaborate about physical testing carried out on caster wheels and raw materials. Obtained results were used in FEA model development in latter chapters. 5th chapter describes the detailed steps carried out in developing simulation model for caster wheel dynamic testing. Then in 6th chapter validation of developed models was done with several case studies comparing simulation results with actual physical test results. Finally, Discussion and conclusions of the developed model included in chapter 7 and 8 respectively.

2. Literature Review

Initially analysis of test standards, physical testing methods and finite element modeling methods available for wheels made form rubber were discussed which includes castor wheels, pneumatic tyres and solid tyres. Various testing methods used to measure parameters of rotating wheel such as turning, rolling, failures, static performance, dynamic performance were also discussed. The various finite element methods used to simulate rubber tyres and rubber other products were analyzed to identify methods used and parameters required for castor wheel simulation.

2.1. Castor Wheel Test Standards

Institute of castor and wheel manufactures association which is a USA based associations has published ANSI ICWM:2012 The ICWM performance standard for casters and wheels. In this standard, wheels are categorized to three main categories as furniture castors, Industrial castor and institutional and medical equipment casters. Sixteen tests are defined in the standard which castor wheels should be tested [4],

- Initial Wheel Play Test
- Initial Swivel Play Test
- Rollability Test
- Conductivity Test
- Initial Wheel Brake Efficiency Test
- Initial Swivel Lock Efficiency Test
- Braking and/or Locking Device Fatigue Test
- Dynamic Test
- Static Test
- Final Wheel Brake Efficiency Test
- Final Swivel Lock Efficiency Test
- Final Wheel Play Test
- Final Swivel Play Test
- Side Load Test
- Caster – Vertical Impact Test
- Wheels – Vertical Impact Test

For given tests, standard describes test apparatus and parameters to be tested. Test parameters and approval limits are different for different castor wheel categories. Standard describes that all the test should be done between 18^{o}C to 24^{o}C environment temperature. Initial wheel play tests are done by measuring castor wheel clearances

when fully assembled. For rollability test, castor wheel should be mounted on to a separate test apparatus and when wheel rotating on a surface rolling and swivelling parameters are measured. Electrical conductivity test is done while wheel is rotating in given apparatus with suitable resistance measuring equipment. Next three tests are done to measure break performance of castor wheels with break option. Dynamic test method given is given in the standard for all three castor wheel categories with recommendation for used any type of track which can be linear or circular, horizontal or vertical but providing required test setup options. Dynamic test is done on wheels to establish dynamic load capacity of the castor wheels. Static and side load tests are done on castor wheels to determine maximum load capacity and deflection of the wheel. Impact test are done to test time to tome extreme load application capacity of the castor wheel. Approval levels and test parameters are given in standard under each category [4].

British standards are established to test castor wheels which are going through application categories furniture castors, industrial castors, castors and wheels for manually propelled institutional applications and hospital beds. BS EN 12527:1999 Castors and wheels test methods and apparatus standard, discuss about test apparatus for the testing defined under given categories. Several test standards are defied to test each given category castor wheels such as,

- BS EN 12529:1999: Castors for furniture. Castors for swivel chairs. Requirements
- BS EN 12530:1999: Castors and wheels for manually propelled institutional applications
- BS EN 12531:1999: Castors and wheels. Hospital bed castors
- BS EN 12532:1999: Castors and wheels. Castors and wheels for applications up to 1,1 m/s (4 km/h)
- BS EN 12533:1999: Castors and wheels. Castors and wheels for applications over 1,1 m/s (4 km/h) and up to 4,4 m/s (16 km/h)

The given standards discuss about various application categories of castor wheels. In the given British standards sixteen tests are defined to be carried out on castor wheels. The failure criteria are defined as no permanent deformation should happen during the test. Each caster shall be capable of carrying out its normal function at the

end of the test program. Testing of a castor wheel starts with wheel clearance tests and rolling analysis. Then conductivity and break efficiency tests are done for several cycles to evaluate the castor wheels. Different types of test apparatus are proposed in standards for furniture castor wheels and industrial castor wheel dynamic tests. Furniture castor wheels test apparatuses designed to load three wheels together to the test which reforms a furniture chair castor wheel arrangement. Industrial castor wheel tests are done with single castor wheel in a linear or circular, horizontal or vertical test apparatus. The static and side load tests are done followed by break efficiency tests. Impact test on wheel and castor are done to identify impact strength of the product [5], [6].

The International Organization for Standardization which is known as ISO has published several standards to standardized castor wheel test procedures. Main categories which are defined under ISO standard are furniture castor wheels, castor wheels for swivel chairs, industrial castor wheels, castor wheels for hospital beds and castor wheels for manually propelled equipment for institutional applications.

- ISO 22878: Castors and wheels – Test methods and apparatus
- ISO 22879: Castors and wheels - Requirements for castors for furniture
- ISO 22880: Castors and wheels - Requirements for castors for swivel chairs
- ISO 22881: Castors and wheels - Requirements for use on manually propelled equipment for institutional applications
- ISO 22882: Castors and wheels - Requirements for castors for hospital beds
- ISO 22883: Castors and wheels - Requirements for applications up to 1,1 m/s (4 km/h)
- ISO 22884: Castors and wheels - Requirements for applications over 1,1 m/s (4 km/h) and up to 4,4 m/s (16 km/h)

In the ISO standard for furniture castor wheels, wheel characteristics and guide lines for fixing system of are defined along with castor types, dimensions and performance level. Normally impact performance test, conductivity test, locking tests, dynamic test, rolling resistance, swivel resistance, static load and stem retention test are done for furniture castor category and castor wheels for swivel chairs categories. For industrial castor category twelve tests are defined by ISO standards to evaluate the performance which is similar to British standard also,

- Initial wheel play
- Initial swivel play
- Electrical resistance
- Fatigue test for break and lock
- Efficiency check of wheel break and lock
- Efficiency check of swivel break and lock
- Dynamic test
- Efficiency check of wheel break and lock after static and dynamic test
- Efficiency check of swivel break and lock after static and dynamic test
- Final wheel play
- Final swivel play

When compared with American standards, British and ISO standards also does same set of tests to evaluate castor wheel performance. However, tests such as static test and impact tests are not included in ISO and British industrial castor test standards compared to American standard.

When analyzing of above three standards for industrial castor wheel testing it was observed that most of tests are related to wheel and fork interaction, clearance, breaking and locking related tests.

Actual wheel part and its strength was checked in five tests which can be categorized into two tests: static and dynamic test as given in Figure 1.4. When dynamic tests of industrial castor wheels are studied, it was observed that standard have only proposed maximum and minimum limits of test parameters which can be adjusted according given guide lines depending on application and customer requirement.

Then study about performance evaluation methods of wheels was done for various aspects. When considered about castor wheels, it was observed that only physical test methods are available in literature for evaluate castor wheel dynamic performance. Several simulations were found on castor wheel vibration analysis and validations. In other rubber product range, such as pneumatic tyres, solid tyres, rubber dampers both physical test methods and finite element simulations methods are available. So mainly for rubber tyres physical testing and finite element simulations can be selected as evaluation methods for dynamic performance.

2.2. Physical Test Methods

As given in international standards various physical tests are conducted on castor wheels to evaluate its performance. Industrial practice of testing castor wheel in dynamic testing is to load castor wheel to the dynamic test drum as described in Figure 1.5. and do the testing according to the guide lines. Given test apparatus is a vertical drum test method where vertical drum rotates while castor wheel is loaded on it to give the castor wheel 4 km/h speed. Other test apparatus methods are also available to have main drum horizontal which will not affect the outcome of the results.

Physical test of castor wheel was found in a study by Kiyoshi Ioi on shimmy vibration using a newly designed 100 mm diameter castor wheel and steel fork. Test variables were running speed, fork height and eccentric length of castor wheel. Industrial running machine was used to do the physical testing. Described test apparatus closely match with the setup given in Figure 1.5. test apparatus. Wheel was loaded on to the test drum and in the test and for various variable values shimmy vibration was recorded by attached pendulum for the test drum. Researcher compared various vibration results with simulation results to evaluate the developed simulation methods [10].

Study on wheel chair castor wheels was done by T.G. Frank to measure turning, rolling and obstacle resistance of wheelchair castor wheels. Turning and rolling resistance of wheel chair castors were measured in three types of indoor surfaces. Rolling resistance was measured by wheel chair deceleration on a flat surface and by direct measurement when wheel was running on a tread mill. Thread mill is linear test apparatus for test castor wheel dynamic performance. Also, horizontal forces required to push wheel chair on a defined step was measured for various wheels. From 800 mm to 200 mm diameter castor wheels were studies in the research [11].

Solid tyre test method also uses a same type apparatus to test solid tyres dynamic loading capacity. Solid tyres are loaded on to bigger scale vertical or horizontal drum which rotates according to given speed. Desired load is applied to the wheel making it pushed in to the rotating drum [12]. Pneumatic industry also uses dynamic tests to evaluate various parameters of pneumatic tyres which is very important for passenger

safety and comfort. Pneumatic tyres are inflated and loaded on to a test drum which is arrange same as described tyre test benches. Then tyres are loaded to desired loads and rotated to given speeds. Tyre static loading, tyre foot print, tyre cornering analysis are few tests done to evaluate pneumatic tyre performance in dynamic applications [13].

2.3. Simulation Methods

Various simulation methods used to simulate rubber castor wheels, pneumatic tyres, solid tyre and other rubber products which are subjected to dynamic load was analysed.

Kiyoshi Ioi in his shimmy vibration analysis, analysed castor wheel using a newly designed 100mm diameter castor wheel and steel fork. For the computer simulation researcher used a wheel running on a flat plate model with Newton-Euler's formulation. Several parameters for the simulation model was measured from material testing and wheel testing, other parameters like the frictional coefficient of rolling motion was expected to be negligible. Testing was done for a small amount of time so castor wheel heat build-up effect was neglected. When comparing vibration results from physical testing with simulation results, it was observed in both results shimmy vibration increases with rotating speed of the wheel. It was seen that the vibration amplitude and frequency increase when the eccentric length of the caster becomes longer. When the experimental results are compared to the simulation results, it is observed that the amplitude and vibration frequency of acceleration has a similar tendency with each other [10].

Ruggero Trivini has patented a hub less castor design which was mainly based on wheel construction and operation mechanism [14]. Another work was studied which was done on Caster wheel having integrated braking means mainly focused on castor wheel and its breaking mechanism by Steven Lewis and Crystal Lewis which was studied to get data about castor constructions and operating mechanisms [15].

Masaki Shiraishi from Sumitomo Rubber Industries, Ltd has obtained a patent for his Method for pneumatic tire simulation. In his method researcher model the tyre profile and inner cavity by finite elements. Researched has given comprehensive details about modelling of pneumatic tyre with selected finite element types according

to tyre construction. Then road surface was model by finite elements and develop wheel model was made to roll on the rod surface by executing the numerical simulation [16].

Study to do temperature prediction of rolling tyre through computer simulation was done by Yeong-Jyh Lin. Study was done for a smooth rubber pneumatic tyre of light truck operated under different speeds, pneumatic pressures, and loading conditions. Initially two separate sets of testing were carried out, namely dynamic mechanical testing and material testing. From material test data static finite element model was developed and total strain energy was calculated from that. Then from DMA data and total strain energy calculated, heat generation rete was calculated inside the wheel. Then again static 2D thermal analysis was used to predict the temperature distribution inside the tyre. Static loading displacement and simulation displacement was compared and found a close match. Then steady state rolling and thermal simulation was done to obtain temperature distribution of the tyre [9].

T.G. Ebbott conducted a research on a finite element-based method to predict tire rolling resistance and temperature distributions. Study was done based on material properties and constitutive modelling as these have a significant effect on the predictions of rolling tyre temperature distribution. A coupled thermomechanical method is described where both the stiffness and the loss properties are updated as a function of strain, temperature, and frequency. Results for rolling resistance and steady state temperature distribution are compared with experiments for passenger and radial medium truck tires [8].

A comprehensive study on Application of Computational Mechanics to Tire Design was done in 2011 by Y. Nakajima. [17] In the study, detailed step by step description was given how Simulation methods are used to simulate pneumatic tyres from past. Researcher divide time frame in to three sections mainly, yesterday from 1970s to 1980s, today from 1990s to 2000s, and tomorrow from 2000s to the future. The axisymmetric FEA was mainly utilized from 1970s to 1980s because of computer and software limitations. Only three kinds of applications such as stress/strain, heat conduction, and modal analysis was done in this time.

In the era of 1990s to 2000s, FEA which was initially use as a problem-solving tool started to evolve as a design tool. New tyre design procedures were developed by combining FEA with optimization techniques. Optimization techniques were used to applications like, tire sidewall shape optimization using the mathematical programming, tyre crown shape optimization by the response surface method using neural network, tyre belt construction was optimization by a genetic algorithm. In late 1990s, software was developed to visualize the streamline in a tire pattern on wet surface by considering fluid–tire interaction. Also, development was done to study tyre-snow interaction, tyre-soil interaction and tyre-air interaction [17].

From year 2000 onwards technology moved towards more coupled simulations and advanced optimizations mainly because of knowledge development, software developments and computer capabilities. Studies like vehicle/tire interaction, Nano simulation for the interaction of polymer and carbon black, Simulation with large strain and deformations, Complete tyre noise simulations are carried out today [17].

In 2007 N. Korunović published a study on Finite Element Model for Steady-State Rolling Tire Analysis. In this study FEA model used for the study was developed to improve accuracy, comprehensiveness and flexibility. Study was done to get simulation data for inflation analysis, analysis of vertically loaded tire, straight line rolling under the action of driving or breaking torque, straight line rolling analysis in fine increments, to find the angular velocity of free rolling, free-rolling cornering analysis. [7] in 2011 same author published a research which was done to study tyre rolling on a drum and comparison of simulation results and physical tests. Rubber components are described using Mooney-Rivlin FEA model. Physical test results and Simulation results were closely matched validating model developed by the author [18].

In study carried out by Robert Smith tyre numerical modelling and prediction of temperature destruction was discussed. Main reason for tyre heat build-up was identified as hysteresis loss in rubber material due to viscoelastic behaviour. Previous work done by Yeong-Jyh Lin [9] was referenced when developing simulation model in this study also. After tyre loading and steady state rolling analysis results from those

simulations were used as an input to thermal analysis to predict temperature distribution. Temperature results for 2 simulation software were compared in the study and found both gives same results within acceptable tolerance [19].

Several studies have been conducted on solidtyre computer simulations to study static behavior, dynamic behavior of solid tyres. In study conducted by U. Suripa, analysis about stress strain development of a solidtyre was done when Tyre was applied a defined static load. Solidtyre 3D model was developed using commercially available ABAQUS software and FEA mesh was created using eight node brick elements using same software. Static load was applied to the model and deflection and stress inside the Tyre was recorded. Deflection data was compared with actual data to validate the model [20].

A study was conducted to analyze heat generation in rubber or rubber-metal springs by Milan s. Bani in year 2012. [21] in this study rubber raw material was tested and parameters were used to develop a visco-elastic constative model. Although modern commercial FE packages are capable of performing full coupling of mechanical and thermal fields researcher mentioned such an approach is highly inefficient when time-temperature superposition is demanded due to huge computational demands. Researcher proposes a novel efficient method, initially hysteresis was calculated by static loading of rubber springs, then from that researcher calculate heat generation rate. Separate simulation was done to predict heat generation of rubber springs. To validate the procedure reaction force of springs were compared, also temperature predicated and actual were compared and found to be correlating to each other.

Several studies on pneumatic tyre temperature predictions and rubber products temperature prediction models were studied to develop the castor wheel temperature prediction models [8], [19], [21]. Most of studies done on pneumatic tyre simulation were started with 2D axisymmetric simulation of tyre inflation. Then 2D FEA profile was revolved to generate 3D FEA model of the pneumatic tyre. If required tyre tread designs were incorporated to the 3D model as revolve of segments. Then static loading simulations and steady state simulations were carried on the tyre model to analyze tyre

loading, cornering. Form steady state rolling analysis energy rate was calculated which was absorbed by rubber tyre in one revolution. With this data, the again 2D axisymmetric simulations were done to predict temperature development inside the tyre when its rotating in steady state condition.

These methods can be adopted to castor wheel temperature prediction tool developments with some modifications. Pneumatic and solidtyre are bigger in size when compared with castor wheels and are mainly made from rubber material and steel beads. Steel beads are incorporated in to the rubber material in order to reinforce selected regions in solid tyres and pneumatic tyres. But in castor wheel designs plastic and rubber materials are placed separately. New material model and material parameters should be included in castor wheel tool for the plastic material analysis. Inflation analysis is not required in castor wheel analysis but should be replaced by solid static analysis. In temperature prediction and failure analysis castor wheel behaves in different way such as wheel run cycle and failure mechanics different from pneumatic or solid tyres.

FEA model presented in Temperature prediction of rolling tires by computer simulation [9] by Yeong-Jyh Lin was selected to study further and used as a base to develop FEA model to castor wheel rolling temperature prediction and failure analysis. This model was used later in several other researches [7], [19] which proves the validity and applicability of the FEA model. In previous researches, other heat generation mechanisms, like friction effects on rubber Tyre was neglected as most of heat was generated by hysteresis in rubber material. Figure 2.1 summaries the procedure developed by the selected study.

Major changes in adaptation of mentioned [9] method to caster wheel is the wheel structure. Where pneumatic tyre is totally different from caster wheel design. Caster wheel consists of two materials as solid structures and pneumatic tyres are made as hollow structures. In addition to that testing cycles are totally different between caster wheel and pneumatic tyres.

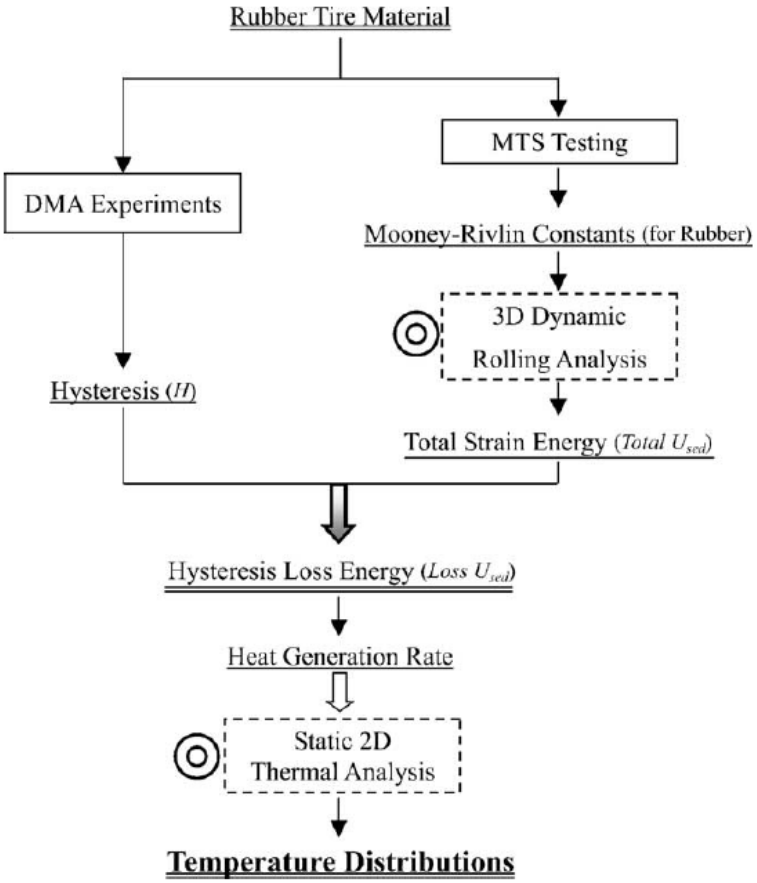

Figure 2.1 : Temperature prediction method for pneumatic tyres [9]

In this model researcher presented a method to develop simulation model with combination of physical testing and FEA techniques. Dynamic mechanical analyzes (DMA) testes were done as physical test and results were used to calculated hysteresis loss energy with combination of FEA analysis. Then separate 2D asymmetry analysis was done to analyze the temperature distributions inside the pneumatic tyre.

3. Methodology

Initially six samples of castor wheels ranging from 100 mm diameter to 200 mm diameter was selected and dynamic test was carried out according to BS EN 12532:1999 industrial castor standard test procedure under several loads [6]. Temperature development inside the castor wheel while in the dynamic test was recorded in four points namely rubber inner, rubber outer, plastic inner and plastic outer. Time each wheel ran on dynamic test before failure was recorded.

Two types of raw material analysis were done namely uniaxial tensile test and dynamic mechanical analyze (DMA) test. Tensile test was performed on both plastic and rubber materials to obtain their stress-strain graph. Plastic uniaxial tensile tests were done according to ASTM D638 test standard with ASTM D638-Type 1 test specimens. Rubber uniaxial tensile tests were done according to ASTM D412 test standard with ASTM D412-Type C test specimens.

DMA test was carried out only for rubber materials because rubber was the main hysteresis heat generation source in a castor wheel when rotated under load. DMA test was carried out according to ASTM D5992 with Rectangular rubber specimen of 35mmx13.5mmx2.8mm size. Test temperature range was selected as -60^0C to $+150^0$C to obtain loss modules and strobe modulus data in each temperature. Testing was carried out in several frequencies selected according to wheel diameter and test speed. It was observed from the results that storage modulus and loss modulus does not change relatively to test frequencies. Calculation was done to obtain energy loss fraction vs temperature graph from obtained loss modulus and storage modulus graphs from DMA test.

For FEA model development 160 mm diameter wheel was selected as case study. FEA model development was done in four steps. Figure 3.1 summarizes the development steps of FEA model starting with 3D static simulation, calculation model for total energy rate, 2D temperature prediction simulation and finally failure analysis simulation.

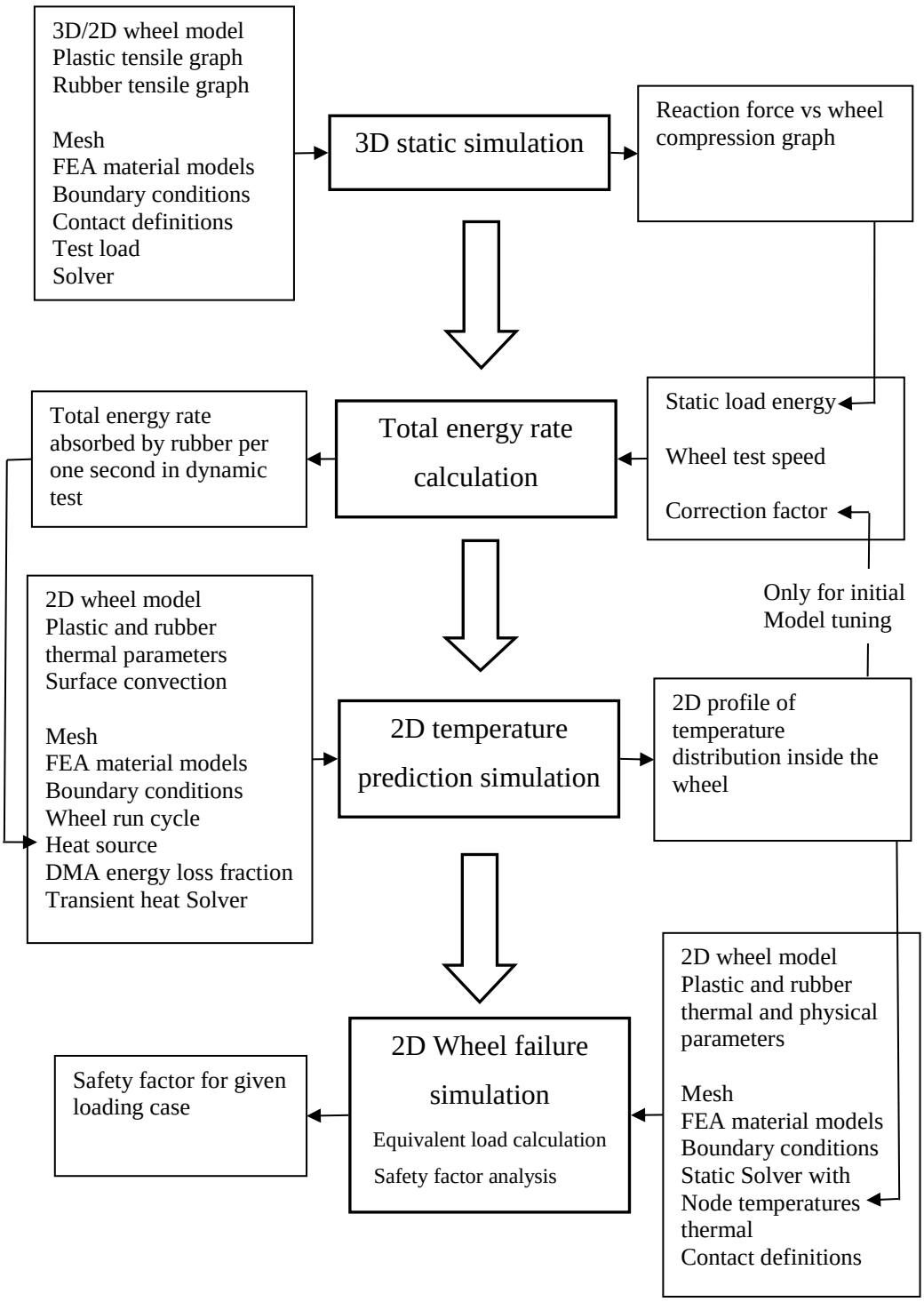

Figure 3.1 : FEA model development methodology

Initially 3D static simulation of the wheel was done under given load. 2D profile of the wheel was imported to the FEA software and 2D plate mesh was created using 8 node plate elements with 5% model size elements. Then 2D mesh was revolved in the FEA software to form 3D mesh of 20 node hexahedron elements. Plastic and rubber tensile graphs were loaded in to the software. Plastic material was selected as elasto-plastic material model. Rubber material was loaded as mooney-revlin material model and constants were calculated from software using a data fitting method. Floor contacts and boundary conditions were model to represent loading condition of the wheel. Nonlinear static solver was used to solve the setup where floor was compressed in to wheel up to 5mm distance. Force applied on the wheel when floor compression in to the wheel was extracted as force vs compression graph.

Extracted graph was integrated up to the point where testing load was applied on the wheel. Results of the integration gave energy absorbed by castor wheel when it was statically loaded to test load. This energy was converted to total energy absorbed by rubber wheel when rotated one second in dynamic test by calculation. Total energy rate was calculated by static energy, number of wheel rotations and correction factor. Initially correction factor was considered as one and simulation were continued until wheel temperature prediction was given. Then by comparing predicted rubber inner temperature with actual temperature of the test, correction factor was adjusted and simulation was done again to evaluate the results. Correct coercion factor was found to be 3.25 which converts static energy to dynamic energy rate correctly in case study. This was used as fixed number in the developed FEA model.

2D axisymmetric model was developed to thermal simulation of the castor wheel. 2D profile was meshed with 8 node plated elements 5% element size as identical to initial static simulation 3D mesh surface. Calculated total energy rate was distributed among rubber elements in the 2D simulation according to static loading stored energy in each element. Initially stored energy density and element volumes of the surface elements of rubber in 3D static simulation was extracted and calculations were done to obtain stored energy in each element. Then 75% of the elements were selected with highest stored energy and stored energy to total energy fractions were calculated. According to calculated fraction relevant 2D profile elements were selected and total

energy rete was applied accordingly. Plastic and rubber material models were defined as static simulation models and relevant elements were assigned to material models. Material thermal data such as specific heat capacity, heat conductivity and surface convection coefficients were extracted from literature, material data sheets and used in this thermal simulation [9] [18]. Transient heat solver was used to analyze the simulation with 1 second time frames up to 10000 seconds. It was observed from results after some time wheel temperatures attain steady state level which was validated in physical testing also.

Wheel failure analysis was done in 2D simulation to simplify the FEA model. This was done in two steps, first one was done without considering thermal data and node temperatures, to identify the equivalent 2D profile load which applies same stress as 3D simulation stress on plastic material. Since 2D simulation was done as axisymmetric simulation, higher load should be applied to the wheel to stress the center part of the wheel to same level as 3D. Only the plastic material stress was considered here because in practical failure was observed in plastic only. Contact definitions and floor was model similar to 3D simulation and nonlinear static solver was used for simulation. Then 2D axisymmetric loading simulation was done with nodal temperatures applied which were predicted in thermal simulation steady state region. Material physical property changes with temperature was considered in failure analysis. This was done using nonlinear static solver with thermal considerations enabled. Safety factor of the 2D profile was analyzed in calculated equivalent load conditions to observe any yield regions in given steady state temperate conditions. Wheel was considered as good design if safety factor was above 1.1 which means no yielding was detected by analysis.

According to the case study steps, general guideline was developed to follow when designing castor wheel to analysis their behavior in dynamic test. Four wheels were selected from sample wheels and developed FEA model was used to predict the temperatures of the wheels. Then comparison was done with practical temperatures to validate the developed FEA model.

4. Physical Testing and Results

Physical testing includes product testing and raw material testes carried out. From these testing, good understanding about wheel failures and their failure modes were obtained. With raw material testing parameters were identified which needs to be fed in to simulation model.

4.1. Product Testing

Actual dynamic testing of selected caster wheels was done as product testing. Initially sample castor wheels were selected and dynamic test was conducted to evaluate castor wheel behavior in dynamic test bench under various loads. Wheels were selected to represent most commonly used castor wheels in both heavy duty and general application range. Test loads were selected as standard load to given caster wheel sizes.

4.1.1. Sample Wheel Selection

Heavy duty range was selected from 200 mm diameter to 125 mm diameter. Theses wheels are made from good quality rubber compounds and nylon centers to carry higher loads and work longer time in industrial applications. In light duty range of castor wheels, most commonly used sizes are 100 mm and 125 mm diameter wheels only. These castor wheels are made from normal rubber compounds and polypropylene centers to carry average loads in day to day applications like shopping trolleys. Table 4.1 indicates the main dimensions, Materials and Wheel loads to test in dynamic tester.

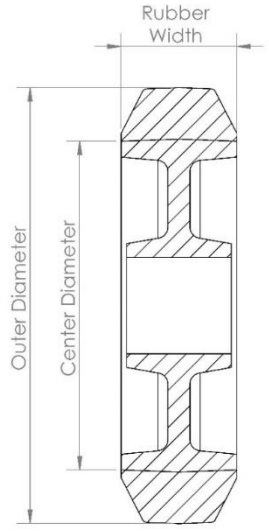

Figure 4.1 : Cross section of a castor wheel

Table 4.1 : Sample Castor wheels and selected test loads

	Dimensions: mm			Material		Load: kg		
Wheel Name	Outer diameter	Center Diameter	Rubber Width	Rubber Material	Center material	Test loads		
Heavy duty wheels								
125x42 Wheel	125	100	40	NR-1	PA-6	375	400	450
160x42 Wheel	160	140	40	NR-1	PA-6	450	500	550
180x42 Wheel	180	140	40	NR-1	PA-6	450	500	550
200x42 Wheel	200	140	40	NR-1	PA-6	450	500	550
General application wheels								
125 Common Wheel	125	100	32	NR-2	PP	80	100	
100 Common Wheel	100	80	32	NR-2	PP	100	125	

NR-1 and NR-2 are identification codes for Natural rubber compounds. Test loads for each wheel were selected according to standard load capacity of each wheel. Additional loading test were done to speed up the wheel failure and analyses the temperature buildup and more deeply.

4.1.2. Dynamic Test

Above selected wheels were tested according to BS EN 12532:1999 test standard which is used to test castor wheel in dynamic test [6]. As described in early chapter castor wheels were loaded on to a rotating drum. Then load was applied to the castor wheel by a pressure controlled pneumatic cylinder to give equivalent kilogram load to the wheel.

In the testing run-stop cycle is also applied to run the caster wheel 3 minutes and stop it for 1 minute throughout the testing. Wheel is rotated to 4 km/h speed to a given number of wheel rotations in the dynamic test. Figure 4.2 shows the dynamic test machine with wheel loaded. In the testing, pneumatic cylinders apply required load to caster wheel from vertical direction through fork of caster wheel.

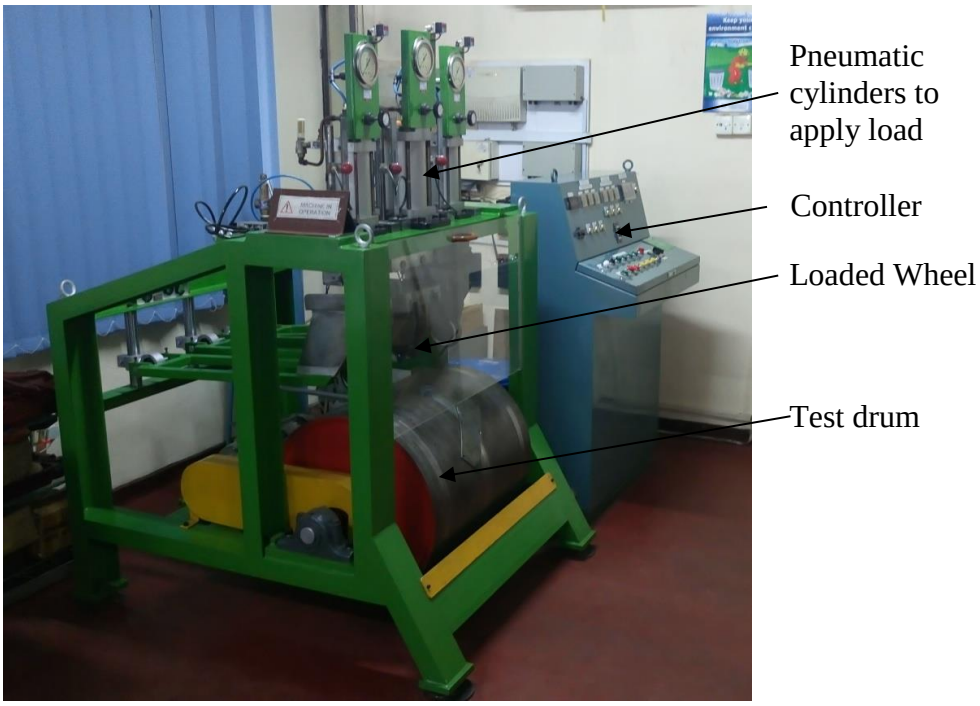

Figure 4.2 : Castor wheel Dynamic test apparatus (Original in colour)

Test Parameters:

Load: As given in table 5.1
Speed of castor wheel: 4 km/h
Run method: 3-minute run, 1-minute stop
Run time: until failure occurs
Obstacles: 0
Standard wheel revaluations required to pass: 15,000

Required 15,000 wheel revelations converted to total run time in seconds considering wheel diameters and speed. Higher run time requirement was obtained for bigger wheels and low requirement was obtained for small wheel according to wheel diameter. But all selected wheels were tested on dynamic test apparatus until failure occurs according to given standard parameters. Main factor for the wheel failures was temperature build up in the rubber due to hysteresis loss [9], [7]. Because of the temperature plastic center starts to yield and eventually fails to hold the wheel original shape. Temperature development of four critical locations of the castor wheel was recorded throughout the testing along with run time until fails. Namely rubber inner, rubber outer, plastic inner, plastic outer temperatures were recorded.

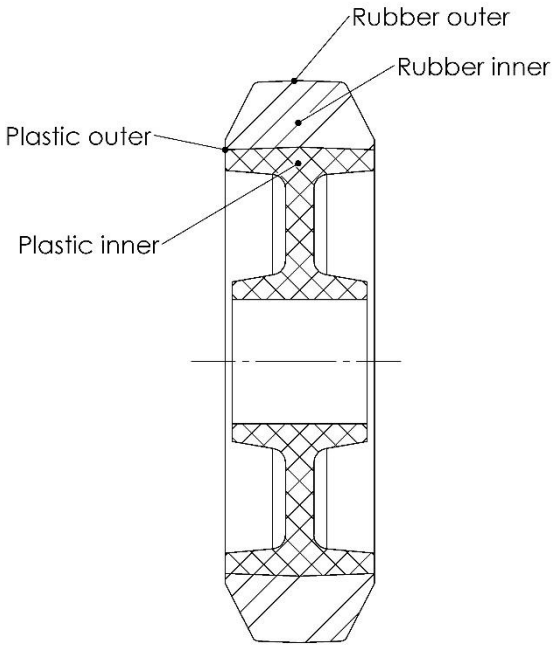

Figure 4.3 : Dynamic test Temperature recorded locations

When failure starts to occur, rotating castor wheel starts to bounce abnormally because of deformed shape. Limit switch is fixed on top of the wheel to detect this abnormal bounce and stop the test when this bounce exceeds the set value.

4.1.3. Dynamic Test Results

It was observed that all the failures were occurred at plastic center. Figure 4.4 shows failed images which show melted and deformed plastics around the failure region.

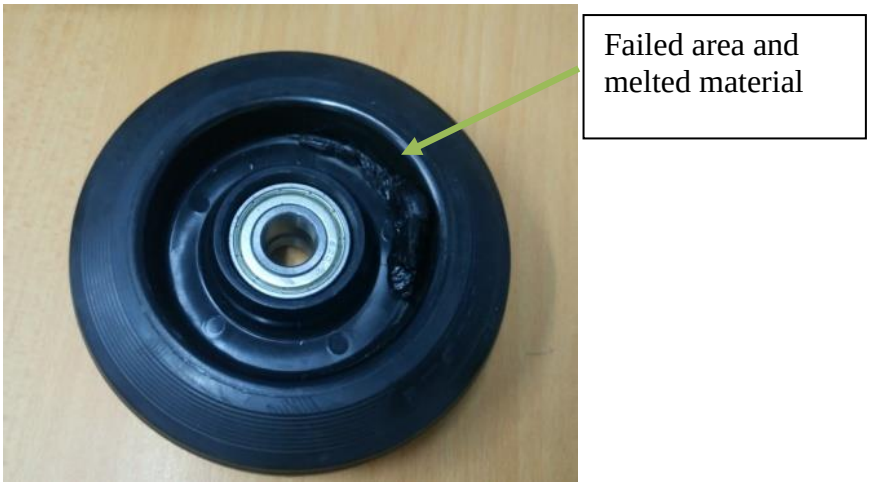

Figure 4.4 : Wheel after failure (Original in colour)

160 mm diameter wheel 450 kg load recorded temperature graph is given in Figure 4.5. Wheel ran for total of 17,220 seconds which is over the required 9,048 seconds test time. It was observed that highest temperature occurred in cater of the rubber where heat generates due to hysteresis loss wheel rotates. Then plastic inner, plastic outer and rubber outer showed the temperatures accordingly. Rubber outer where wheel contact with steel rotating drum of the testing machine, showed lowest temperature build up as this area has higher heat dissipation to steel drum.

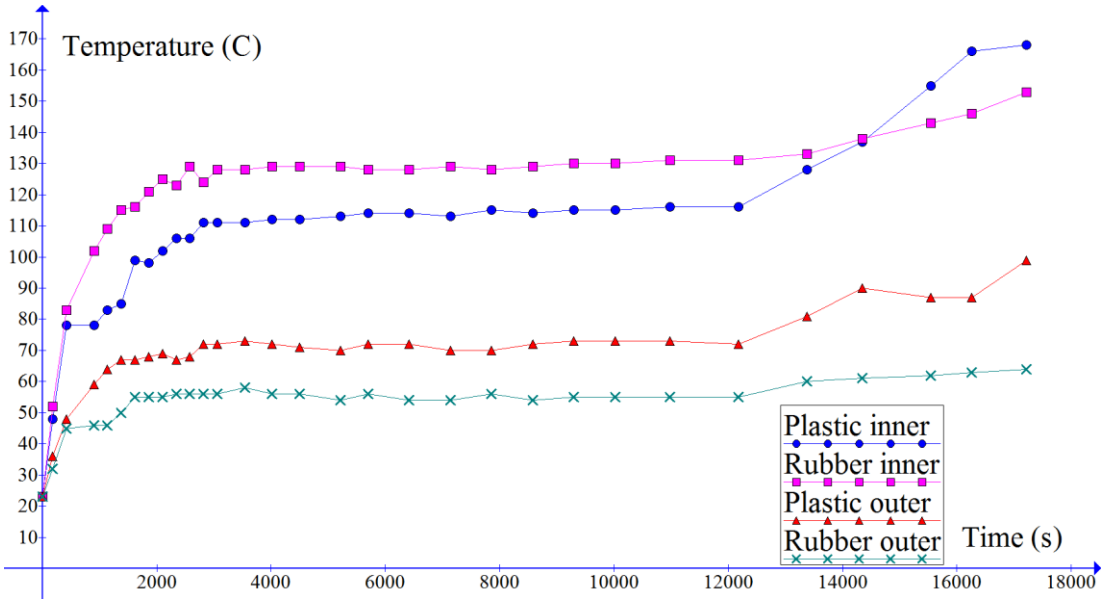

Figure 4.5 : 160 mm Wheel 450 kg Dynamic test temperature record

Summary of all sample wheel dynamic test temperature records are given in appendix 1 which shows that six wheels were failed before required 15,000 revaluations of the wheel test cycle.

It was observed that when wheel rotates, temperatures raises and then attain steady state level after some time, then again temperature went up when wheel was about to fail. Wheel run-stop cycle temperature variation was not captured here as measurements were taken right after wheel stops only. From the obtained graph, interesting phenomena of the temperature development was observed. From each temperature development curves, it was observed that temperature development happens in three stages.

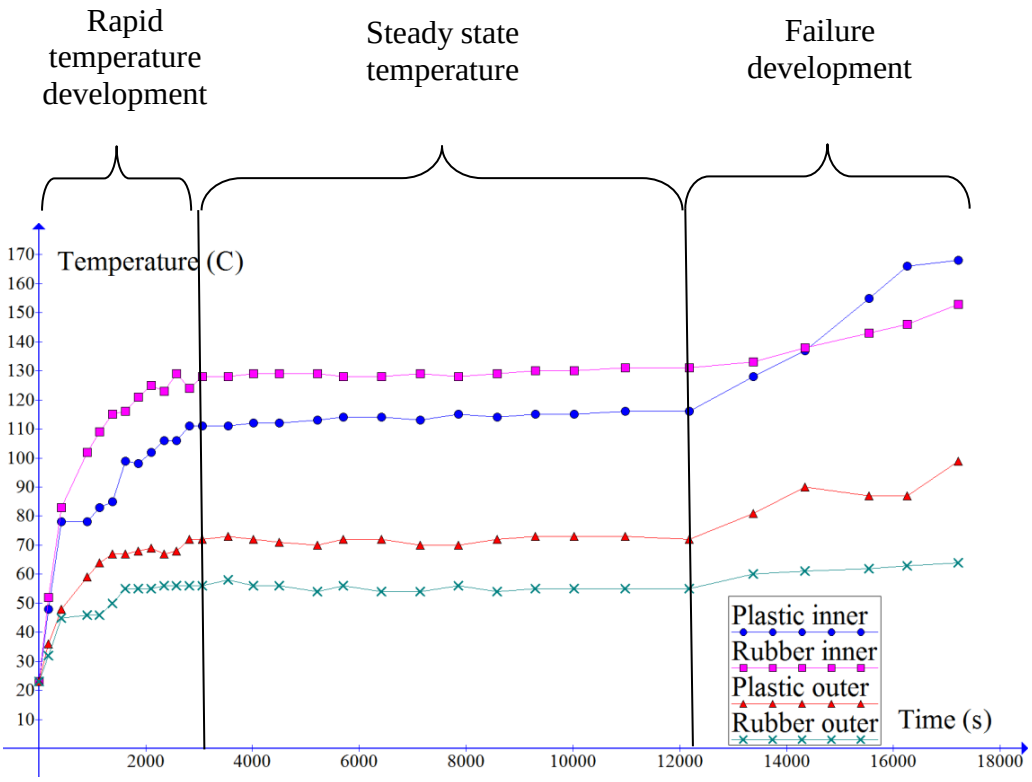

Figure 4.11 : Castor wheel temperature development stages

It was observed that at the start of the dynamic tests wheel goes through a rapid temperature development stage. In the given case, all recorded temperatures showed a rapid increase until about 3,000 seconds. Then it was observed that wheel comes to a steady state level where no clear temperature increase happens. At this region heat generated inside the wheel was assumed to be equal to the heat loss from outer surface. But after some time, it was observed that temperature started to increase again and then wheel failure occurred.

From the observation, it was decided that even in the steady state level micro changes happens inside the wheel material which leads to failure at the end. This temperature increase at the end of the test was happened because of wheel abnormal bounce which happens near to the failure. Wheel material was deformed and castor wheel shape was changed near to failure of the wheel which resulted abnormal bounce of the wheel near to failure of the wheel. Same behavior was observed from other wheels also. In higher loads, some of wheels were failed before entering steady state level.

4.2. Raw Material Testing

Raw material tests include testing of plastic and rubber materials.

4.2.1. Tensile Test

Uniaxial Tensile test was carried out in rubber, polypropylene and nylon material to evaluate stress strain behavior of the materials. All the test pieces were made in house and tested with available tensile test machine Tinius olsen 5ST machine [22].

Plastic material tensile test

Uniaxial tensile test of plastic materials was carried out under ASTM D638 standard. Tensile pieces were made by injection moulding according to standard type 1 dumbbell shape pieces as given is test standard.

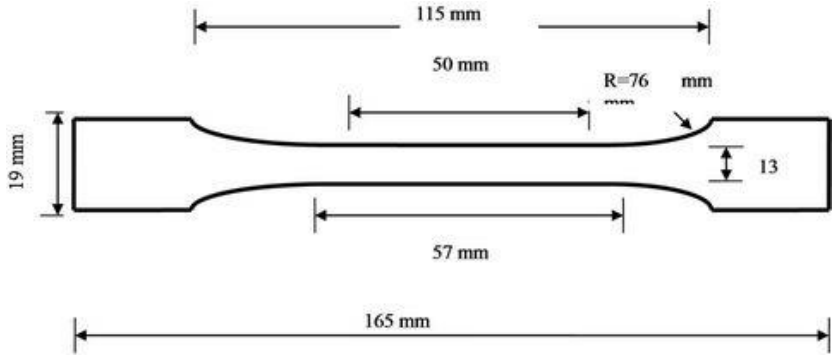

Figure 4.20 : ASTM D638-Type 1 test piece dimensions

Test was carried out in average recommended strain rate of 50mm/minute in controlled lab temperature of 23ºC. strass-Strain graph for the test was extracted from the tensile machine. This data was used to calculate modulus and yield stress when giving parameters for the FEA software.

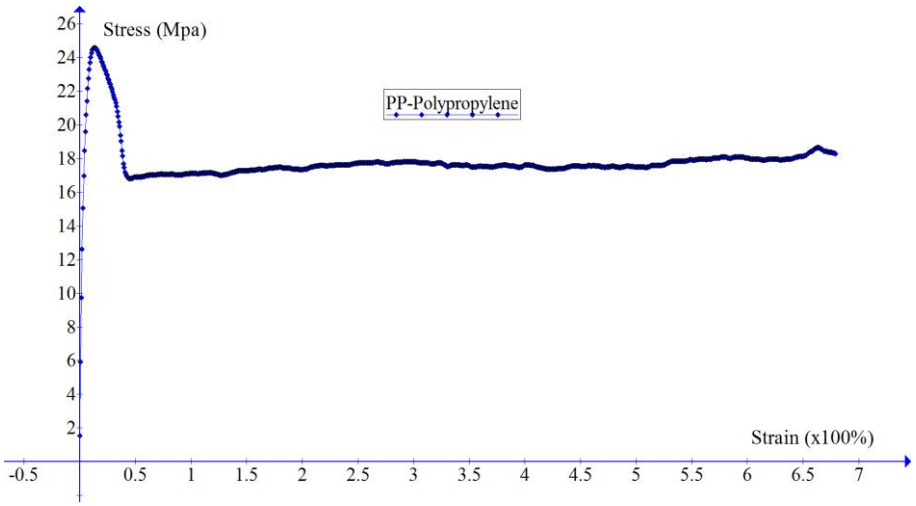

Figure 4.29 : Polypropylene Stress-Strain graph at 23ºC

Figure 4.8 shows stress-strain graph of polypropylene material used in castor wheel. Yield stress of the material is 24.5 MPa according to the obtained graph with approximately 700% post yield strain.

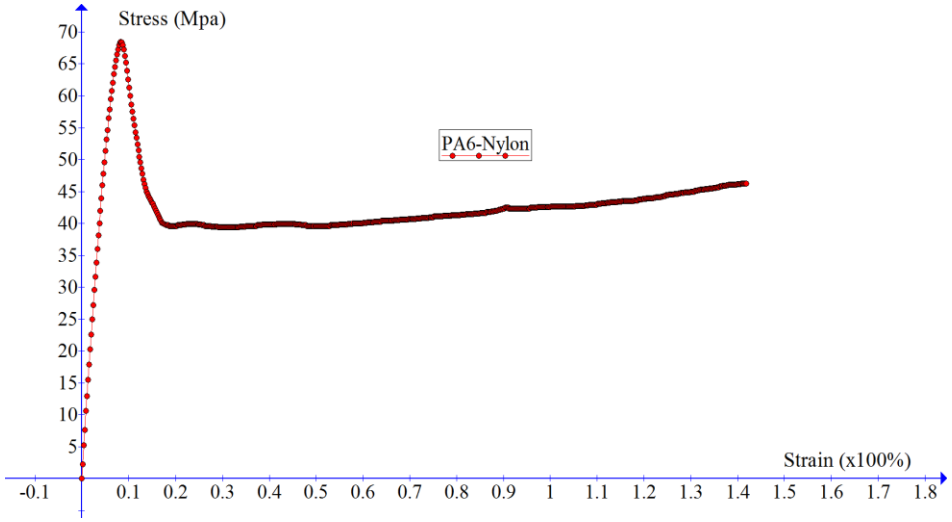

Figure 4.36 : Nylon Stress-Strain graph at 23^{o}c

Figure 4.9 shows Stress strain graph of nylon used for castor wheels. Yield stress of nylon was 68.4 MPa, which was 2.8 times higher than polypropylene. But nylon maximum strain was 200%. This higher strength and yield stress was main reason for use nylon material in heavy load application castor wheels.

Table 4.2 : Plastic material tensile test results

Units	MPa	MPa	(x100%)	(x100%)
Material	Modulus	Yield Stress	Strain at yield	Max Strain
PA6 (Nylon)	821.2	68.4	0.083	1.5
PP (Polypropylene)	194.5	24.6	0.126	7.0

Rubber material tensile test

There were two rubber compounds used in selected castor wheel sample set namely NR-1 and NR-2. Both those compounds were tested in uniaxial tensile test to get stress-strain data for each material. ASTM D412 Standard Test Methods for Vulcanized Rubber and Thermoplastic Elastomers was used as standard to test rubber materials. Initially compounds were mixed and milled as normal procedure. Then

rubber 150mmx150mmx2mm rubber sheets was made by compression moulding. ASTM D412-Type C die was used to cut dumbbell pieces from those moulded sheets.

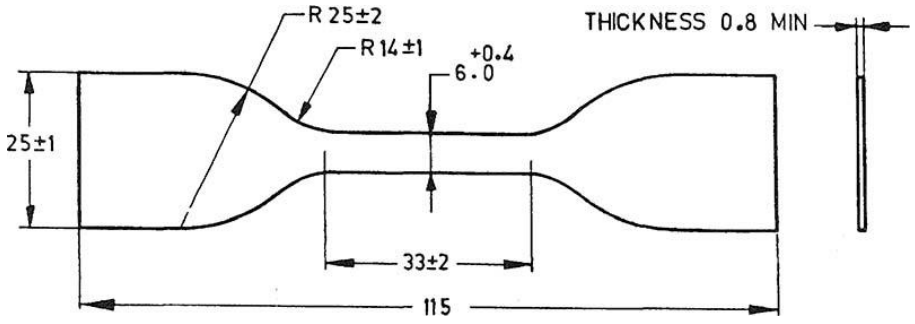

Figure 4.37 : ASTMD 412-Type C rubber specimen dimensions

Standard 200mm/minute speed was used to test those dumb-bell pieces in same tensile machine. Obtained Stress-Strain graph showed similar behavior and in average max stress recorded was 15 MPa with about 390% strain. Those graphs were directly used in FEA software for calculation of material model coefficients. X axis of the graph represent strain amount of test piece. Y axis shows the stress inside the test piece.

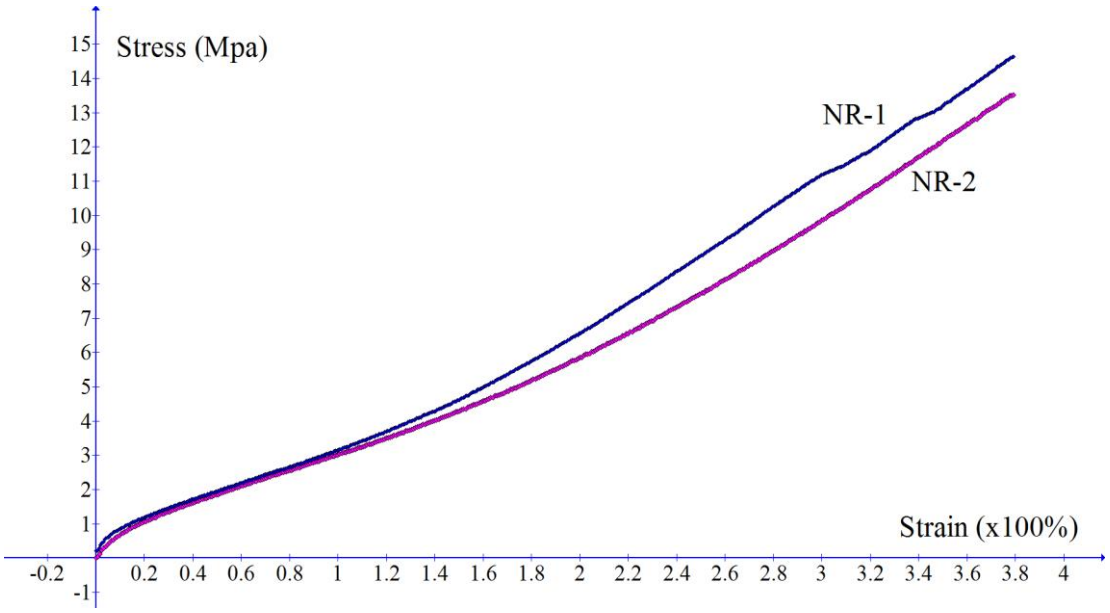

Figure 4.38 : Rubber Stress-Strain graph at 23^{o}c

4.2.2. DMA Test

DMA which is named as dynamic mechanical analyze is mostly used to analyze viscoelastic behavior of polymers. DMA measures the properties of materials as they are deformed under periodic sinusoidal stress, which is very similar to behavior of material when a tyre or castor wheels are rotated under load. Loss modulus and storage modulus of a viscoelastic material and their variation with temperature can be extracted by DMA test [23]. The storage modulus represents the stiffness of a viscoelastic material and is proportional to the energy stored during a loading cycle. The loss modulus is defined as being proportional to the energy dissipated during one loading cycle. For example, it represents the energy lost as heat, in a loading cycle of a viscoelastic material [23].

When castor wheels are rotated under load heat generation happens inside of the rubber material due to this loss energy because of viscoelastic property of the rubber material [19]. So only rubber materials were tested in DMA test as it contributes most of energy for the heat generation inside the wheel.

[24] Various methods are available to test rubber materials in DMA test. ASTM D5992 Standard Guide for Dynamic Testing of Vulcanized Rubber and Rubber-Like Materials Using Vibratory Methods was followed when testing rubber in DMA tester.

Rectangular rubber piece 35mmx13.5mmx2.8mm in size, which is cut by previously described moulded rubber sheet was used as specimen for DMA test. The test specimen is clamped between the movable and stationary fixtures, and then enclosed in the thermal chamber. Oscillation frequency and a temperature range appropriate for the material were given to tester. The Analyzer applies oscillation to the test sample while slowly moving through the specified temperature range.

Materials were tested for several oscillation frequencies in between -60^{o}C to +150^{o}C. frequency was selected according to castor wheel rotation speed of 4 km/h and wheel diameter.

$$\text{Frequency} = \frac{\text{Wheel Speed}}{\text{Wheel Circumference}} \qquad (1)$$

Table 4.3 : DMA test oscillation frequency

km/h	mm/s	mm	mm	
Wheel Speed	Wheel Speed	Wheel diameter	wheel circumference	Frequency
4	1111.1	80	251.3	4.4
4	1111.1	125	392.7	2.8
4	1111.1	160	502.7	2.2
4	1111.1	180	565.5	2.0
4	1111.1	200	628.3	1.8

It was observed that very similar data curves were given by the DMA test for various frequencies which suggest this viscoelastic property of the material doesn't depend of oscillation frequency. DMA graph for both materials which was done at 2.2 Hz frequency was selected for further studies.

loss modulus and storage modulus was extracted in between given temperature range -60^{o}c to 150^{o}c as data points from the DMA test machine. Temperate range selected according to temperatures occurred in castor wheel dynamic testing. As referenced research paper [9] energy input modulus for the DMA test specimen in each temperature can be calculated as,

$$\text{Energy input modulus} = \sqrt{(\text{Storage modulus})^2 + (\text{Loss Modulus})^2} \quad (2)$$

Then Energy loss fraction of the rubber material at a given temperature can be calculated as,

$$\text{Energy loss fraction} = \frac{\text{Loss modulus}}{\text{Energy input modulus}} \quad (3)$$

Energy loss fraction vs temperature graph was analyzed in both NR-1 and NR-2 rubber compounds and recorded to be used in FEA model creation. Calculated Graphs are given in Figure 4.12. It was observed in both graphs energy loss fraction started around 0.08 and went up to 0.2 around -20^{o}C temperature. Then this Energy loss drops back to0.09 after -15^{o}C and steadily follows similar values after that. in this research area interest are of the curve was above 23^{o}C which is steady around 0.9-0.8 energy

loss fraction. Very similar behavior was observed between NR-1 graph and NR-2 graph.

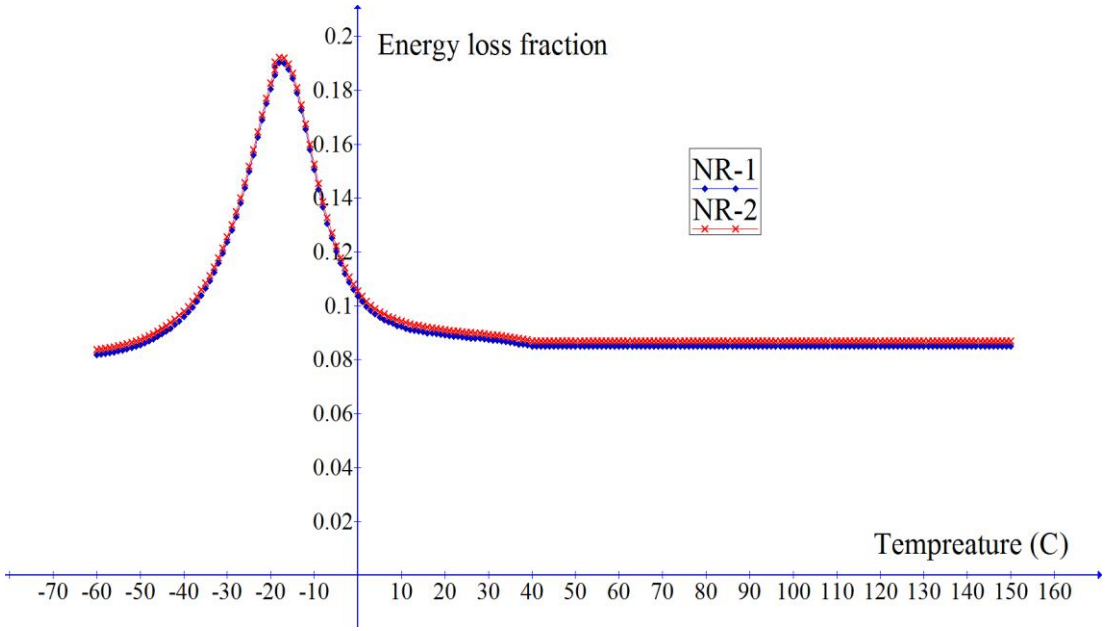

Figure 4.42 : NR-1 & NR-2 Energy loss fraction vs temperature graphs

From energy loss fraction, energy loss at given cycle can be calculated if Total energy input for the particular cycle is known. These obtained data were checked against previous researches done on this DMA testing and was fond to be very closely matching with research data. [9] Yeong-Jyh in his research presented pneumatic tyre tread rubber material DMA test data which was done at frequencies from 0 Hz to 25 Hz and temperatures from 0^{o}C to 100^{o}C. it was presented that energy loss fraction was not varied according to variation of frequency. Also from 25^{o}C to 100^{o}C energy loss fraction was measured as 0.1 in given test which is closely matching with observed test data.

5. Finite Element Model Development

Finite element analysis (FEA) is well established technology to virtually simulated real world application and behaviors. When a product is analyzed through FEA for a loading condition, the setup is broken in to small elements and analyzed in simplified manner then combined again to give the full results [25].

After castor wheel dynamic tests and raw material testing next step was to develop finite element simulation model to predict temperature profile of a rotation castor wheel under load. The simulation models were developed according to Figure 3.1 given in methodology. Initially simulations were done to predict temperature profile of rotating castor wheel in a given time, the with predicted temperature data simulation was done to analysis failures of the wheel. To simplify the simulation, 2D plate simulations were used where ever possible. 160 mm wheel with 450kg load was used to develop the FEA model as case study.

5.1. Static Loading

Static load simulation of the castor wheel was done to understand stress level of wheel with given load and to analyze total energy required to load the wheel. For the simulation, commercially available mid-range FEA software Strand7 [26] was used with nonlinear static and dynamic analysis capability.

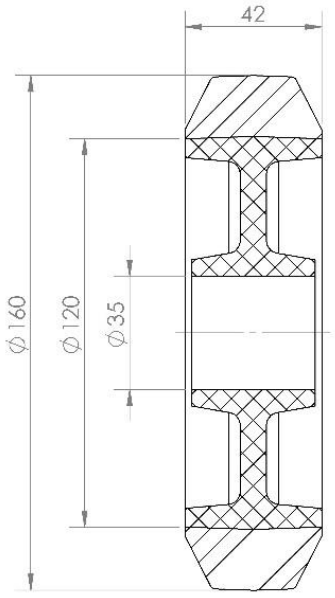

Figure 5.1 : 160 mm Castor wheel dimensions

3D FEA analysis was done for the static loading simulation because loading was done from one location when wheel statically loaded. When considered about this loading case, it was observed that symmetricity could be considered for this dividing loading area and 3D model in to ¼ of the model. Figure 5.2 demonstrate the proposed ¼ symmetric model with loading conditions.

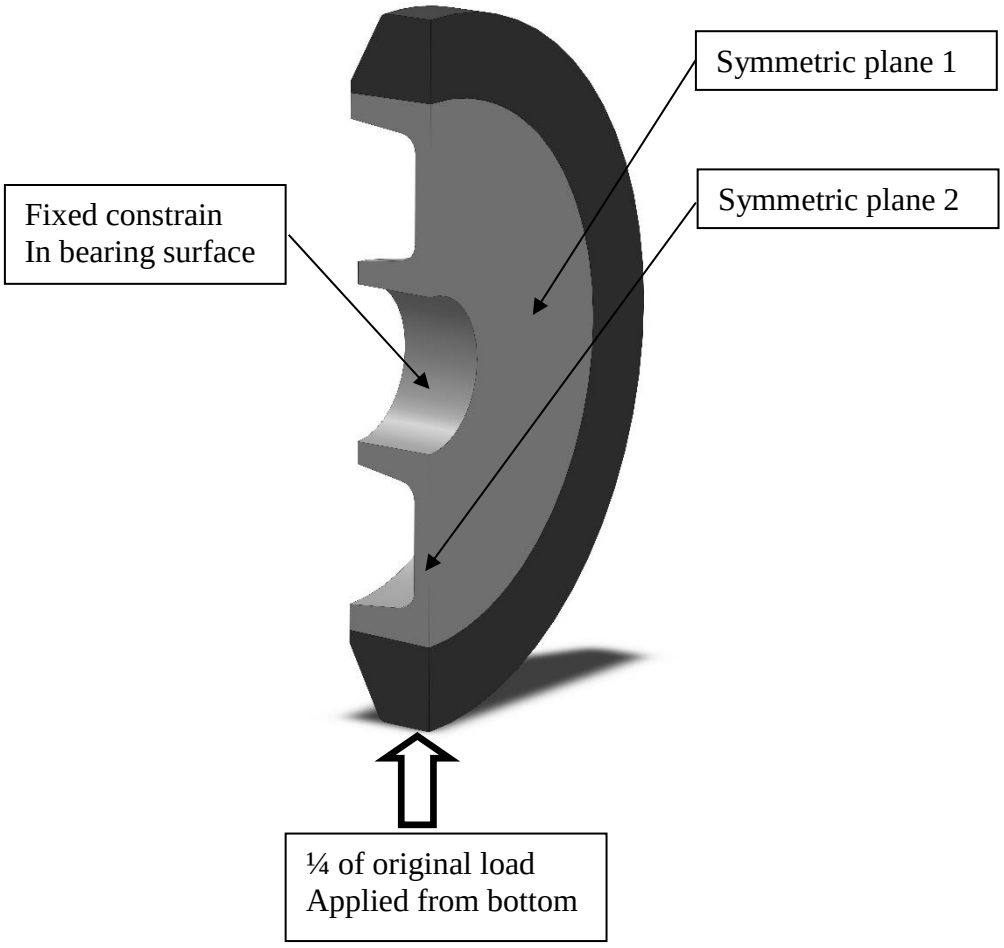

Figure 5.2 : proposed ¼ castor wheel model for FEA

Obtained tensile graph of the NR-1 rubber material was loaded in to the software as a Stress-Strain graph. Tensile graph of nylon was also loaded to the software as stress-strain graph.

5.1.1. Mesh Creation

when considered about required 3D model mesh, several element types are available as given in Figure 5.3 to mesh a model and do analysis. Element type was selected according to literature of rubber and plastic product simulations. Mostly 20 node hexahedrons were used in 3D simulations and 8 node plate elements were used in 2D simulations in literature to simulate filled rubber components and plastic components because of results accuracy and efficiency. Same element type was used in this research also [26] [27]. Element size of the mesh was selected after several analyses done by possible element size and developing a convergence graph. Initially ½ of 2D profile of the wheel was imported to FEA software. Then according to selected element size 2D profile was meshed with 8 node plate elements and revolved to form 20 node hexahedron elements in 3D mesh.

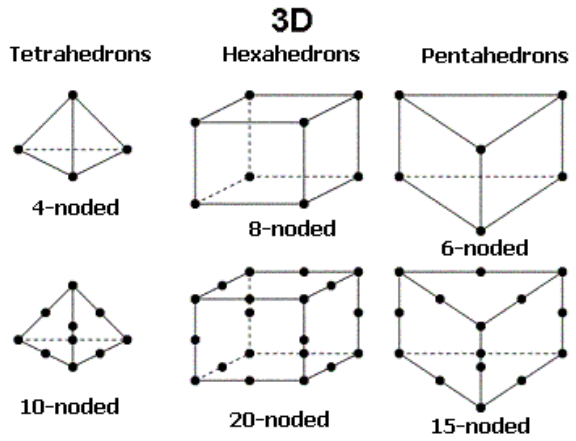

Figure 5.3 : FEA Elements available for 3D simulation

Convergence plot was developed to select the best element size for the simulation. Model was simulated in various element sizes and maximum stress developed in the plastic region of the model for given load was recorded and plotted.

Stress in the plastic region was selected because rubber region stress was much lower value than plastic region. Mesh size was defined as percentage for the maximum dimension in the model so when wheel size changed accordingly proper mesh size can be derived from percentage.

Table 5.1 : Max stress in plastic vs Element size

	mm	kg	MPa
2D Element size	Element size for 160 mm wheel	Wheel load	Max Stress in plastic
9.0%	14.4	450	17.50
8.0%	12.8	450	19.50
7.0%	11.2	450	20.10
6.0%	9.6	450	20.50
5.0%	8.0	450	20.63
4.0%	6.4	450	20.64
3.0%	4.8	450	20.65
2.0%	3.2	450	20.66

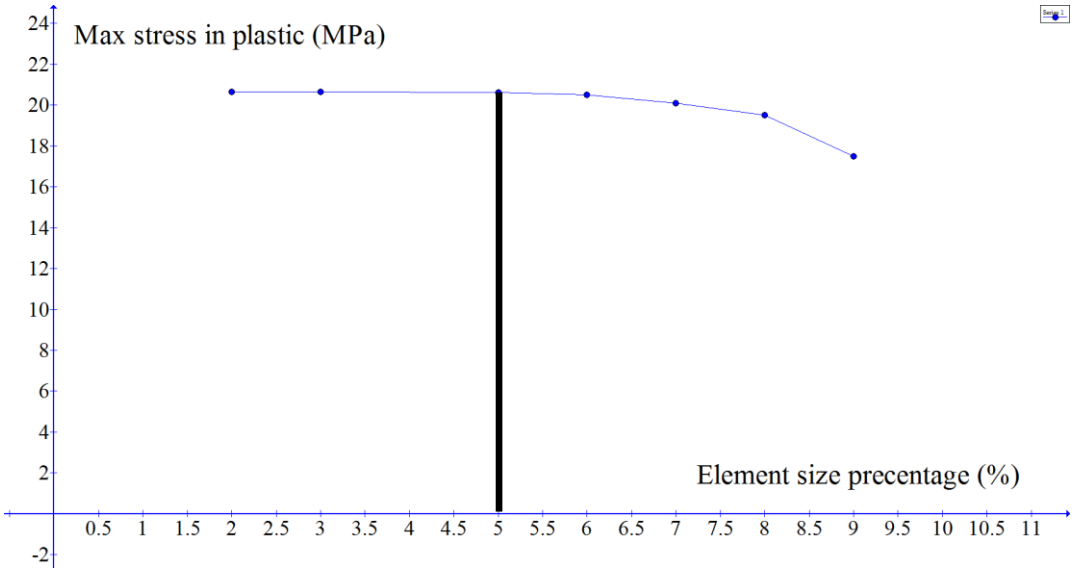

Figure 5.4: Convergence analyze for selecting mesh size

From Figure 5.4 it was observed that before 5% element size graph converge to a stable value. for Castor wheel 2D profile 8 node plate elements were created in the size of 5% from maximum dimension of the castor wheel model. Then they were revolved around wheel axis initially by 2 degrees until 30 digress, and the by 6 degrees until 180 degrees. Initial 2 degrees were created more densely to be used in contact analysis. the Same element size percentage was selected to mesh the models of all the wheels.

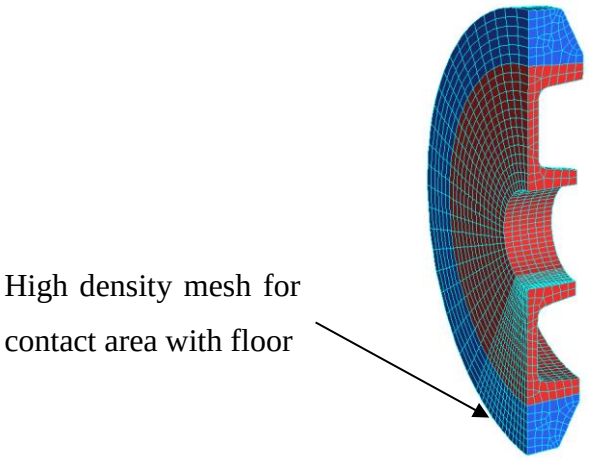

Figure 5.5 : Meshed 3D model of 160 mm Castor wheel

5.1.2. Boundary Conditions

Fixed boundary condition for the bearing area was applied as model is supported by bearings. In the 3D model bearings were not modeled, boundary conditions were applied to the plastic center bearing area directly to simplify the simulation. Bearing effect was not considered in simulations.

Symmetric boundary conditions for both symmetric planes were applied as next step. Separate boundary conditions were defined for fixed location and two symmetric planes where castor wheel was split to simplify the FEA model.

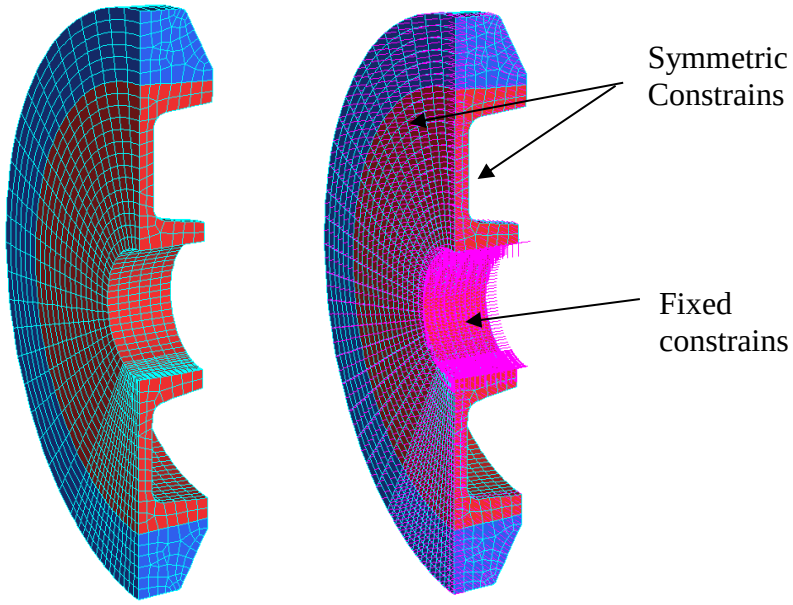

Figure 5.6 : Meshed model with boundary conditions

Load was applied on the castor wheel as compression force which applied through floor. Initially contact between castor wheel and floor was defined by contact element. Strand7 software use “node to node” contact method to define contact between two bodies. Other advance contact definitions are “surface to node” and “surface to surface” which needs higher computational power and generally used with complex contact problems. In the castor wheel simulation floor to wheel contact is straightforward and “node to node” contact definition is the most effective contact definition to be used here [26], [28].

From 3D mesh approximately contact area of the rubber wheel was selected and nodes in that area were extruded to form floor nodes with beam elements. The point contact definition was used to define those beams, so when beam length becomes 0 it acts as contacted node.

Then all those floor nodes were connected with rigid beams to form a one cluster node. Cluster node was given constrain to move upwards along with the floor until floor compresses rubber wheel generation a reaction force on the cluster node. From the reaction on the cluster node load acted on the wheel was calculated to a given wheel compression.

Contact element parameters were selected as standard parameters and kept as fixed values throughout case study models to maintain uniformity.

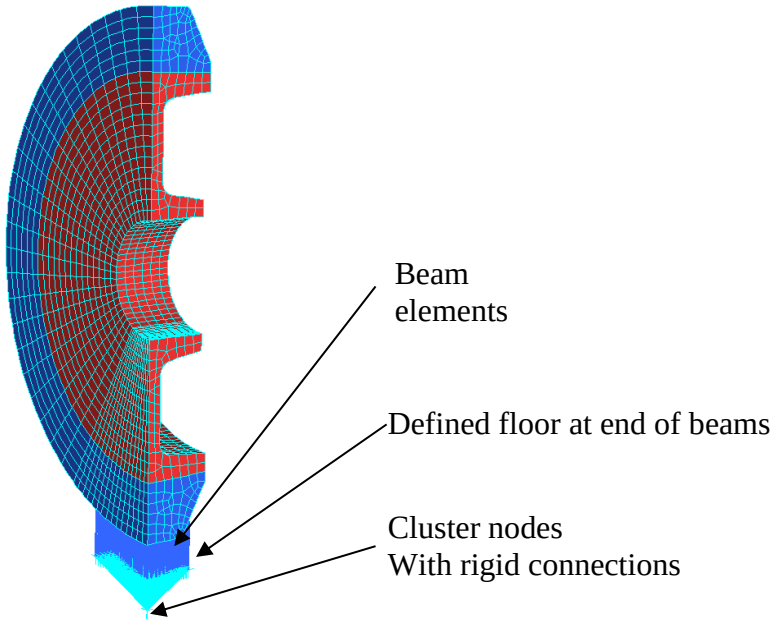

Figure 5.7 : FEA model with loading conditions

5.1.3. Material Models

Lots of material models are available in FEA to various types of materials and behaviors. For plastic materials, separate material model was defined and for rubber material separate material model was defined in the FEA software. All the elements belong to plastic category was assigned with plastic material model and all the elements belong to rubber material was assigned with rubber material model.

Material models related to plastic and rubber in FEA can be divided in to four main categories namely elastic, elastic-plastic, hyperelastic and viscoelastic. Apart from this, various other material models also available to define different types of materials. for example, sand or water behavior modeling in FEA is done in their own material models. Elastic-Plastic material model is an extension of Elastic model to plastic region.

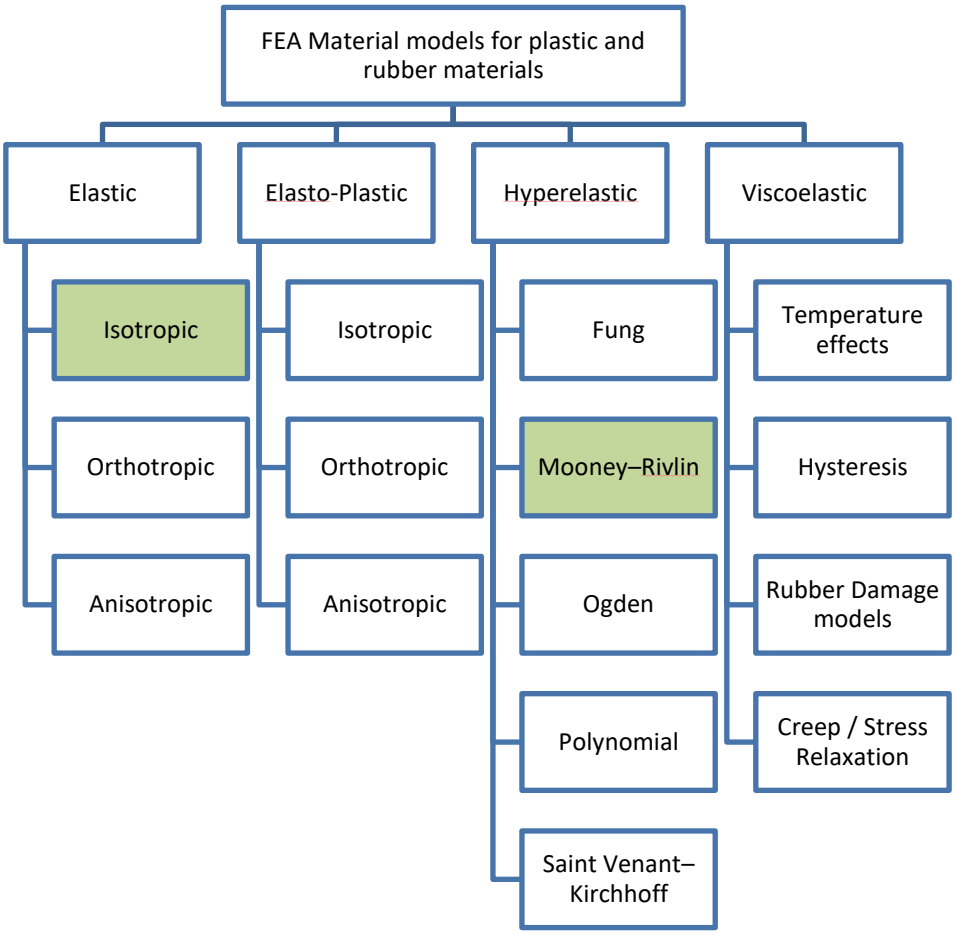

Figure 5.8 : Material models used in FEA

Plastic material model was selected as Elastic-Plastic Isotropic material model according to plastic material behavior. Generally, plastics are defined as isotropic material which means physical property has the same behavior when measured in different directions. Initial linear elastic region and after yielding plastic deformation region was observed in tensile graphs of both polypropylene and nylon which qualify them for Elastic-Plastic behavior. Both polypropylene and nylon materials were defined as Isotropic Elastic-Plastic material model. For 160 mm wheel simulation, previously loaded tensile graph of nylon was assigned to defined material models inside the software along with relevant elements.

Selection of appropriate material model for rubber material was done considering literature data provided in previous research works done. Both hyperelastic and viscoelastic material can be used in modelling rubber material.

Viscoelastic material models are advanced material models which can simulate time, temperature dependency of rubber material. Those models incorporate Hysteresis effects, rubber damage, creep and stress relaxation effects of rubber material. Complex material property analysis relevant to each and every application, need to done to define those material models in FEA and get accurate results. Very high computation power also required to solve these material models.

Hyperelastic material models are relatively simple material models for rubber material. These models are time independent models which means separate methods need to follow if those types of simulations are needed with hyperelastic models. Material models can be defied with simple tensile test and require less computational power to solve and get accurate results.

Generalized Mooney-Rivlin material model under hyperelastic category was selected to model rubber material in castor wheel simulation based on successful literature [7] [9]. This material model was recommended by Strand7 software supplier also for filled rubber product simulation. Mooney-Rivlin constants which are needed to define the material model, were calculated from the provided tool in Strand7 software directly from loaded rubber tensile graph.

5.1.4. Solver Setup

Developed castor wheel was used with nonlinear static solver. Nonlinear solver was used because of nonlinear behavior of rubber material, high strain levels in rubber and contact element definitions in the FEA model which violates linear solver limitations. For the static loading case, Nonlinear Static solver was selected.

Solver parameters can be defined to break the full analysis to small fractions. When defined, solver solves each fraction of the analysis at a time to evaluated and capture the nonlinear behavior of the simulation model. In the study fractions were defined as floor compression movement in to the wheel. Defined floor was compressed in to the castor wheel by 5mm through solver in 50 steps. 5mm was divided to equal 50 fractions of 0.1mm and solver pushed the floor up by 0.1mm in each step. Since rubber wheel was fixed from center, when floor was pushed in to the rubber generated a reaction force on floor which is equivalent to wheel load at given solver step. Iterative solving was done for each step until forces and resultant displacements in FEA model gets to equilibrium and stabilized. Then again solver goes to next step. In each step, all the calculations for stress build up, reaction force, node shape change were done and recorded in results file as 50 steps.

5.1.5. Simulation Results

Reaction force on the cluster node in each step was extracted from results file to find the step which 450 kg load was applied to the castor wheel. Since ¼ of the model was used in the simulation reaction equivalent to ¼ of 450 kg would give the relevant step.

Case study load on wheel = 450 kg

Equivalent Force = 450x9.81

= 4414.5 N

Because ¼ of the model is used in FEA simulation,

Relevant FEA model reaction = 4414.5 / 4

= 1,104 N

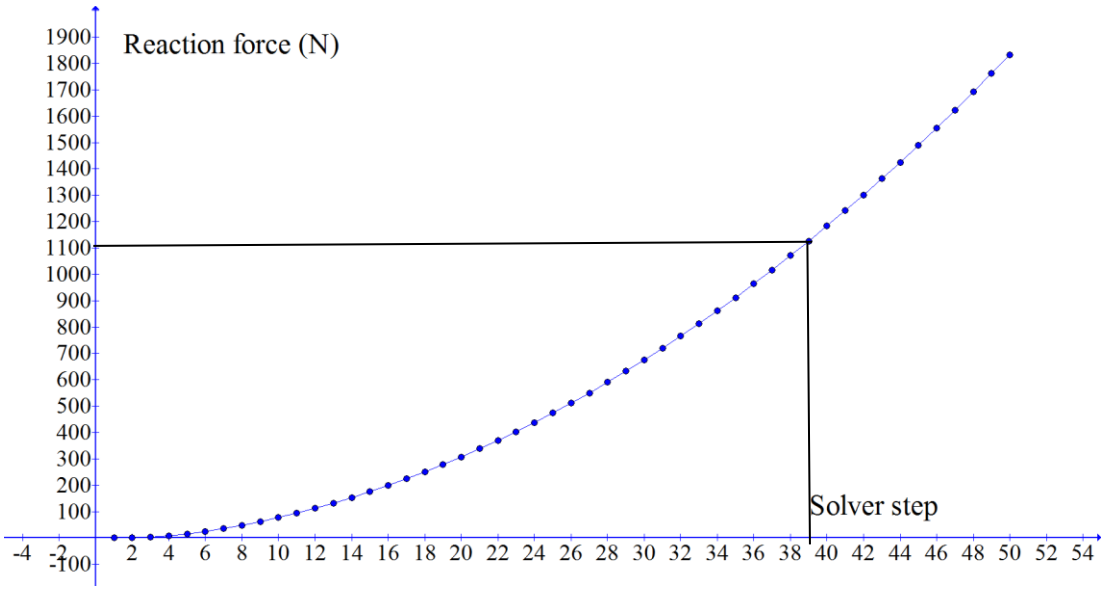

Figure 5.9 : Reaction force vs Solver step graph of 160 mm wheel

It was observed that solver step relevant to 450 kg wheel load is 39th step from the given graph. At the given 39th step stress inside the wheel was analyzed. To define the stress inside the rubber and plastic material von Mises definition was used. This given stress can be directly compared with plastic yield stress for yielding or safety factors using von Mises yield criterion [29]. Reaction force vs wheel compression graph was observed to get the wheel compression which was 3.9 mm at given wheel load of 450 kg.

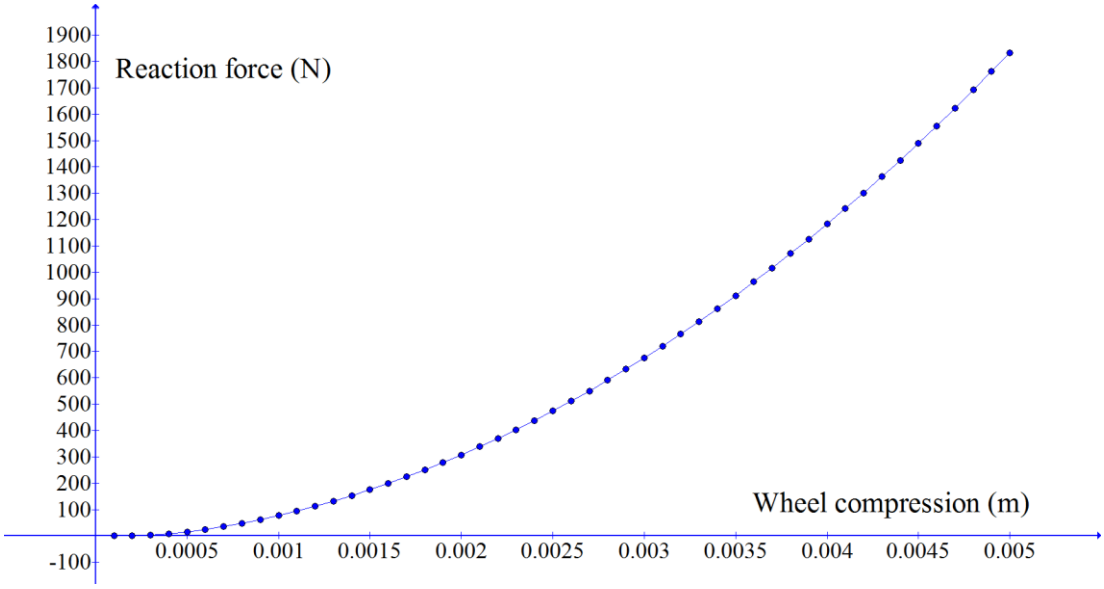

Figure 5.10 : Reaction force vs Wheel compression of 160 mm wheel

Stress distribution of the wheel was observed at load 450 kg and found close relation for the wheel failures at dynamic test. Highest von Mises stress was recorded in plastic center in the area were wheel fails at dynamic load.

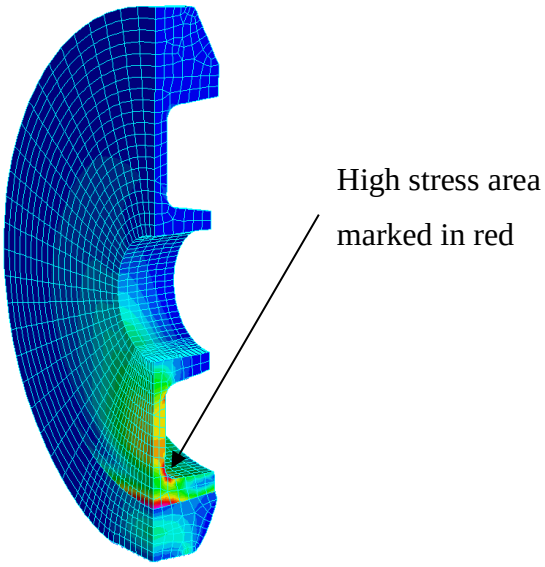

Figure 5.11 : von Mises stress distribution of 160 mm wheel

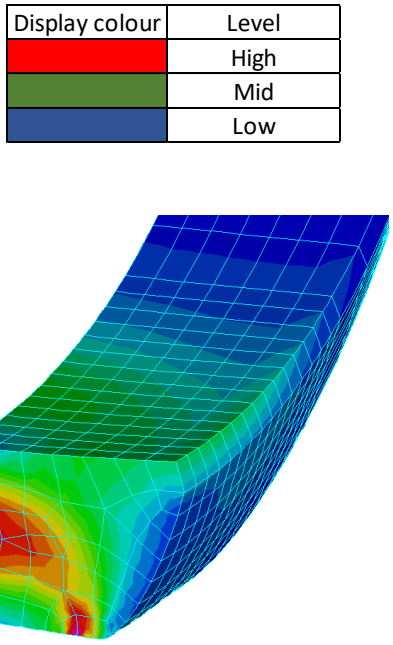

Figure 5.12 : Stress in rubber 160 mm wheel (Original in colour)

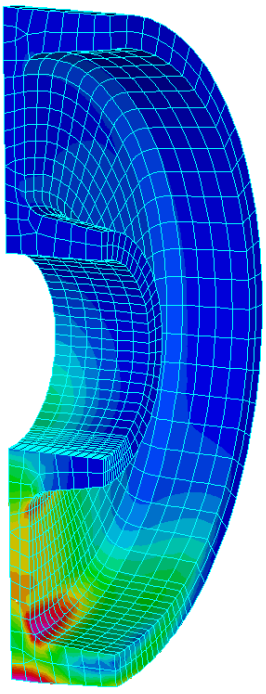

Figure 5.13 : Stress in Plastic 160 mm wheel (Original in colour)

Stress developed in castor wheel for 450 kg static loading given in table.

Table 5.2 : 160 mm wheel, 450 kg static load safety factor

	MPa	MPa	MPa	MPa		
load	Stress in nylon centre	Stress in NR-1 rubber	Nylon yield stress	NR-1 max stress	Safety factor for nylon centre	Safety factor for rubber wheel
450 kg	20.6	6.9	68.4	15.0	3.3	2.2

3.3 safety factor was observed for the Nylon center of the 160 mm wheel for 450 kg load. 2.2 safety factor was observed from the rubber wheel for 450 kg load in static loading condition.

5.2. Total Energy Rate Calculation

Total energy rate inside the rubber when castor wheel was rotated under load was calculated for 160 mm wheel 450 kg dynamic test simulation. This was done by combining static load simulation results and DMA test results.

Initially total energy given to the wheel when wheel was statically loaded to 450kg was calculated. Wheel reaction load vs Wheel compression graph given in Figure 5.10 was extracted from the static FEA simulation data and used to calculate total energy input to the system. 3.9mm compression was observed from the graph when wheel was loaded with 450 kg. Area under graph was calculated from x=0 to x=3.9mm to get total energy input to the system to load wheel up to 450 kg load. To calculate the area under the curve Riemann sum method with right boundary rectangle approximation was used. Graph was divided in to small rectangles with 0.1mm “x” width and height of “y” value where right boundary of rectangle touching the graph [30].

Then area of all these rectangles was sum to get area under the curve. Figure 5.10 Graph shows reaction force from developed ¼ model, so given force was multiplied by 4 in each step to get actual force to load full castor wheel.

From appendix 2:

$$\text{Total energy input to static loading at 450kg load} = 6.3\ \text{J} \quad (4)$$

Then static energy was converted to energy input to the system in one second when wheel was rotated under 450 kg load at 4 km/h speed, which is called as total energy rate

$$\text{Total Energy rate} = 6.3 \times \text{Number of wheel rotations in one second} \times \text{correction factor} \quad (5)$$

Number of wheel rotations in one second calculation,

Wheel rotation speed	= 4 km/h
Wheel rotation speed	= 1111.1 mm/s
Wheel diameter	= 160 mm
Wheel perimeter	= 160 x Pi
	= 502.65 mm
Number of wheel rotations per second	= 1,111.1 / 502.6
	= 2.2

Correction factor calculation,

Correction factor was introduced in this calculation to convert static loading energy to steady state rolling energy. Initially correction factor was set to 1 and modeling was continued till castor wheel temperature prediction model. Then rubber inner temperature was compared in prediction model and actual. In actual heat inside the rubber at Steady state was recorded as 131^{o}C. then with trial and error method correct factor was selected. This factor was used as fixed factor for other validation models.

Table 5.3 : Correction factor calculation

Correction factor	Actual temperature ^{o}C	Predicted temperature ^{o}C
1	131	90
2	131	110
3	131	120
3.1	131	126
3.2	131	130
3.25	131	131

Selected correction factor = 3.25

Total energy rate for 450 kg loaded rotating wheel in one second, From equation (5)

Total Energy rate = 6.3 x 2.2 x 3.25 J/s

= 45.25 J/s

Total energy rate is the energy absorbed by castor wheel in one second when wheel is rotated under 450 kg load. Due to viscoelastic behavior of the rubber part of this energy is converted in to heat energy. This loss energy was calculated by combining DMA test data with total energy rate.

In Figure 4.12 graph shows rubber materials energy loss fraction against temperature in cyclic loading. Hence to get energy converted to heat energy by rubber wheel in one second heat generation rate was defined,

$$\text{Heat generation rate} = \text{Total energy rate x Energy loss fraction} \quad (6)$$

Heat generation rate inside the rubber was calculated from equation 6. It was assumed that total energy given to the system is totally absorbed by rubber and energy absorbed by plastic is negligible.

5.3. Temperature Prediction

A FEA model to predict castor wheel developed temperature profile after a given time of dynamic test was developed. 2D axisymmetric FEA model was used to this temperature profile prediction model. Computational cost of model is reduce because of the use of this axisymmetric model.

In this model wheel was modeled as 2D profile and input was given to software to consider as axisymmetric along a selected wheel center line axis, which means software assumes the model as revolved profile. 8 node 2D plate elements were used with 5% selected element size to mesh the model. 2D simulations are very effective simulation which takes very less time to solve and give accurate results.

5.3.1. 2D Model and Mesh Creation

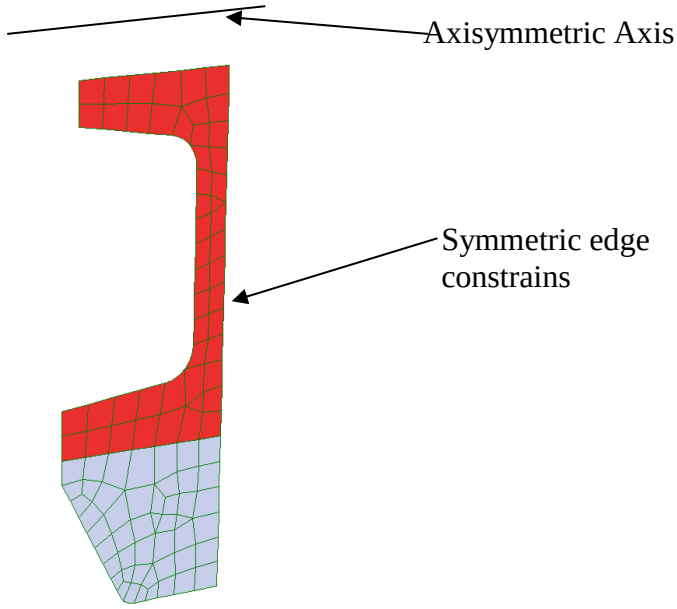

Figure 5.14 : 2D axisymmetric model

2D profile of castor wheel was imported to the software then meshing was done according to 5% mesh sizes to elements sizes to be identical with 3D mesh. Then axisymmetric boundary conditions and symmetric boundary conditions were applied to the developed mesh.

5.3.2. Heat Generation Rate

Previously calculated total energy rate was used as heat source inside the rubber wheel for the thermal simulation. To distribute the total energy rate among 2D model rubber elements, stored energy of rubber element in the 3D static 450 kg loading case was used.

According to the stored energy in static loading case surface elements, total energy rate was distributed among initial 75% of the elements. Each element storage energy was calculated ad divided by total energy to get relevant distribution factor. Distributed total energy rate was applied as heat sources at each rubber element. Calculation is given in Appendix three.

Table 5.4 : Total energy rate distribution

	j/s
Element ID	**Total energy rate**
136	4.27
121	4.13
586	2.98
676	2.91
106	2.68
151	2.60
391	2.43
601	2.24
376	2.02
406	1.89
616	1.85
46	1.85
421	1.68
706	1.67
451	1.62
571	1.61
61	1.52
646	1.40
556	1.36
241	1.28
31	1.24

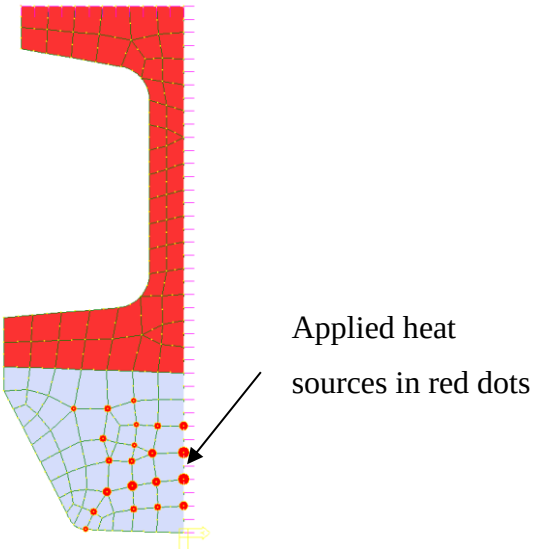

Figure 5.15 : 2D profile with heat sources applied to relevant elements

From total energy rate, heat generation rate should be calculated as,

$$\text{Heat generation rate} = \text{Total energy rate x Energy loss fraction} \qquad (7)$$

Energy loss fraction graph according to the Figure 4.12 was loaded in to the software and instructions were loaded to software to calculate the heat generation rate accordingly in each calculation according to part temperature. Energy loss fraction was calculated from rubber material DMA tests according to proven literature. This graph can be varied according to temperature also according to the details fed in to software.

Heat generation rate was controlled according to time also since castor wheel dynamic test was carried out as 3-minute run and 1 minute stop. At one minute stop time, heat generation rate should be zero inside the rubber.

To achieve this another table was defined in the FEA software and wheel run cycle was loaded as given in Figure 5.16. Calculated heat generation rate was multiplied by 1, in first 3 minutes and in next minute it was multiplied by 0. This cycle was continued until 300 minutes which is more than maximum wheel run time.

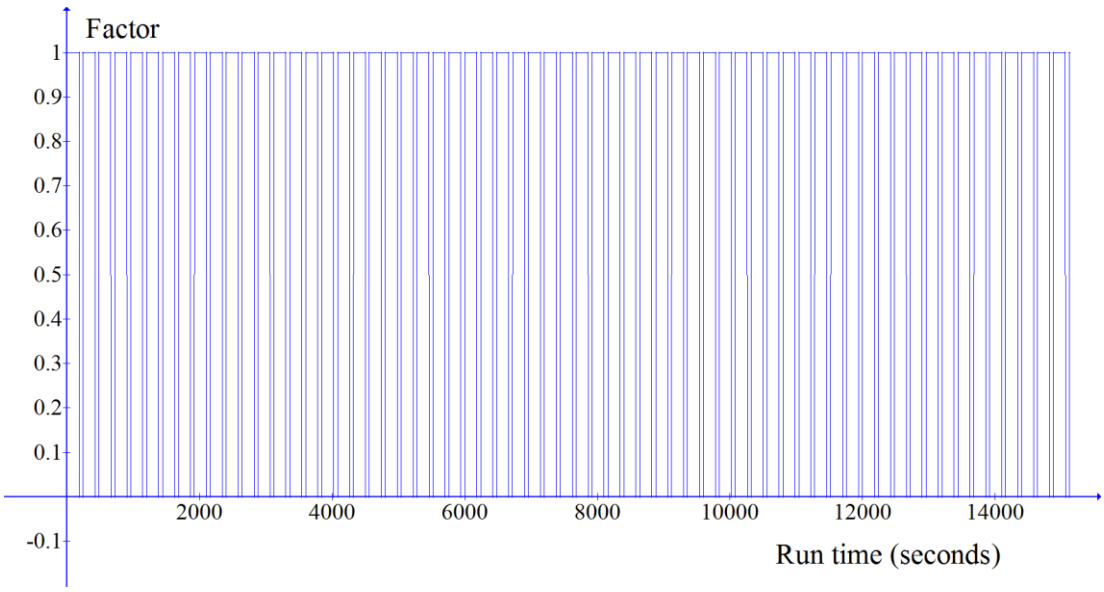

Figure 5.16 : Castor wheel run cycle graph

5.3.3. Thermal boundary conditions

Thermal boundary conditions for the castor wheel model which includes heat capacity, heat conductivity of materials, convection heat loss from surface was loaded to the software next. These data were needed to define the proper simulation model. It was assumed that these data do not change with time or temperature during the course of simulation.

Data was extracted from literature data where FEA thermal simulations were done with success [9] [18]. Mass density of rubber and plastic was measured by in-house specific gravity tester and calculated accordingly. Each material data was assigned to relevant rubber and plastic elements through the software. Surface heat convection coefficient and initial temperatures of the model was also allocated to relevant elements and element surfaces.

Table 5.5 : Material properties for thermal simulation

Material	Mass Density	Specific Heat capacity	Heat conductivity	Forced Convection-Air	Rubber to floor
	kg/mm3	W/kg/k	W/mm/c	$W/mm^2/c^\circ$	$W/mm^2/c^\circ$
PP	$9.1x10^{-7}$	1800	$1.8x10^{-4}$	$6\ x10^{-6}$	
Nylon	$1.25x10^{-6}$	1700	$2.6\ x10^{-4}$	$6\ x10^{-6}$	
NR-1	1.210^{-6}	1700	$2.39\ x10^{-4}$	$6\ x10^{-6}$	$1\ x10^{-4}$
NR-2	$1.2x10^{-6}$	1700	$2.39\ x10^{-4}$	$6\ x10^{-6}$	$1\ x10^{-4}$

5.3.4. Solver setup

Transient heat solver was used to simulate the developed model with 1 second intervals until 10,000 seconds which equals to dynamic test time of 160 mm wheel under 450 kg load. Each second solver solves the equations and record temperatures and other property data.

Then according to the developed temperatures next solving was done. This simulation was a very accurate and efficient simulation because the use of 2D simulation.

5.3.5. Simulation results

Temperature development inside the castor wheel in previously defined temperature measuring points was analyzed from the model. In each measuring point how temperature increases with the time was plotted in graph through the software.

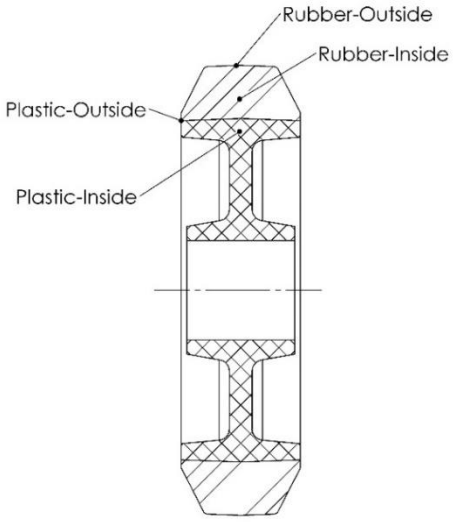

Figure 5.17: Temperature extracted points from 2D simulation

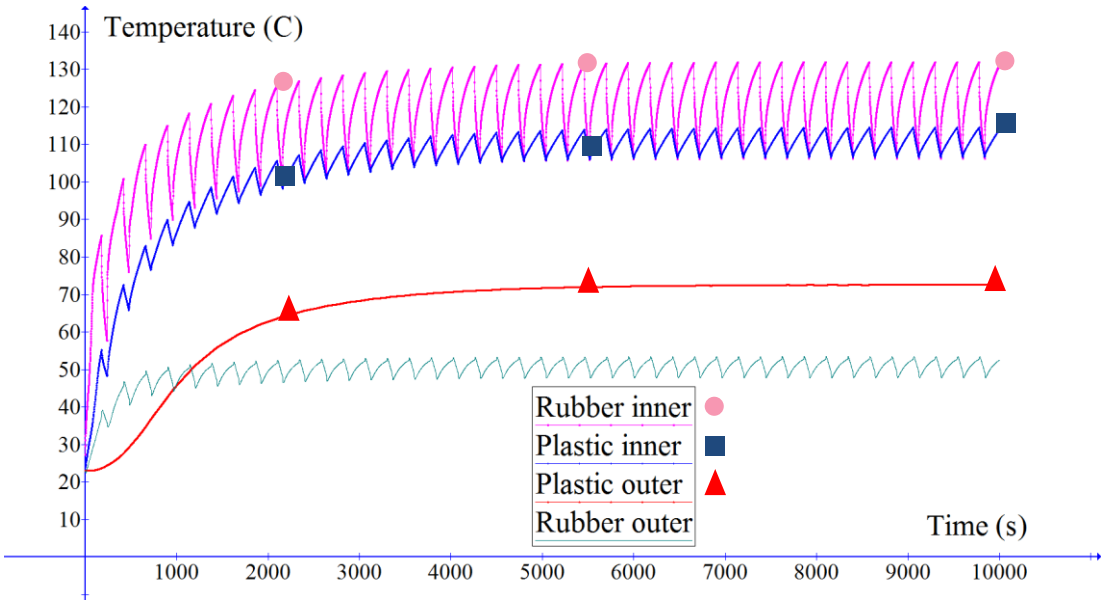

Figure 5.18 : 160 mm 450 kg FEA simulation temperature prediction

It was observed from the graph that temperature raise and drops cyclic manner relative to wheel run and stop time. But this behavior was not prominent in plastic outer location. Max temperature recorded was observed and rubber inner temperature was the highest recorded in the simulation which went up to 131^{o}C. Then plastic outer

recorded a temperature at 115°C before plastic inner temperature of 76°C. Lowest temperature of 53°C was recorded at rubber outer where higher convection rate was defined because rubber touches the floor.

Also from the graph we could see that temperature development in the castor comes to a steady state level roughly after about 3,200 seconds when run stop behavior was neglected. For the simulation results steady state was defined as when temperature difference is less than 0.5°C in adjust temperature points just after wheel enter stop cycle. This temperature distribution after 3,200 seconds, maximum temperature recorded given in Figure 5.19. It was observed that in actual dynamic test also wheel attain this steady state level. Then after some time temperature starts to go up again because of abnormal bouncing of the wheel which generate higher amount of heat than normal rotation.

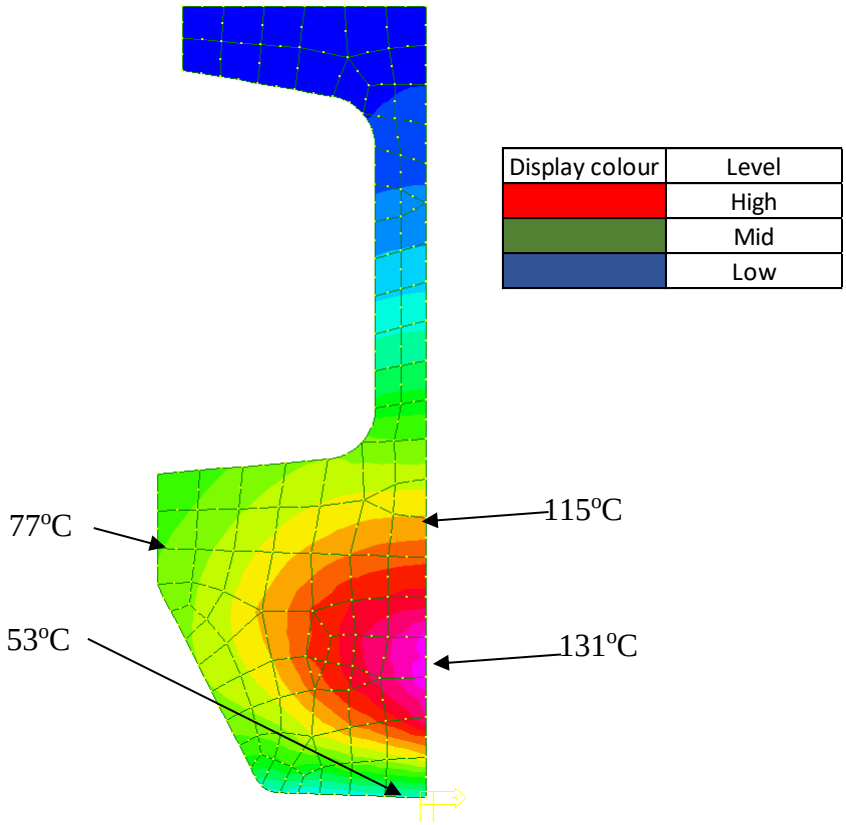

Figure 5.19 : Steady state max temperature profile, 160 mm 450 kg

Temperature profile of maximum temperature attained by the simulation was analyzed. Profile exhibits the same values as measured temperatures from the actual dynamic test. There was no clear region between plastic and rubber boundaries because of close thermal material properties of rubber and plastic.

Also, it was observed that center area of the wheel which connects to bearing, was heated to very low temperature because of effective length from heat generation area and surface convection of developed heat, heat transferred to that area was low.

Temperature graphs obtained from the prediction was compared with actual results. From equation 5 correction factor was calculated based on rubber inner temperature only, so other temperature components were compared with predicted temperature values to observe validity of the calculated correction factor.

In actual for 17,000 s wheel continued dynamic test, but from Figure 5.18 graphs it was observed that steady state level was achieved after about 3,200 s.

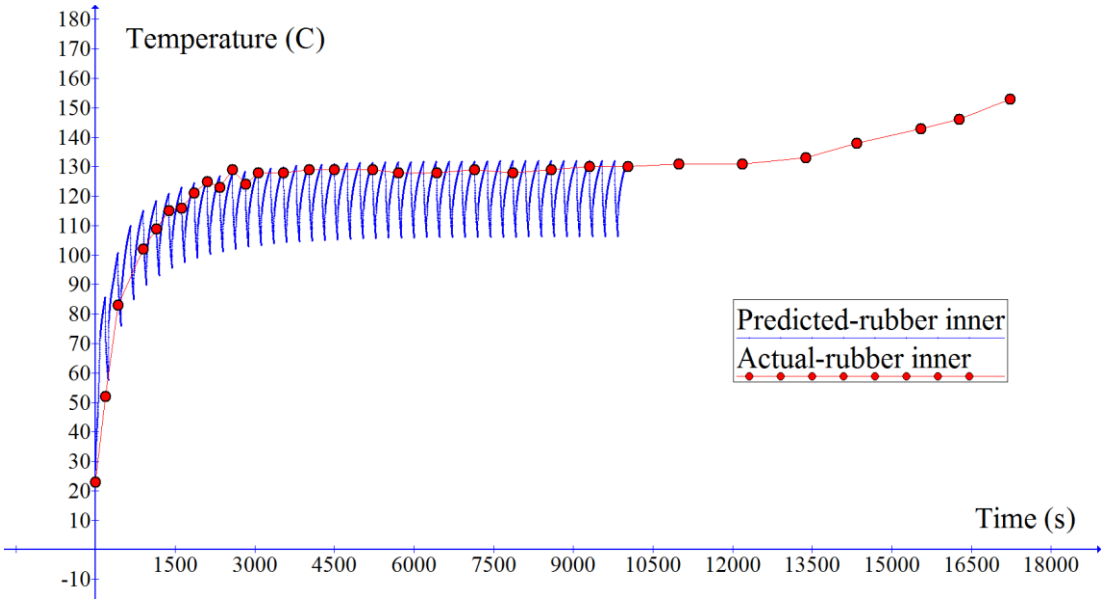

Figure 5.20 : Rubber inner temperature comparison, 160 mm 450 kg

Steady state rubber inner temperature was selected to tune the FEA temperature prediction model which was the reason for very close matching of the comparison. Tuning was done only for first case study. This was used as fixed number for the rest of simulations.

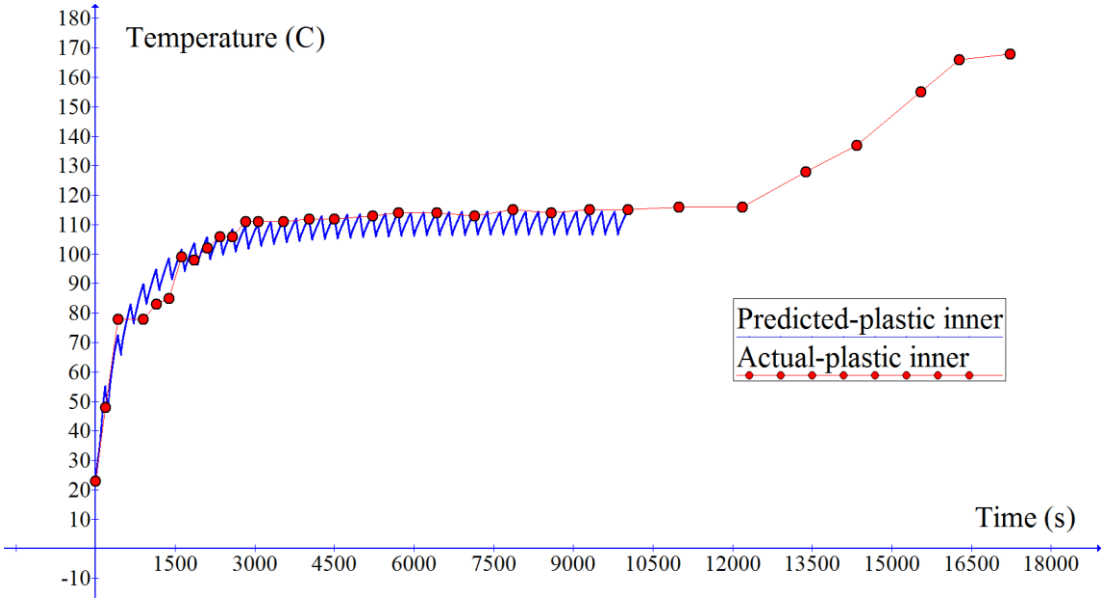

Figure 5.21 : Plastic inner temperature comparison, 160 mm 450 kg

It was observed that steady state temperatures of actual and predicted plastic inner Figures also very close to each other. But in actual after 13,500 s it was observed that center temperature was increased further. In most of test results this temperature raise was observed when wheel was close to failure, abnormal bouncing of the wheel close to failure was the reason for this which was not captured in this simulation model.

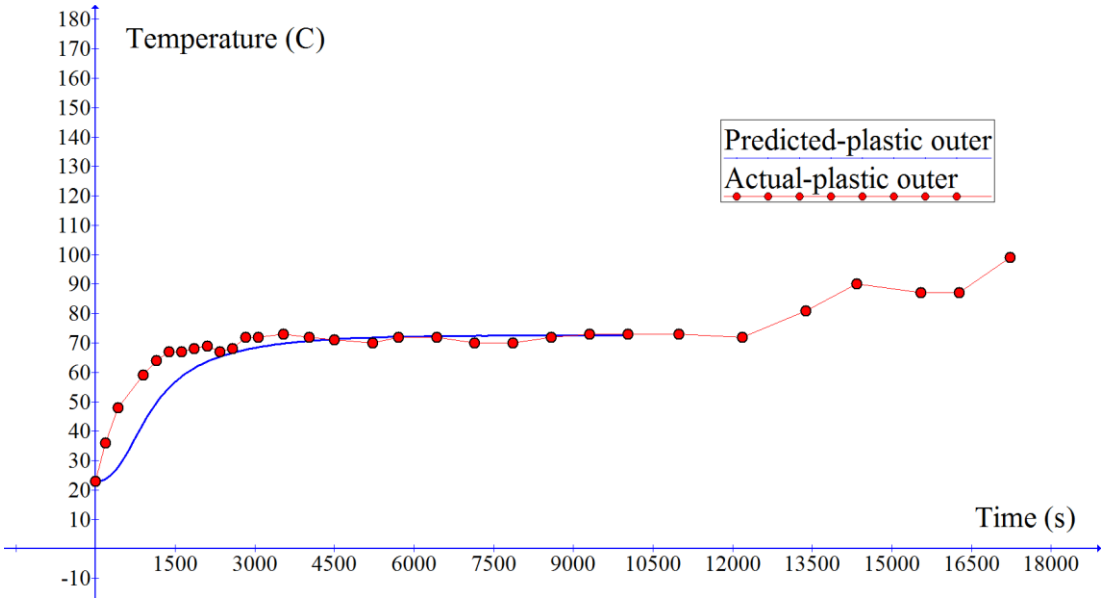

Figure 5.22 : Plastic outer temperature comparison, 160 mm 450 kg

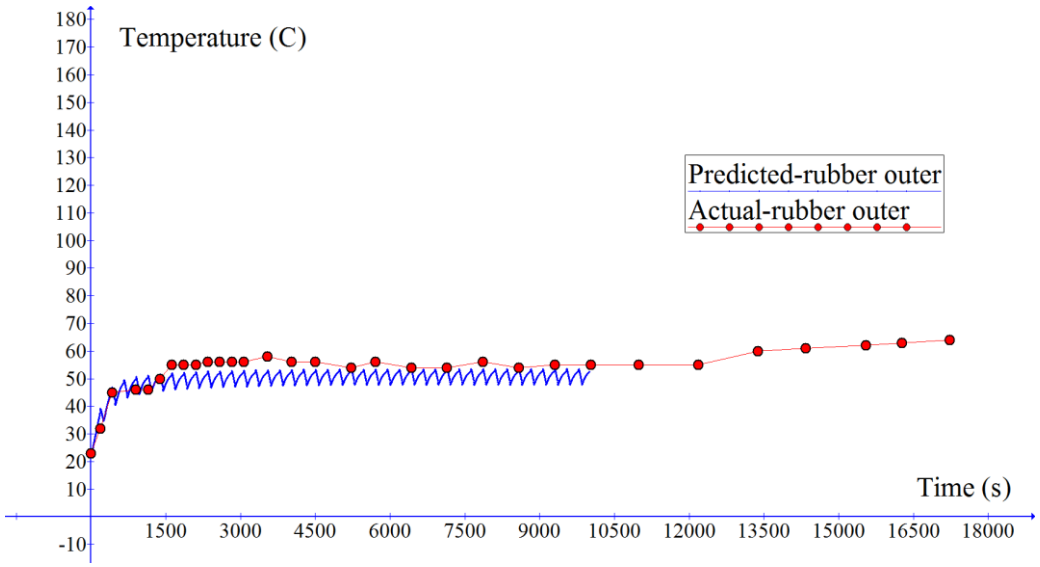

Figure 5.23 : Rubber outer temperature comparison, 160 mm 450 kg

Both plastic outer and rubber outer temperatures also found to be closely prediction actual steady state temperatures. For temperature comparison observations 3.25 correction factor calculated in equation 5 was validated.

5.4. Failure Analysis

Failure was observed from the center part of the wheel in actual dynamic simulation. So, the failure analysis was focused on detecting center part failures through FEA simulation when wheel was heated by hysteresis energy loss from the rubber. Temperature, applied load and material property changes with temperature mainly contributes for center plastic failure. When wheels are rotated under load they achieve steady state temperature level and then after some time temperature starts to raise again close to wheel failure due to yielding and bouncing of wheel. This final failure mechanical involves very complex physical behavior which was very complex to solve in general FEA application. It was observed that wheels at lighter loads continued on dynamic test longer than wheels at higher loads which failed sooner in dynamic test. Failure analysis was done to identify wheel failures at steady state level, if wheel was identified as failed at steady stated level it would fail in dynamic test sooner, if wheel was identified as not failed at steady state level, it would continue longer time at steady state level on dynamic test before actual failure.

A 2D axisymmetric model was developed to analyze those effects and identify failures at steady state level. Use of 2D analysis was effective at this stage as temperature prediction was also done as 2D axisymmetric simulation. 2D model solver treats loads are applied all around the wheel, unlike 3D static load simulation. It was required to calculate the equivalent load on 2D static model to stress the center part to same level as 3D static model at 450kg load.

5.4.1. Equivalent Load Calculation

Same 2D profile as Figure 5.14 was used for this simulation. Meshing of the model was done according to 5% of maximum model dimension which gives same mesh as thermal simulation. Material properties and boundary conditions were loaded as 3D static loading case for this axisymmetric 2D model. Beam elements were modeled as point contact elements and floor was defined at the end. For the beam contact parameters, same parameters were used as 3D static loading model. Nonlinear static solver was used to push the floor in to the rubber by 5mm generating reaction force on cluster node. Initially maximum stress developed in the center was analyzed and solver increment was identified which gives same stress in center as 3D static simulation result. For the solver step, reaction force was recorded which gives same stress. It was assumed that in those both cases, 3D static simulation with 450 kg load, 2D axisymmetric simulation with recorded reaction force, Loads and stress acting in the center part of the wheel was same. So, comparison can be done and predictions can be done about 3D behavior of the wheel under 45 0kg load, from developed 2D model under recorded reaction force.

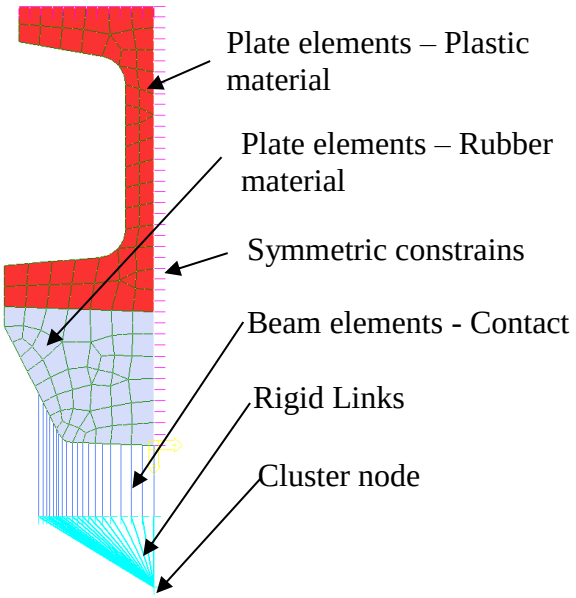

Figure 5.24 : 160 mm castor wheel 2D profile

In the 3D static load simulation, it was observed that center was stressed up to 20.3 MPa at 450kg load as given in table 6. In the 2D simulation same stress level of 20.3 MPa was developed in the center part at 28th solver increment. This increment was selected by analyzing Stress profiles and Stress levels of each increment given by the software.

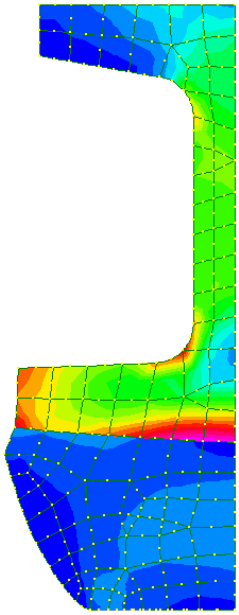

Figure 5.25 : 160 mm wheel 2D profile stress distortion

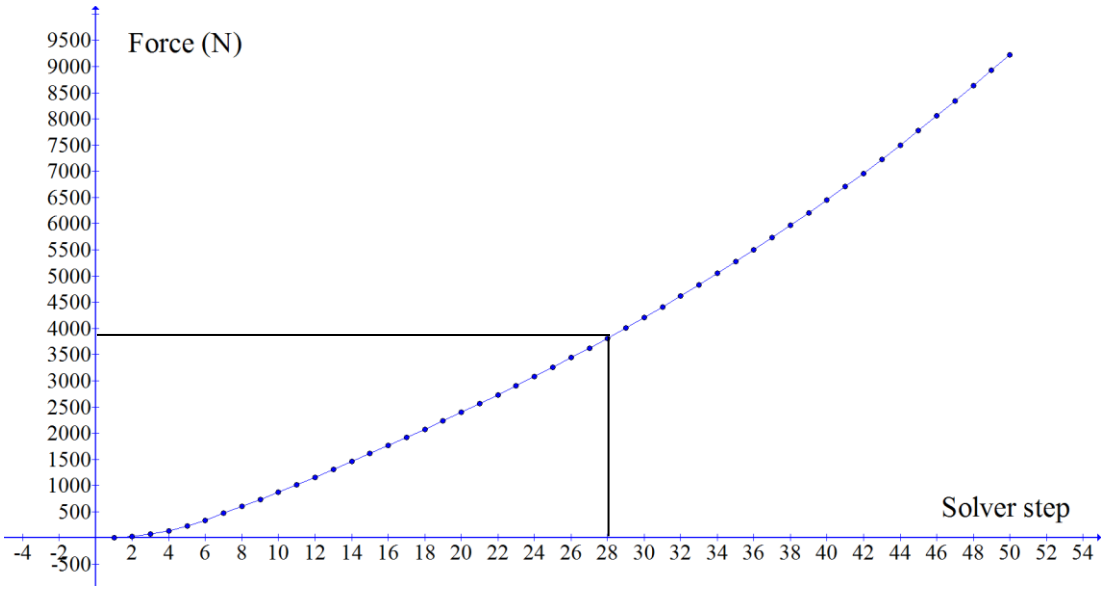

Figure 5.26 : Reaction force on cluster node vs Solver increment

From the Figure 5.26 reaction force at increment 28 was observed as 3,814 N. for the 160 mm wheel 450 kg loading case we can define equivalent load as,

2D 450 kg static loading Equivalent load = **3814 N** on cluster for 2D simulation

From other way, when 2D model was loaded up to 3,814 N load to the cluster node, behavior inside the center would be equal to static 3D model 450 kg loading case behavior. Analyzing of the 2D profile was very fast and effective way to evaluate stress development in the wheel loading.

5.4.2. 2D simulation Model with Temperature Effects

After calculation of equivalent load, same 2D model was used to simulate the loading case with temperature effects. Material tensile graph which were loaded as fixed property graphs where changed to variable property graphs according to material temperature. Then again 2D static simulation was done to observed stress development. In the model solver increment, which was loaded to 3,814 N at cluster node was analyzed to obtain relevant stress levels.

Tensile properties of plastic were tested in elevated temperatures to obtain modulus and yield Stress in relevant temperature and analyze effect of temperature to material properties. These results were compared with material data sheets, literature data and validated for the final results [31]. Those results were summarized in to a table to be loaded in to the FEA software directly. Table 10 & 11 summarized the results obtained from testing and literature.

Table 5.6 : Nylon Tensile data variation with temperature

Temperature (°C)	Modulus(MPa)	Yield (MPa)
23	821.2	68.4
140	614.0	19.9

For nylon material, tensile test 23°C gave 82.21 MPa modulus and 68.4 MPa yield stress. It was observed that at 140°C these values were reduced to 614 MPa and 19.9 MPa respectively. Since these values indicated the strength of the material it was observed that strength of the material reduced with increased temperature. Between

those temperature values 23°c and 140°c it was assumed that material property changes were linear.

Table 5.7 : Polypropylene Tensile data variation with temperature

Temperature (°C)	Modulus(MPa)	Yield (MPa)
23	194.5	24.6
120	152.0	9.2

194.5 MPa modulus and 24.6 MPa yield stress was observed for polypropylene tensile results at 23°C. those parameters were reduced to 152 MPa and 9.2 MPa respectively at 120°C elevated temperature tensile testing.

Recorded nylon material properties were loaded in to the FEA software for loading simulation with temperature.

Steady state region maximum temperature profile of 2D temperature simulation of 160 mm wheel at 450 kg load was directly imported as fixed temperatures at nodes. Since both models have same elements and mesh, it was possible and easy to import temperatures from previous simulations. These temperatures we imported as separate loading case for the 2D model then from the solver temperatures were applied before loading of the model.

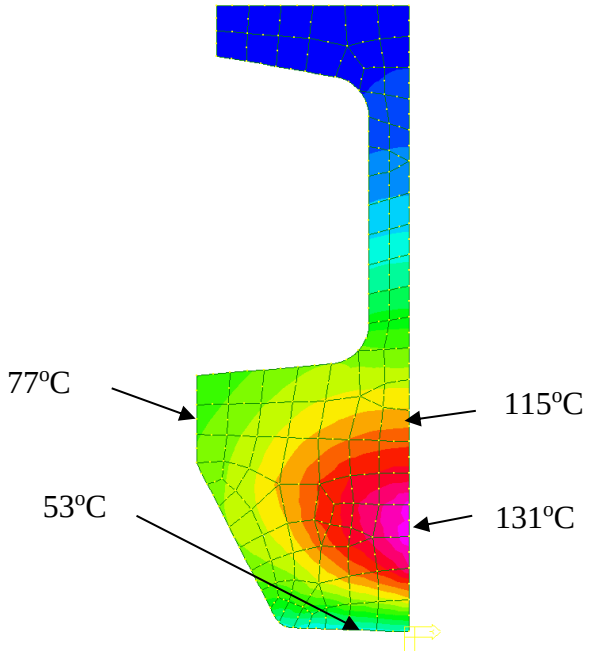

Figure 5.27 : Applied temperature profile, 160 mm wheel, 450 kg loading

5.4.3. Simulation results

Nonlinear static solver was used with temperature effects enabled to simulate the given models and obtain results. Initially given temperatures were loaded to the nods before applying the loads. Then floor was pushed in to the rubber wheel by 5mm to generate reaction load on cluster note where wheel loading was calculated. From the results reaction load on cluster node vs Solver step graph was obtained and analyzed. Solver step which applies 3,814 N load on cluster node was identified from the graph. 3,814 N was the calculated equivalent load for 160 mm wheel 450 kg loading case, so at this identified solver step stress development inside the center would give an idea about 3D loading condition. At this step stress inside the center was analyzed to study yielding of the center part to detect failures.

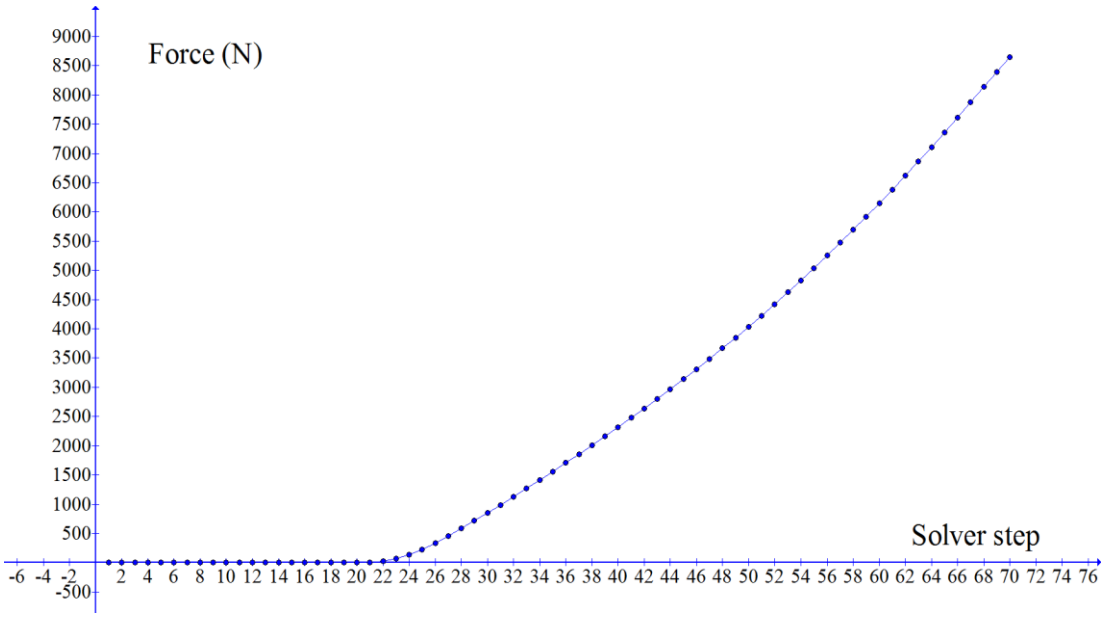

Figure 5.28 : Reaction force vs Solver step for temperature effect simulation

Initial 20 steps in the solver was used to apply the temperature gradually from 23^0c to defined temperature profile. Hence reaction force on cluster node was 0 on these steps. Floor was pushed in to the rubber and load was applied from 21^{st} to 70^{th} solver steps where reaction force on cluster node was developed. It was observed that 3,814

N was developed in cluster node at 49th increment of the solver. Stress developed inside the center was observed in selected 49th increment.

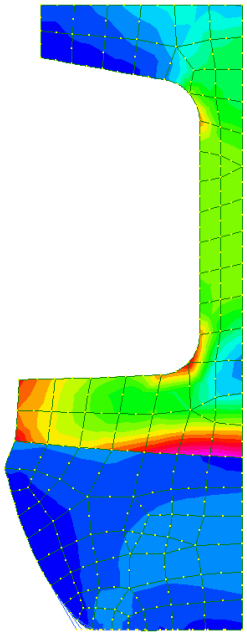

Figure 5.29 : 160 mm castor 450 kg stress profile

Table 5.8 : 160 mm 450 kg wheel safety factor

	MPa	MPa	
Equivalent load	Stress in nylon centre	Nylon yield stress at 118°C	Safety factor for nylon centre
450 kg	20.5	29.0	1.41

Maximum of 20.5 MPa von Mises stress was observed inside the center part of the wheel. According to von Mises criteria this stress can be compared with yield stress of the material to find failure locations of the wheel. It was defined that if Developed stress exceeds Yield stress of the material it would yield and cause possible failures. Since this analysis was done in elevated temperature stress at give point should be compared with material properties of the given point temperature.

Highest temperature of 118°C inside the center was recorded in the same place where highest stress was recorded according to Figure 5.29. Since same place recorded

highest stress and highest temperature same location was the lowest safety factor location. safety factor was compared between given location yield stress according to temperature and observed 20.5 MPa von Mises stress.

1.41 Safety factor was observed in steady state level of the castor wheel which suggest wheel would run on dynamic test for a longer time. Form physical test data also it was observed that wheel ran total of 17,220 seconds until it fails (Appendix 1). Actual standard requirement was to run wheel up to 9048 seconds which suggest wheel passed the test in physical test. From safety factor analysis also, castor wheel was marked as pass as it achieved more than 1 safety factor at steady state level.

Steady state was achieved by the castor wheel after 3,200 seconds, so between 3,200 seconds and 17,220 seconds wheel was running with 1.41 safety factor. While running of the wheel this safety factor might be lowered gradually due to complex material behavior under dynamic load to fail the wheel at 17,220 seconds.

5.5. Generalized model

From case study data and material tests used, Generalized FEA model was developed to simulate castor wheel designs to evaluate castor wheel dynamic test performance. Steps done in the given study was summarized and developed to be followed when new design evaluations are to be done. Given steps describes the generalized model steps one by one,

- 2D profile of the castor wheel new design should be developed and should be simplified considering symmetry.
    - 2D profile should be ½ of axisymmetric model if symmetrical

Figure 5.30 : Example models for 2D profile

- Developed models should exported as IEGS, STEP format to import in to FEA software
- Materials used for the center part and rubber should be selected
- Raw material testing to be carried out to test center material and collect material parameters or get data from Appendix 4 / Material data sheets
    - Uni-axial tensile test 23^{o}c
    - Uni-axial tensile test in elevated temperature 120^{o}C,140^{o}C
    - Poison ratio
    - Material density
    - Heat conductivity

    - Specific heat capacity
    - Surface convection coefficient to air
- Raw material testing to be carried out to test rubber/Outer ring material and collect material parameters or get data from Appendix 4 / Material data sheets
    - Uni-axial tensile test 23^{o}c
    - DMA test
    - Poison ratio
    - Material density
    - Heat conductivity
    - Specific heat capacity
    - Surface convection coefficient to air
- 2D IGES/STEP file should be imported to FEA software and meshed by 5% of the total model size 8 node plate elements. This model should be save as main mesh file.
- Copy of main mesh file should be renamed as 01-Static loading.
- 01-Static loading simulation
    - 2D meshed profile should be revolved from FEA software to from ¼ of 3D model. Revolve should be done as 2 degrees x15, 6 degrees x25

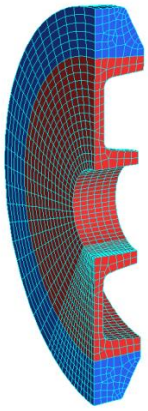

Figure 5.31 : 3D FEA model of castor wheel

    - 3D model elements should be 20 node hexahedrons
    - Tensile graph of the plastic material at 23^{o}c should be loaded in to FEA software as Stress-Strain graph

- Center part elements should be selected and assigned with Elasto-Plastic material model with loaded tensile graph
- Tensile graph of the rubber material should be loaded in to FEA software as Stress-Strain graph
- Outer ring part elements should be selected and assigned with rubber material model Mooney-Revlin.
- Tensile graph of rubber material should be assigned to Mooney-Revlin material model to calculate coefficients automatically
- Fixed constrains and symmetric surface constrains should be applied to relevant nodes in relevant planes
- Beam elements should be created from outer ring approximate contact area to form floor
- Bean element should be defined as point contact elements
- End of those beam elements should be connected to one node called cluster node which compresses the rubber wheel by 5 mm in simulation.

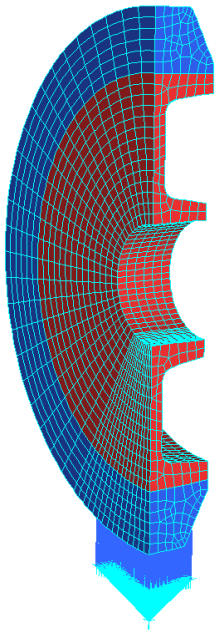

Figure 5.32 : 3D FEA model with beam and cluster node at bottom

- Nonlinear static solver should be used to solve the defined FEA model

- Reaction force on cluster node vs Solver step graph should be obtained and step should be identified which applies given load for the wheel considering symmetry
- At given step von mises stress inside the rubber and plastic can be compared with material yield stress to identify static safety-factor

- 02-Total energy rate calculation
  - From 01-static load simulation Reaction force vs rubber ring compression graph should be obtained
  - Integration to be used to calculated the area under the defined graph up to identified solver step in previous simulation for given load
  - Integration results give the energy spent to compress wheel under given load in static loading.
  - This can be assumed as energy absorbed to rubber ring
  - From this static energy calculation, should be done to obtain the energy absorbed by rubber ring to one rotation in dynamic loading.
  - Total Energy rate =
    Static energy x Number of wheel rotations in one second x correction factor
  - Number of wheel rotations per one second was calculated according to dynamic test speed and wheel diameter
  - Calculated correction factor = 3.25
  - Form equation total energy rate should be obtained to be used in temperature prediction FEA model
  - From rubber material DMA test data energy loss fraction vs temperature graph should be obtained
    - DMA test gives storage modulus and loss modulus of material and their variation according to temperature
    - $\text{Energy input modulus} = \sqrt{(\text{Storage modulus})^2 + (\text{Loss Modulus})^2}$
    - $\text{Energy loss fraction} = \frac{\text{Loss modulus}}{\text{Energy input modulus}}$
    - From given equations energy loss fraction can be calculated and graph according to temperature

- 03-Tempreature profile prediction model

- Copy of main mesh file to be renamed as 03-Tempreature prediction model
- Calculated total energy rate should be distributed to relevant rubber elements to represent their heat generation when dynamic test
- From 3D static simulation model relevant surface rubber elements were selected and from FEA software stored energy density in elements and element volumes should be extracted.
- Then from that data energy stored in elements should be calculated to static loading case.
- First 75% of the elements should be selected and among them which has maximum stored energy
- Calculated total energy rate should be distrusted according to calculated stored energy among those elements in 2D temperature simulation model as heat sources.

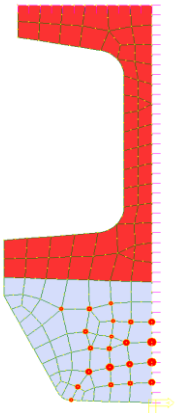

Figure 5.3350 : Temperature prediction 2D model with heat sources

- Energy loss fraction graph from DMA test should be loaded in to software and assigned total energy rate should be multiplied by loss energy fraction to obtain heat generation rate in a given temperature
- Material thermal properties tested or extracted from Appendix 4 should be loaded in to the software
- Convection coefficients should be assigned to relevant surface edges with initial temperature

- Transient heat solver should be used with time step of 1s up to 10,000s to analyze the temperature development inside the wheel

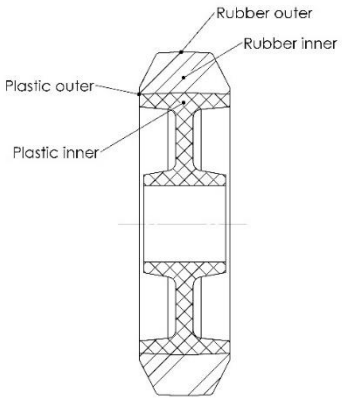

Figure 5.34 : Temperature analyze locations

- Nodes should be selected to represent rubber inner, rubber outer, plastic inner, plastic outer and temperature vs time graph should be obtained to observed temperature development.
- Time till wheel comes to steady state should be identified
- Temperature at steady stated should be identified

- 04-Wheel failure analysis
  - Copy of main mesh file should be renamed as 04-faliure analysis-1
  - As 3D static loading simulation material properties, contact elements, symmetric conditions should be applied to this 2D model.

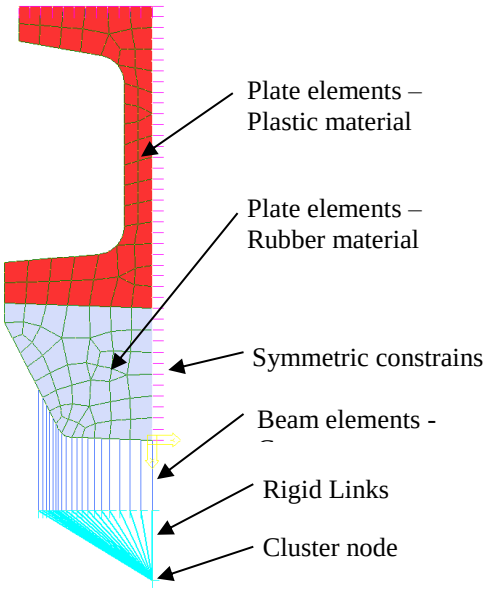

Figure 5.35 : 2D castor wheel FEA profile

- First equivalent force on cluster node to stress the center to the same stress level as 3D static simulation should be calculated
- Nonlinear static solver should be used to solved the model which compressed the floor 5mm in to the rubber wheel to apply the load same as 3D static simulating case
- von Mises stress of the center part should be analyzed and stress equivalent to 3D static simulation loading should be identified with particular solver step
- From reaction force vs Solver step graph, reaction force should be identified and recorded
- Copy of 04-faliure analysis-01 file should be renamed as 04-faliure analysis-02
- This analysis should be done considering temperature development and property changes due to temperature taking in to consideration
- Loaded plastic material properties were changed to temperature dependent plastic properties according to test data or Appendix 4 material data
- Node temperature for each node should be imported from 03-tempreature profile prediction model at steady state region maximum.
- After loading above data nonlinear static solver setting should be change to apply temperature load first for 0-20 solver steps
- Then floor should be pushed in to rubber by 5mm from 21^{st} solver step to 70^{th} solver step
- Form nonlinear static solver results reaction force vs solver step graph to be obtained and solver step should be identified which generated same reaction force as identified equivalent force
- In the given solver step von Mises stress and material yield stress should be analyzed to get safety factor to identify wheel failures when wheel enters steady state level
- It was defined as good design if wheel doesn't yield when it's in steady state temperature level

6. Validation

Generalized model of Castor wheel evaluation for dynamic test was used and analysis were conducted according to given guidelines. Validation case study wheels were selected among selected samples wheels from initial dynamic test. According to wheel size and dynamic test performance given in appendix 1, wheels were selected to carry out validation case studies. Smallest wheel diameter was 100 mm and biggest wheel diameter was 200 mm so both wheel sizes were selected for analysis. Wheel pass and fail status were also considered in case study selection. Validation was carried out by compared each temperature development curves with time from prediction and physical tests. Then failure analysis results from physical test was compared with simulation failure analysis to validate the developed model.

6.1. Case Study 1

For 160 mm wheel with 500 kg load was selected to case study 1 simulation. FEA models used in development case study was used. All 3D and 2D models, mesh and material data was used for case study simulation according to given guide.

Static Loading Simulation

Simulation was done and results were analyzed to identify solver step for 500 kg load. Cluster node reaction force for 500kg load was calculated as 1,227 N considering model symmetry. To identify the solver step same graph given in Figure 5.9 can be used and this is same 160 mm wheel design. It was observed that 1,227N was applied on the cluster note at 41st solver step.

Total Energy Rate Calculation

Force vs compression graph given in Figure 5.10 was used and integration was done to find energy applied on static loading to load castor wheel for 500 kg load. It was observed that at 500kg wheel compression was 0.0041m, up to that limit graph was integrated and value was recorded as 7.29 J. (Appendix 3)

Number of wheel rotation per second was calculated as 2.2

Correction factor from guide 3.25

total energy rate = 52.36 J/s (From equation 5)

Since it was the same rubber material, energy loss fraction graph given in Figure 4.12 was used to get heat generation rate from above total energy rate.

Temperature Prediction

2D models used for the 160 mm 450 kg load studies were used for this 160 mm 500 kg simulation. Calculate total energy rate of 52.36 J/s was distributed among rubber elements. 3D static simulation was analyzed at 41 solver step which applies 500 kg load and stored energy density and rubber element volumes were extracted from surface elements. According to the stored energy in each element first 75% present elements were prioritized and total energy rate was distributed among respective elements of 2D profile the according to stored energy percentages. Those distributed total energy rate was applied to relevant nodes as heat sources for FEA simulation.

Table 6.1 : Element energy rate in 160 mm 500 kg case

	J/s		J/s
Element ID	**Total energy rate**	**Element ID**	**Total energy rate**
136	4.92	616	2.13
121	4.78	421	1.95
586	3.45	706	1.92
676	3.36	451	1.88
106	3.12	571	1.87
151	3.00	61	1.79
391	2.81	646	1.62
601	2.58	556	1.58
376	2.35	241	1.50
406	2.19	31	1.46
46	2.17		

Material thermal properties and convection data were loaded to model according to appendix 4. Transient solver was used to solve the model with transient heat solver with 1 second time steps up to 10,000 seconds. Temperature development was extracted from the results in given points of the model to represent rubber inside, rubber outside, plastic inside, plastic outside temperatures.

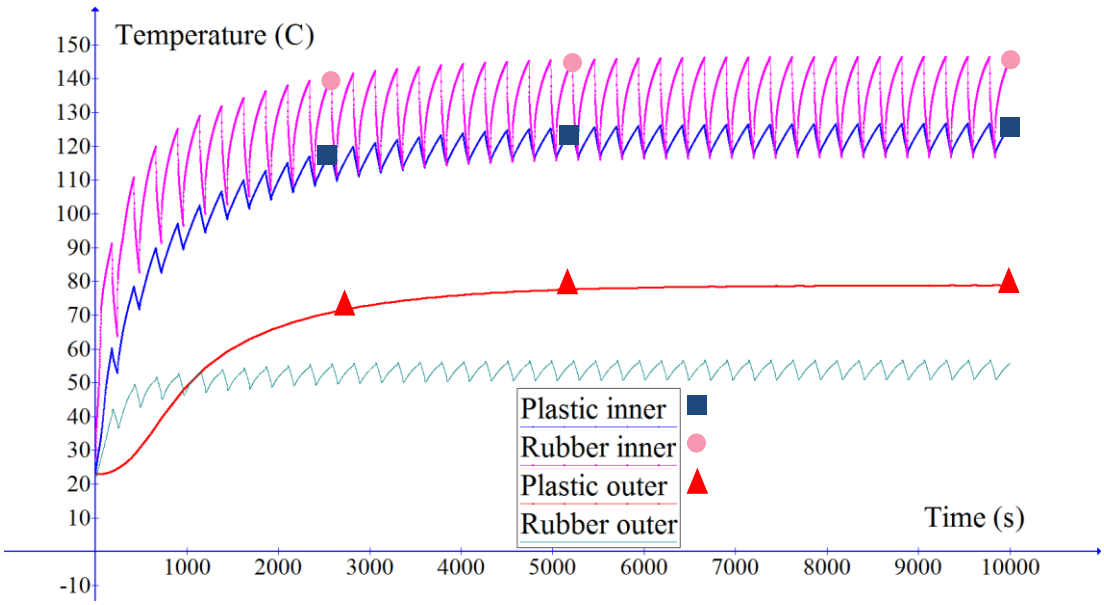

Figure 6.1 : 160 mm 500 kg load temperature prediction

inside the rubber of 146^{oC} and next, inside the plastic was recorded 125^{o}C. plastic outside temperature was recorded as 78^{o}C and lowest temperature was recorded at rubber outer of 57^{o}C temperature. Plastic outside temperature was very slightly varied due to wheel run-stops cycles because of temperature measuring point was far away from heat sources loaded. Big variation was visible in plastic and rubber inner locations due to wheel run-stop cycle. Obtained temperature graphs were compared with actual dynamic test results to validate the simulation model. Actual temperature recorded from the 160 mm castor wheel 500 kg dynamic test was compared with each location predicted temperature from simulation.

Temperature Comparison

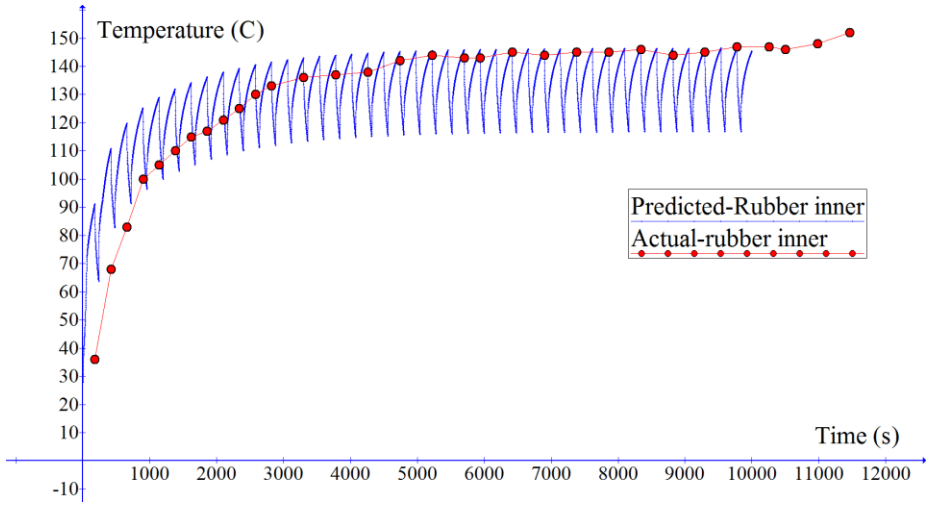

Figure 6.2 : Rubber inner temperature comparison, 160 mm 500 kg

In actual dynamic test, wheel continued for about 11,500 s before fail. From the Figure 6.1 it was observed that actual wheel achieves steady state around 4,000 seconds which proves selected 10,000 s range was enough for temperature prediction simulation. Actual temperature graph was recorded at 180 s intervals immediately after wheel was stopped according to cycle, hence run cycle variation was not captured in actual temperature measuring. Comparing the maximum temperature of each simulation and actual temperature it was observed that close prediction was done by simulation also for rubber inner temperature. Predicted Rubber outer temperature was closely matched with actual rubber outer temperature of the dynamic test.

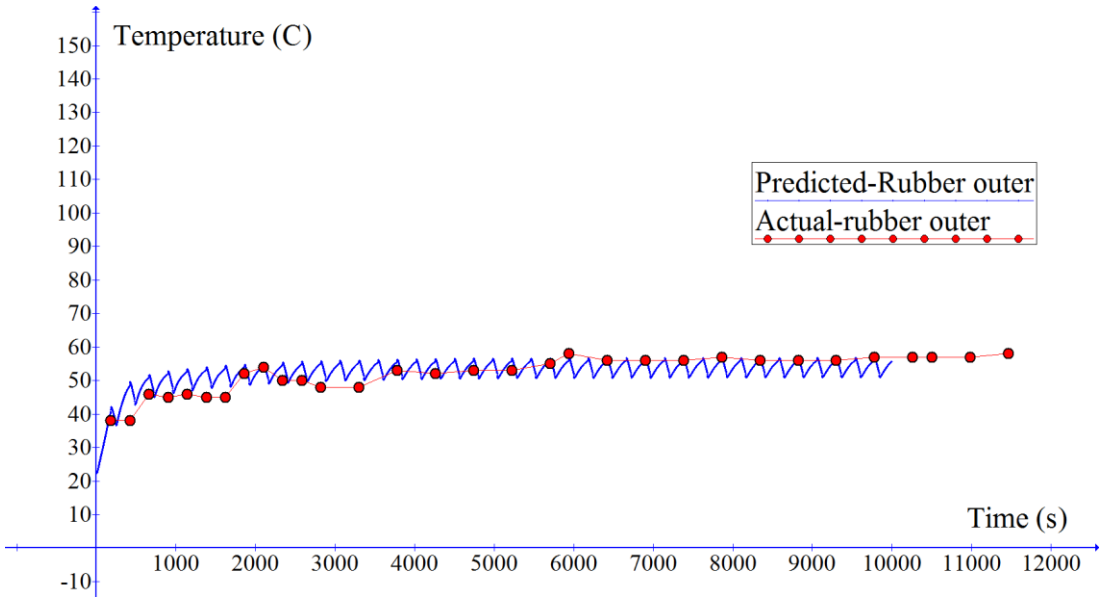

Figure 6.3 : Rubber Outer temperature comparison, 160 mm 500 kg

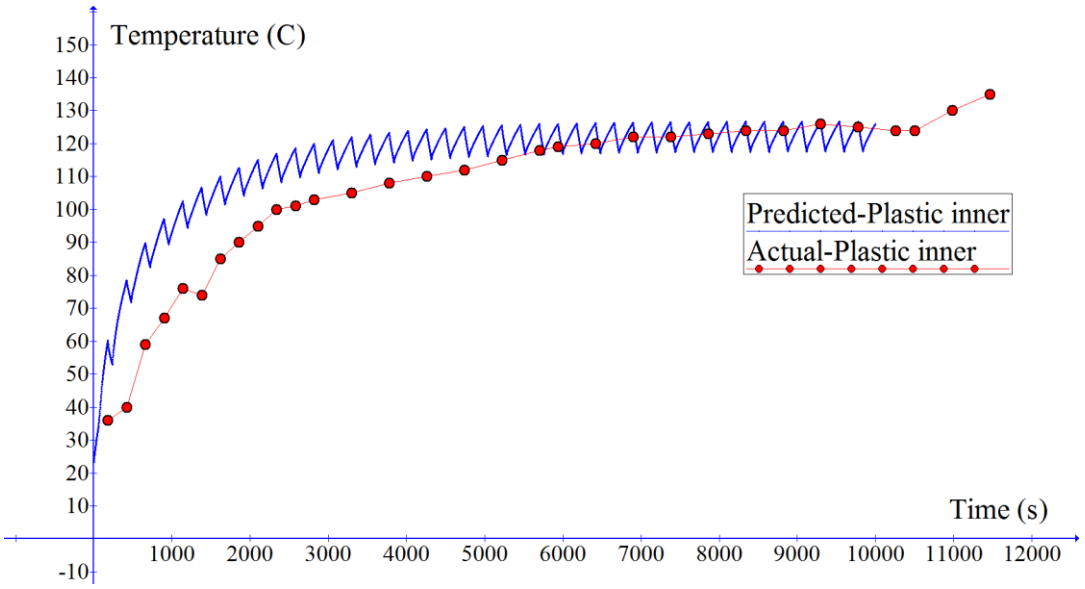

Figure 6.4 : Plastic Inner temperature comparison, 160 mm 500 kg

Predicted Plastic inner temperature was closely matched with actual rubber outer temperature of the dynamic test.

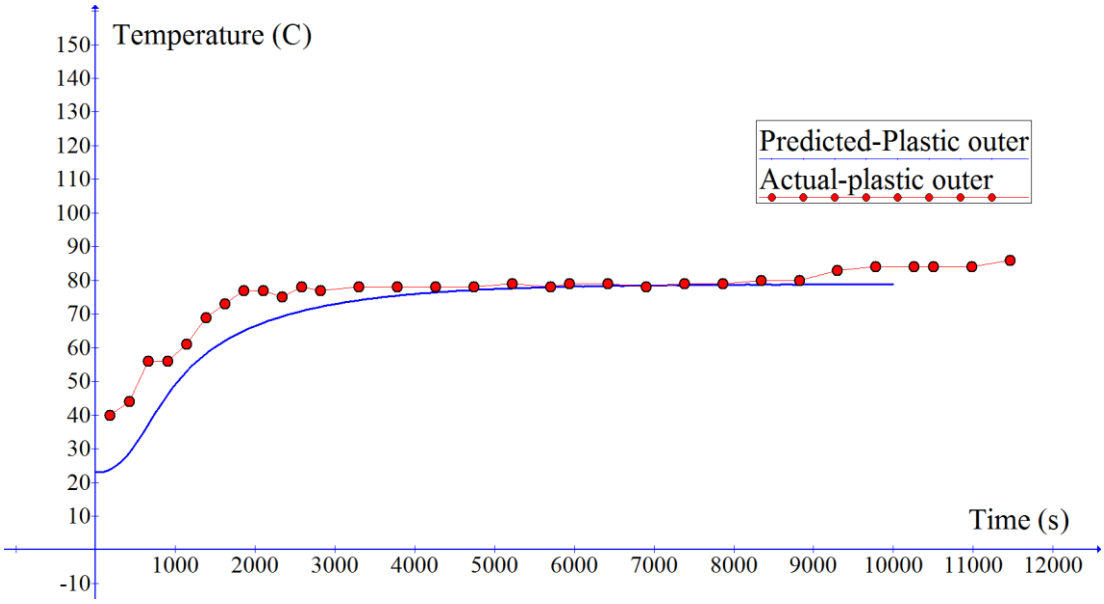

Figure 6.5 : Plastic Outer temperature comparison, 160 mm 500 kg

Predicted plastic outer temperature was slightly deviated from actual one at start but when considered the steady state level, it was observed that both parameters are very close to each other.

At steady state level, all predicted temperatures and actual temperatures are very close to each other validating the proposed methods capability to predict temperature through FEA simulation.

Failure Analysis

Initially equivalent load to 2D profile which stresses the center to the same level as 3d Simulation 500kg loading was calculated. In 3D static simulation center stress was 22.7 MPa when loaded to 500 kg load.

From 2D static simulation solver step 30 was identified as giving same stress to canter of 22.7 MPa. 4203.5 N was applied on cluster node at given solver step.

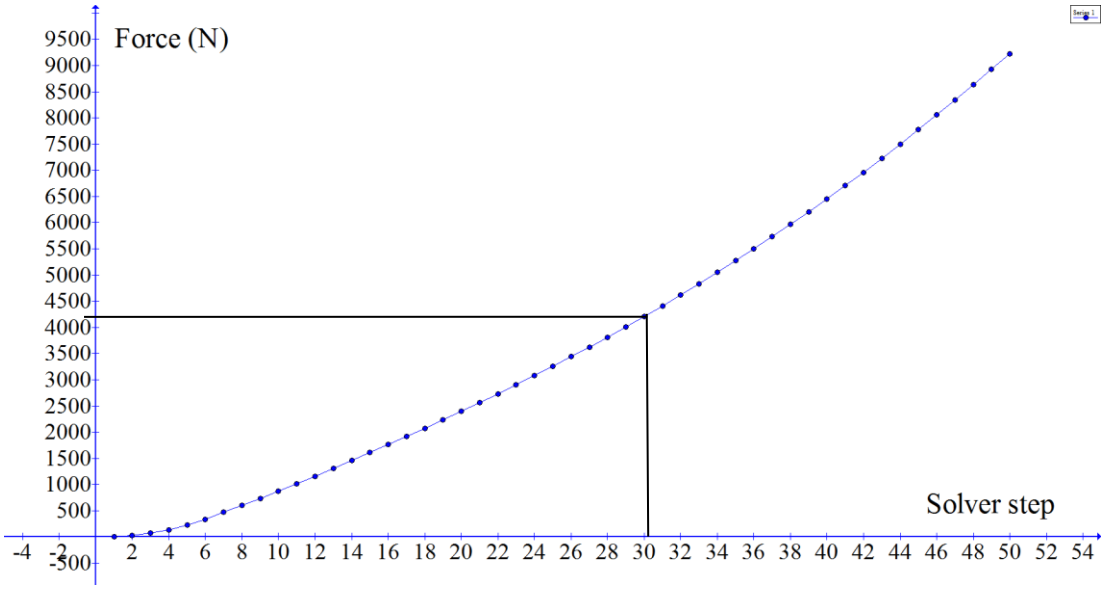

Figure 6.6 : Reaction force vs solver step 160 mm wheel 500 kg

Then from appendix 4 temperature dependent material properties were loaded to the created 2D FEA file. Temperature profile was imported from transient temperature prediction simulation file at steady state region maximum temperature at 5938 seconds. Nonlinear static solver was used to simulate the temperature application and loading case to analyze failure of the 160 mm wheel at 500 kg load dynamic test.

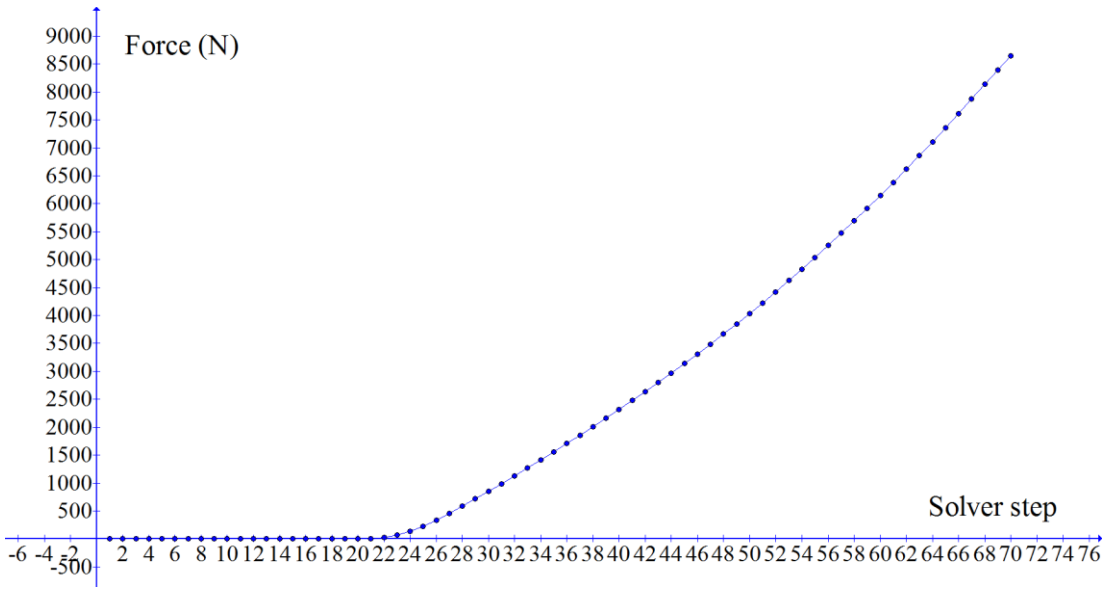

Figure 6.7 : 160 mm 500kg load failure analysis

It was observed that equivalent load of 4,203.5 N was applied to the reaction node at 51 solver step. At this step stress inside the center and material yield stress was studied to analyze failure.

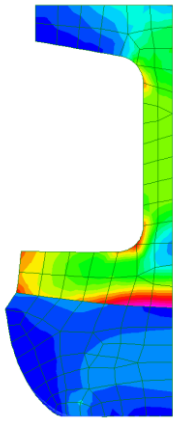

Figure 6.8 : 160 mm wheel 500 kg load with temperature stress profile

22.5 MPa stress was observed inside the center part of the 160 mm wheel at 500 kg load to the wheel with temperature profile applied. At this level yielding of the wheel was analyzed by safety factor analysis. Highest temperature recorded inside the center was 128^{o}C same place where highest stress was recorded.

Table 6.2 : 160 mm 500 kg wheel safety factor

	MPa	MPa	
Equivalent load	Stress in nylon centre	Nylon yield stress at 127^{o}C	Safety factor for nylon centre
500 kg	22.5	25.3	1.12

Safety factor of 1.12 was calculated for the 160 mm wheel 500 kg load after achieving steady state level. Wheel ran for 11,460 seconds before failure at the actual dynamic test (Appendix 1). Standard requirement of the test was to run the wheel until 9,048 seconds which makes the wheel successful in dynamic test. From safety factor analysis also, wheel achieved lowest 1.12 safety factor at steady state level which suggest wheel was capable of handling 500 kg load in dynamic test.

6.2. Case Study 2

125 mm common wheel with 125 kg load was selected from table 1 for validation of the FEA model. 125mm wheel was made from polyproline center and NR-2 rubber compound which is different from case study material. Geometric dimensions and design also comparably different from case study.

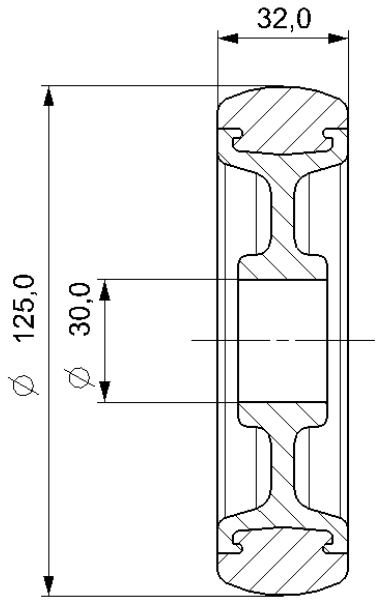

Figure 6.9 : 125 mm Castor wheel

Static Loading Simulation

According to developed model FEA static simulation was done. Instead of nylon material data, polypropylene data was fed in to the FEA software as this wheel was made from poly propylene an NR-2 rubber compound as given in table 1.

Contact elements and floor definitions were given according to the guide. Nonlinear static solver was used to solved the setup. For 125 kg load, calculated load on ¼ of FEA model was 306.5 N. at this load stress inside the wheel was studied.

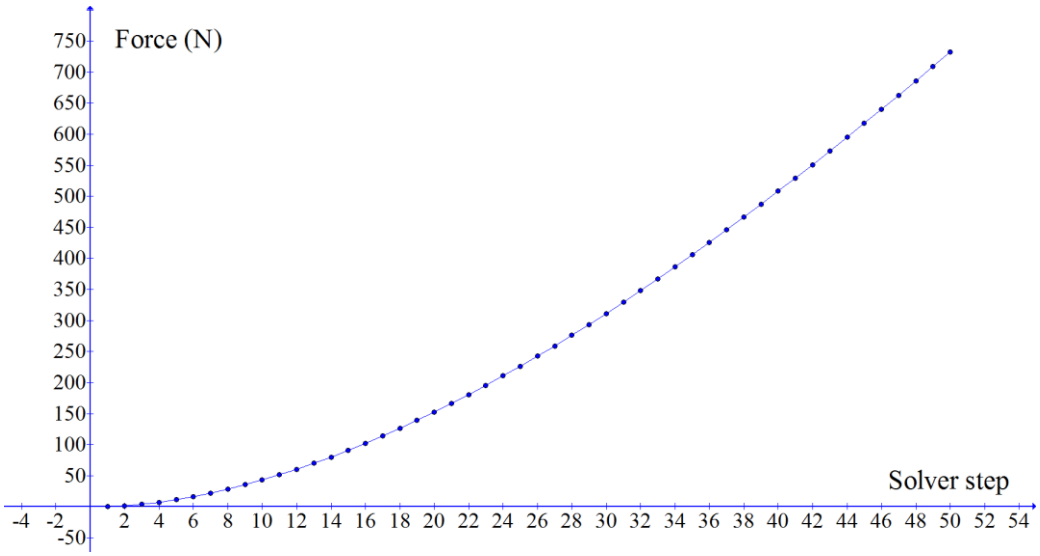

Figure 6.10 : 125 mm 125 kg static loading

From the extracted graph 306.5 N load was applied in 30th solver increment. At this step stress inside rubber and plastic was analyzed and given in table

Table 6.3 : 125 mm 125 kg case static loading stress

	MPa	MPa	MPa	MPa		
load	Stress in centre	Stress in rubber	PP yield stress	NR-2 max stress	Safety factor for PP centre	Safety factor for rubber wheel
125 kg	9.9	3.6	24.6	14.5	2.5	4

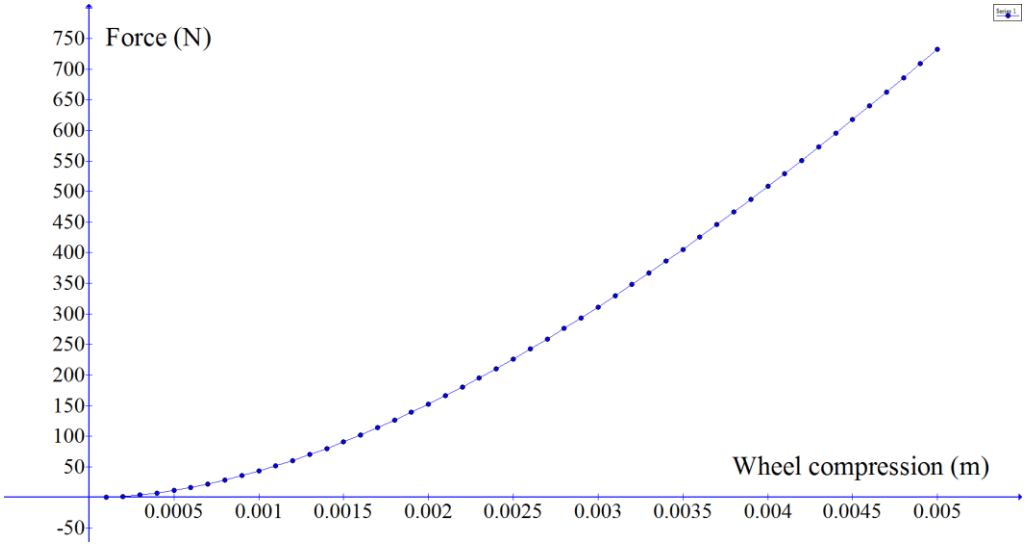

Figure 6.11 : 125mm 125 kg case force vs wheel compression

Total Energy Rate Calculation

Force vs compression graph given in Figure 6.11 was used and integration was done to find energy applied on static loading to load castor wheel for 125 kg load. It was observed that at 125 kg wheel compression was 0.003 m, up to that limit graph was integrated and value was recorded as 1.41 J. (Appendix 5)

Number of wheel rotation per second was calculated as 2.8

Correction factor from guide 3.25

total energy rate = 13 J/s (From equation 5)

Energy loss fraction graph given in Figure 4.12 was used to get heat generation rate from above total energy rate. Wheel run-stop cycle was also loaded to FEA model to control the heat sources according to run-stop time.

Temperature Prediction

Total energy rate was distributed among 2D temperature prediction model according to table 13. Material Thermal parameters along with convection coefficients were added to the FEA model according to appendix 4 data.

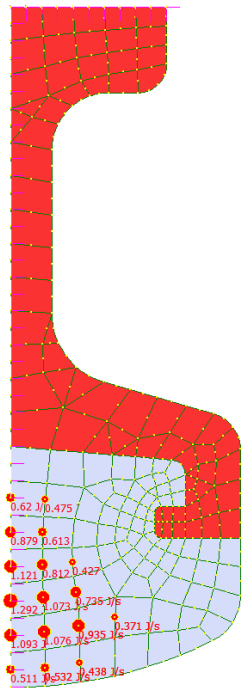

Figure 6.12 : 125 mm 125 kg temperature prediction setup

Table 6.4 : 125 mm 125 kg case total energy distribution

Element ID	Distributed total energy rate (J/s)
316	1.292
331	1.121
301	1.093
1006	1.076
1021	1.073
991	0.935
346	0.879
1036	0.812
1111	0.735
361	0.620
721	0.613
271	0.532
286	0.511
496	0.475
256	0.438
1051	0.427
976	0.371

After solving temperature for defined four points were extracted given in Figure 6.13

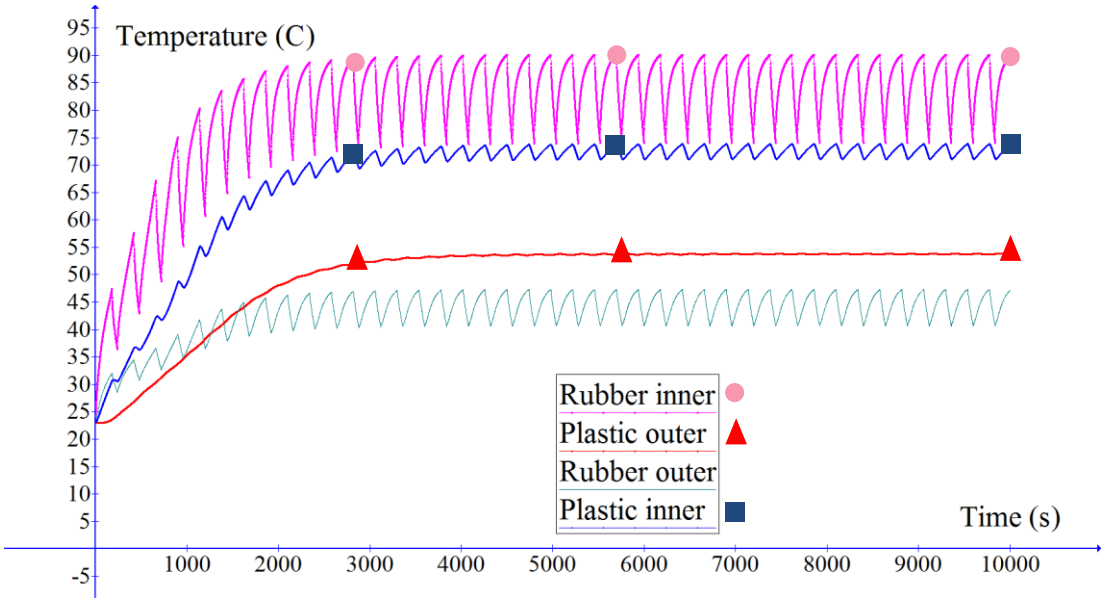

Figure 6.13 : 125 mm 125 kg temperature prediction

Temperature Comparison

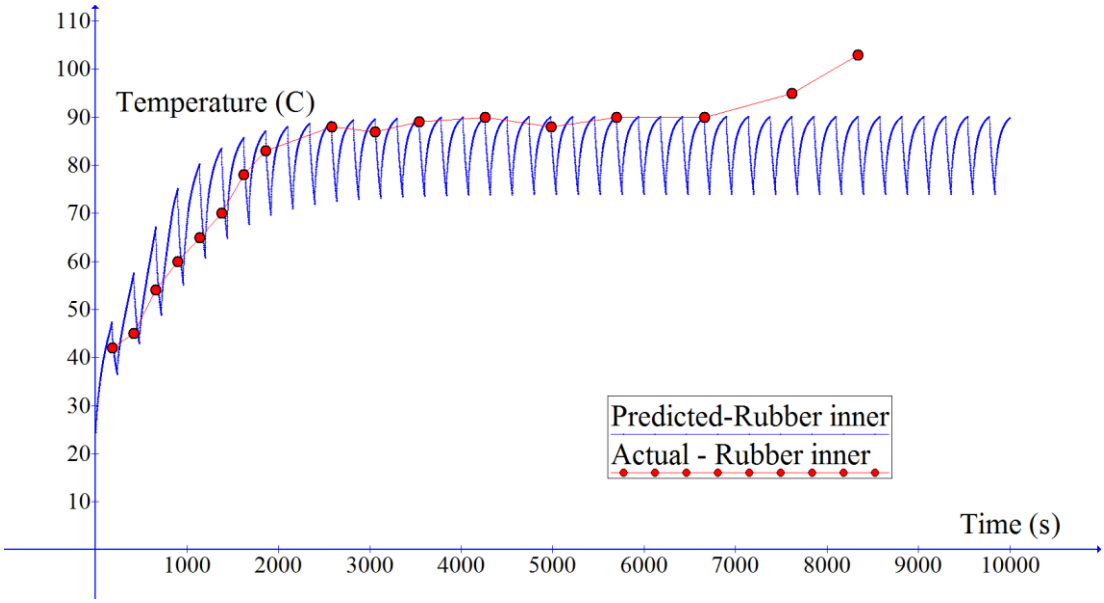

Figure 6.14 : rubber inner temperature comparison, 125 mm 125 kg

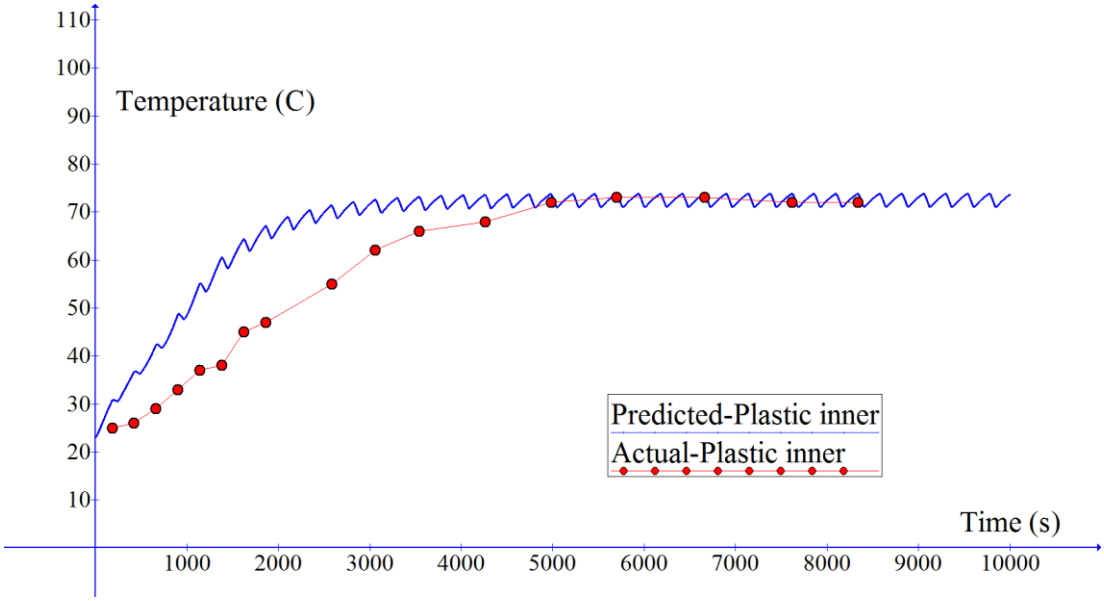

Figure 6.15 : Plastic inner temperature comparison. 125 mm 125 kg

From above graphs we can observe good agreement of predicted temperature with actual temperature. Predicted temperature curves and actual temperature curved shows very good agreement in steady state region.

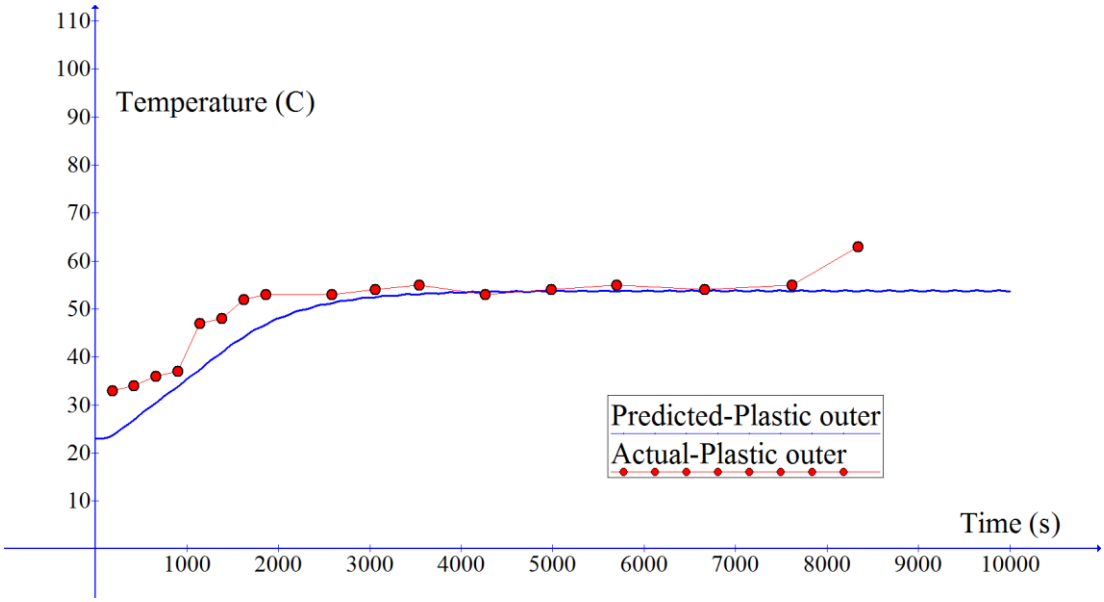

Figure 6.16 : Plastic outer temperature comparison, 125 mm 125 kg

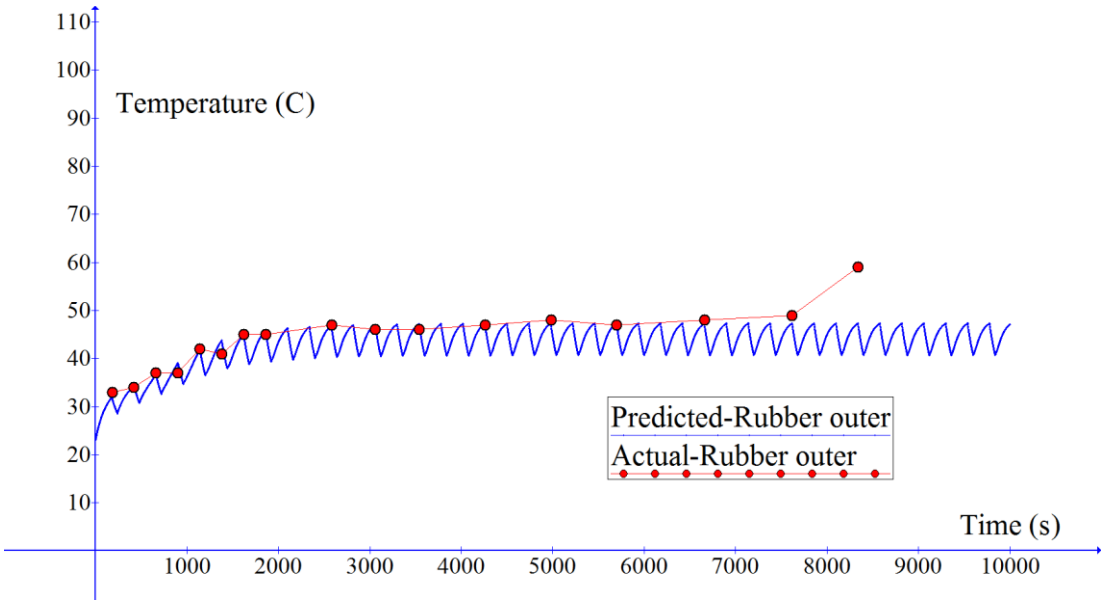

Figure 6.17 : Rubber outer temperature comparison, 125 mm 125 kg

Compared temperature graphs of actual testing and predicted temperatures graphs found to be very closely matching with each other. Which proves validity of the model to simulate both polyproline and nylon castor wheel in both heavy-duty and general application range.

Failure Analysis

Initially equivalent load was calculated from 2D axisymmetric FEA setup with nonlinear static solver. It was observed that at 22nd solver step center was stress up to 9.9 MPa von Mises stress which is equivalent to static loading stress.

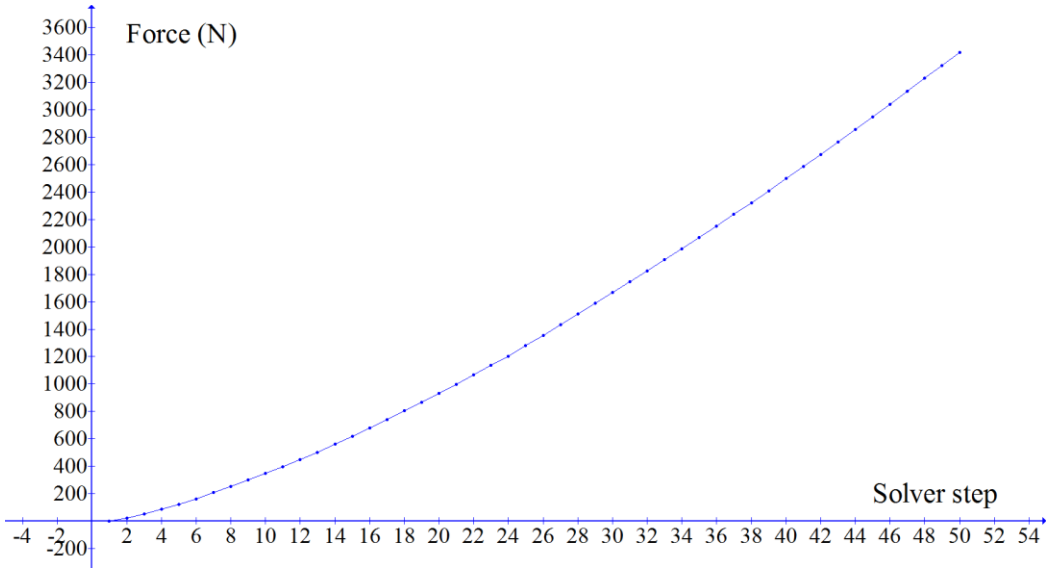

Figure 6.18 : 125 mm wheel 125 kg Force vs solver step

From graph, equivalent load on 2D axisymmetric profile was calculated as 1,067 N. Then failure simulation was carried out considering maximum node temperatures and material parameter changes with temperature.

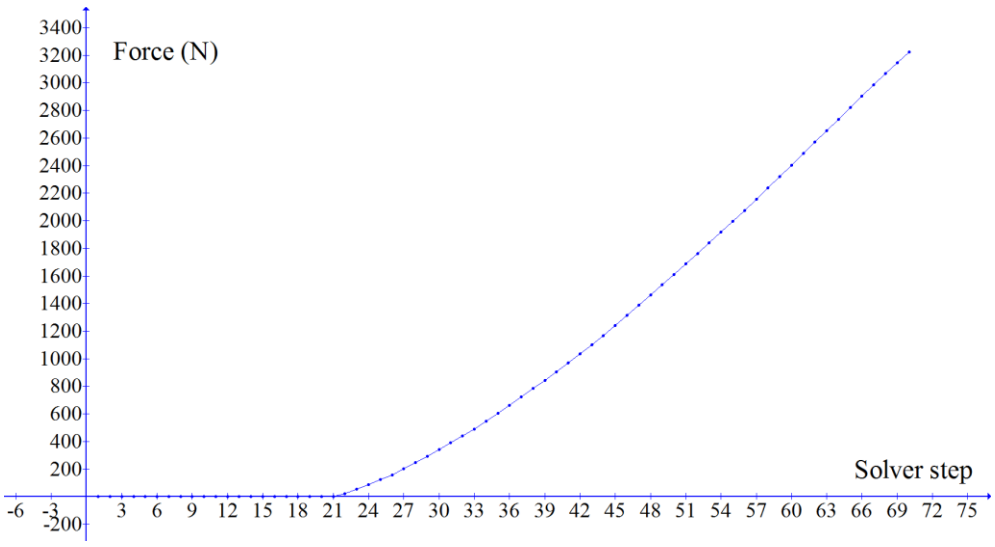

Figure 6.19 : 125 mm wheel failure analysis

From Figure 6.19, solver step 43 was identifies as generating same load of 1,067 N on 2D axisymmetric model. Maximum von Mises stress of 10.1 MPa was observed in the center part of the wheel after failure simulation.

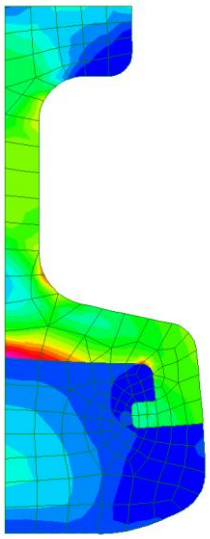

Figure 6.20 : 125 mm 125 kg stress distribution at steady state

Maximum temperature of 75^{o}C temperature was recorded inside the center part.

Table 6.5 : 125 mm 125 kg safety factor

	MPa	MPa	
Equivalent load	Stress in PP centre	PP yield stress at 75^{o}C	Safety factor for PP centre
125 kg	10.1	16.3	1.61

1.61 safety factor was achieved by 125 mm common wheel at 125 kg dynamic test. In actual dynamic test wheel ran for 8340 seconds which is more than required by the standard (Appendix 1). In the simulation also 1.61 safety factor suggest wheel would run more time in steady state level. Wheel was evaluated as pass from simulation model also.

6.3. Case Study 3

100 mm common wheel with 100 kg load was selected from table 1 for validation of the FEA model. This wheel was failed at dynamic test before completing the required revaluations. 100mm wheel was made from polypropylene center and NR-2 rubber compound. Basic wheel structure is same as Figure 6.9 with outer diameter 100 mm.

Static Loading Simulation

According to developed model FEA static simulation was done. Polypropylene data and NR-2 rubber compound data were fed in to FEA software. Contact elements and floor definitions were given according to the guide. Nonlinear static solver was used to solve the setup. For 100 kg load, calculated load on ¼ of FEA model was recorded as 245 N. at this load stress inside the wheel was studied.

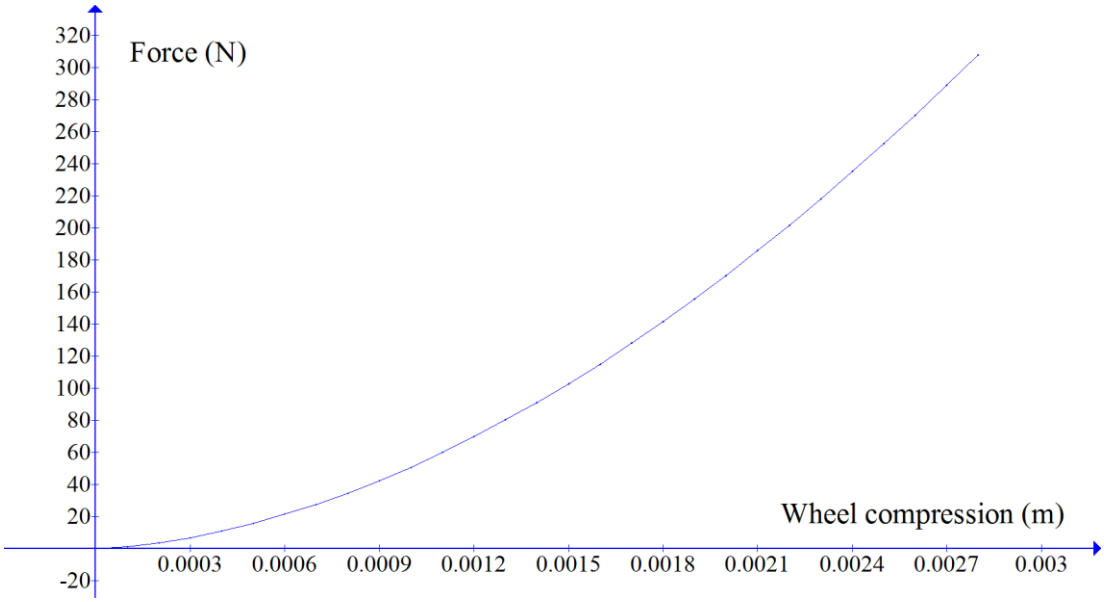

Figure 6.21 : 100 mm 100 kg case force vs wheel compression

Table 6.6 : 100 mm 100 kg case static loading stress

	MPa	MPa	MPa	MPa		
load	Stress in centre	Stress in rubber	PP yield stress	NR-2 max stress	Safety factor for PP centre	Safety factor for rubber wheel
100 kg	14.9	3.7	24.6	14.5	1.6	3.9

Total Energy Rate Calculation

Force vs compression graph given in Figure 6.21 was used and integration was done to find energy applied on static loading to load castor wheel for 100 kg load. It was observed that at 100 kg wheel compression was 2.5 mm, up to that limit graph was integrated and value was recorded as 0.94 J. (Appendix 7)

Number of wheel rotation per second was calculated as 3.5

Correction factor from guide 3.25

Total energy rate = 10.7 J/s (From equation 5)

Energy loss fraction graph given in Figure 4.12 was used to get heat generation rate from above total energy rate. Wheel run-stop cycle was also loaded to FEA model to control the heat sources according to run-stop time.

Temperature Prediction

Total energy rate was distributed among 2D temperature prediction model according to calculation method given in simulation model given in appendix 8. Material Thermal parameters along with convection coefficients were added to the FEA model according to appendix 4 data.

After solving temperature for defined four points were extracted given in Figure 6.22

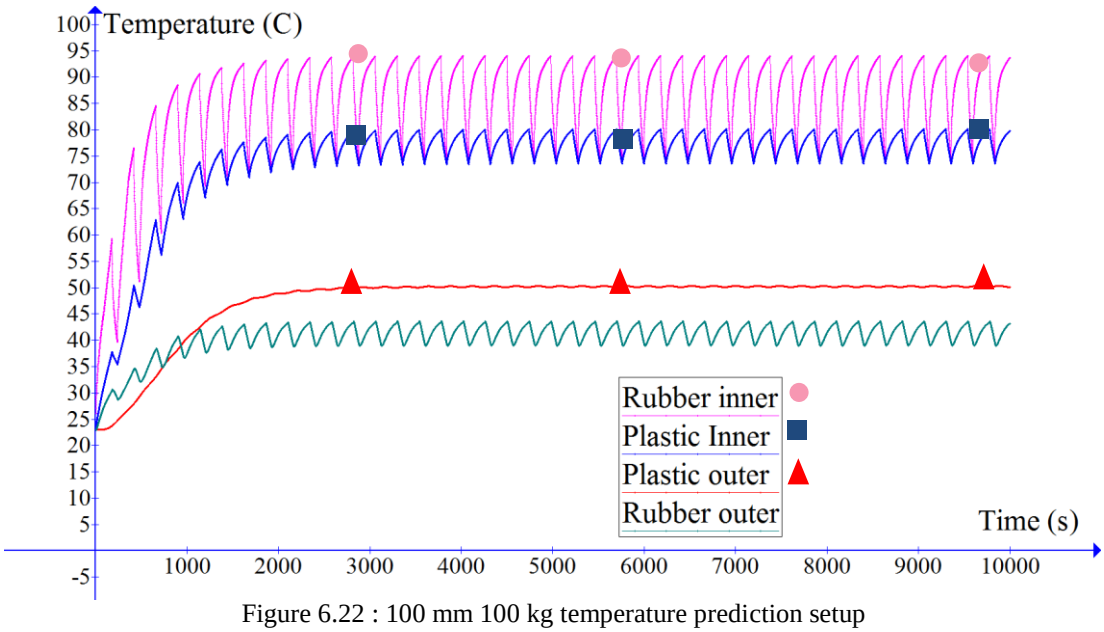

Figure 6.22 : 100 mm 100 kg temperature prediction setup

Temperature Comparison

It was observed from actual dynamic test wheel continued on test up to 2,820 seconds only. To pass the dynamic test wheel has to run until 5,655 seconds. Actual temperature recorded until 2,820 seconds was plotted to validate the temperature prediction.

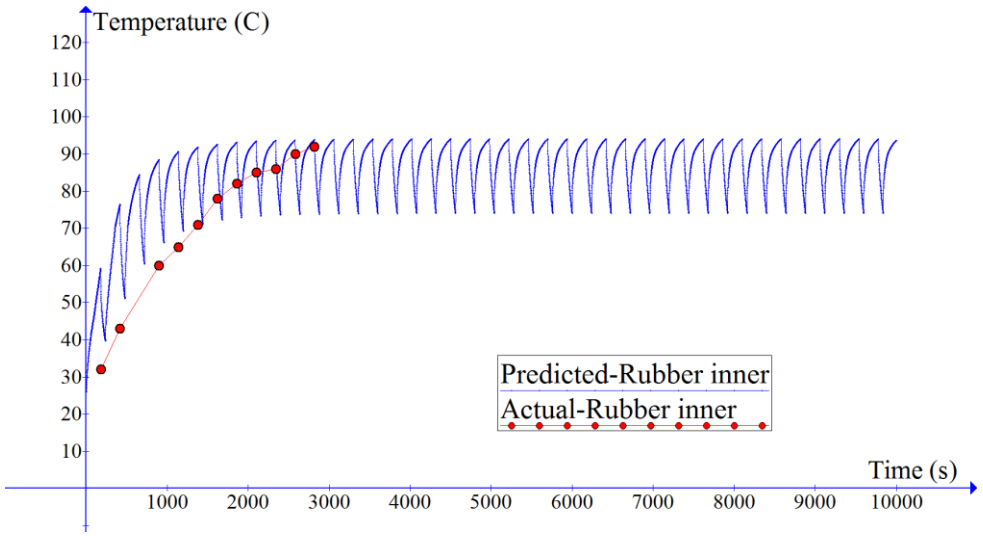

Figure 6.23 : rubber inner temperature comparison, 100mm 100 kg

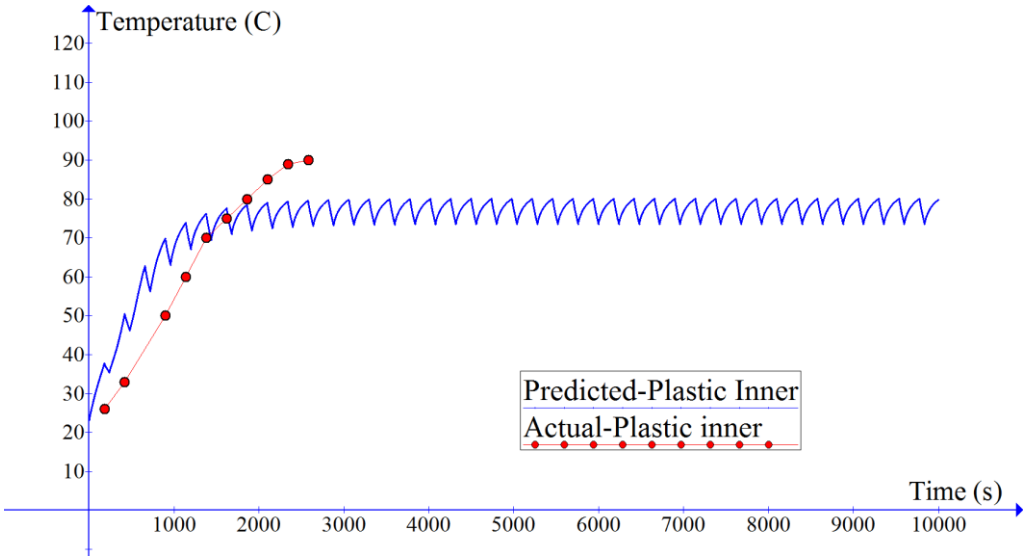

Figure 6.24 : Plastic inner temperature comparison. 100 mm 100 kg

From actual temperature graphs, it was observed that wheel fails early in dynamic testing before going in to steady state temperature region.

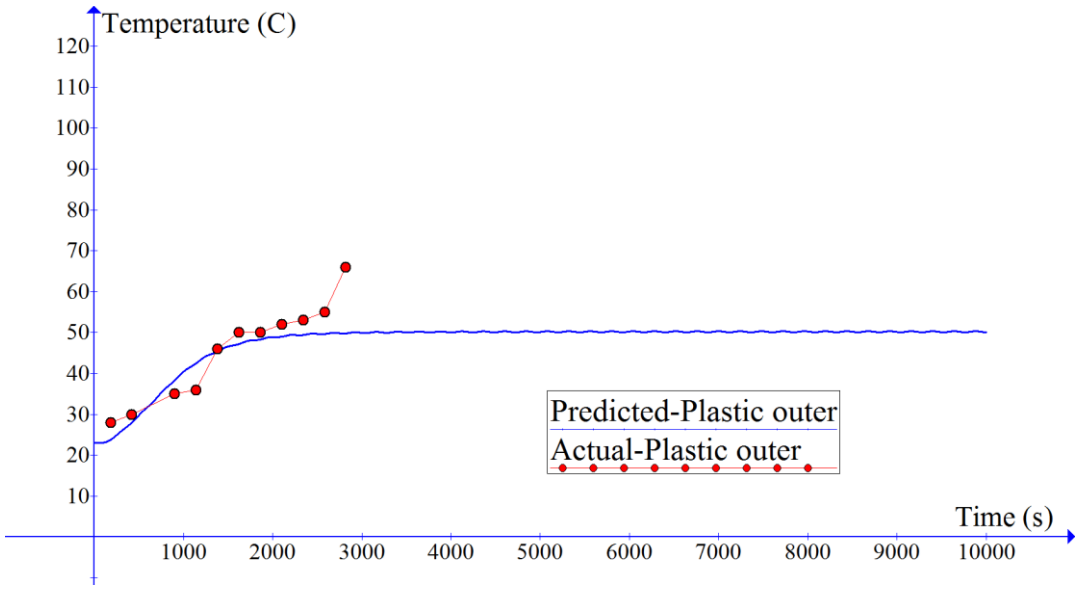

Figure 6.25 : Plastic outer temperature comparison, 100 mm 100 kg

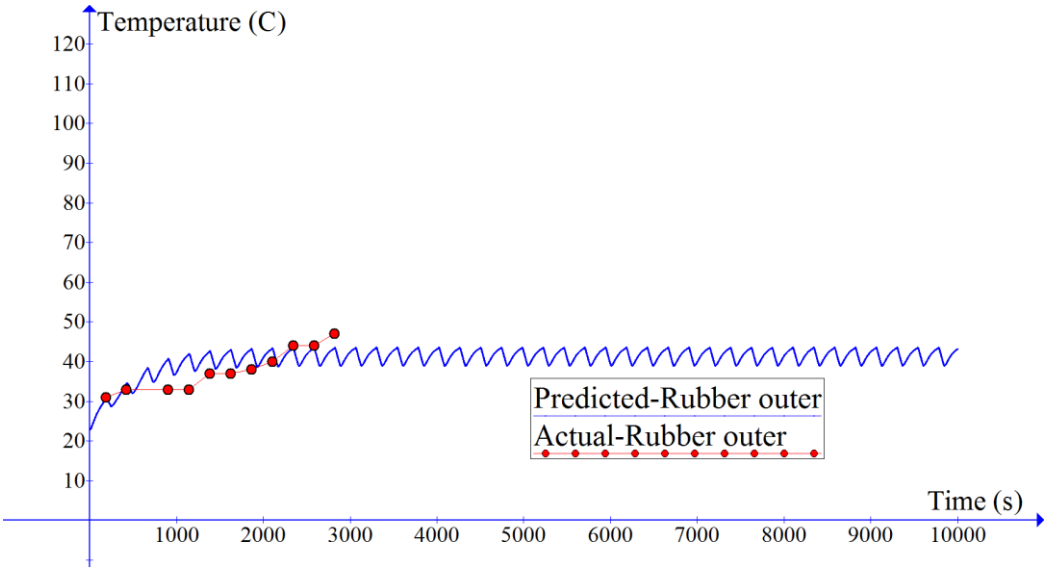

Figure 6.26 : Rubber outer temperature comparison, 100 mm 100 kg

Rubber inner rapid temperature develop region showed slightly deviated temperature but in steady state level same temperatures were observed. Other temperature compared temperature graphs of actual testing and predicted temperatures graphs found to be matching with each other. I

t was observed that steady state region was not prominently visible in actual temperature developments like in previous records.

Failure Analysis

From initial static load analysis plastic center was stressed up to 12.1 MPa. From 2D axisymmetric static loading simulation required load was calculated to stress the center to same level. 821 N was required to be applied on 2D model to stress center up to 12.1 MPa von Mises stress. Temperature data were loaded to the model and failure analysis was carried out to evaluate wheel failure at steady state level.

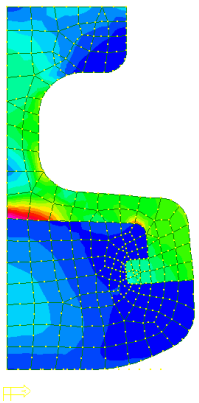

Figure 6.27 : 100 mm 100 kg stress distribution at steady state

Maximum 15.2 MPa von Mises stress was observed in the center part of the wheel at steady state level. Same place was identified as highest temperature of 85°C recorded at steady state level. Safety factor analysis was done to evaluate yielding of the wheel at steady state level.

Table 6.7 : 100 mm 100 kg safety factor

	MPa	MPa	
Equivalent load	Stress in PP centre	PP yield stress at 85°C	Safety factor for PP centre
125 kg	15.2	14.7	0.96

From safety factor analysis, it was observed that plastic was yielded when entering steady state level. Since plastic yields before steady state level in actual test, it was observed that no steady state region was prominent in dynamic test. Wheel was failed at 2,820 seconds before the intended run time of 5,655 seconds.

6.4. Case Study 4

200 mm wheel with 550 kg load was selected from table 1 for validation of the FEA model. This was the highest diameter wheel in the sample lot and wheel was failed at dynamic test before completing the required revaluations. 200 mm wheel was made from Nylon center and NR-1 rubber compound.

Static loading simulation

According to developed model FEA static simulation was done. Nylon material data and NR-1 rubber compound data were fed in to FEA software. Contact elements and floor definitions were given according to the guide. Nonlinear static solver was used to solve the setup. For 100 kg load, calculated load on ¼ of FEA model was recorded as 1,348 N. at this load stress inside the wheel was studied.

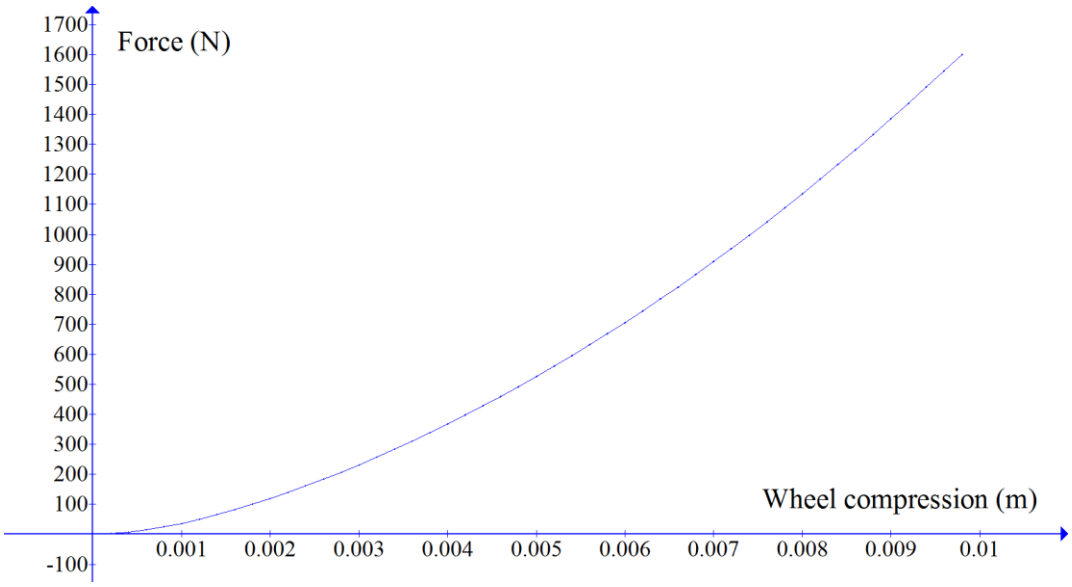

Figure 6.28 : 200 mm 550 kg case force vs wheel compression

Table 6.8 : 200 mm 550 kg case static loading stress

	MPa	MPa	MPa	MPa		
load	Stress in centre	Stress in rubber	Nylon yield stress	NR-2 max stress	Safety factor for nylon centre	Safety factor for rubber wheel
550 kg	26.4	2.8	68.4	15.0	2.6	5.3

Total Energy Rate Calculation

Force vs compression graph given in Figure 6.29 was used and integration was done to find energy applied on static loading to load castor wheel for 550 kg load. It was observed that at 550 kg wheel compression was 9 mm, up to that limit graph was integrated and value was recorded as 19.4 J. (Appendix 9)

Number of wheel rotation per second was calculated as 1.7

Correction factor from guide 3.25

Total energy rate = 107 J/s (From equation 5)

Energy loss fraction graph given in Figure 4.12 was used to get heat generation rate from above total energy rate. Wheel run-stop cycle was also loaded to FEA model to control the heat sources according to run-stop time.

Temperature Prediction

Total energy rate was distributed among 2D temperature prediction model according to calculation method given in simulation model given in appendix 8. Material Thermal parameters along with convection coefficients were added to the FEA model according to appendix 4 data.

After solving temperature for defined four points were extracted given in Figure 6.30

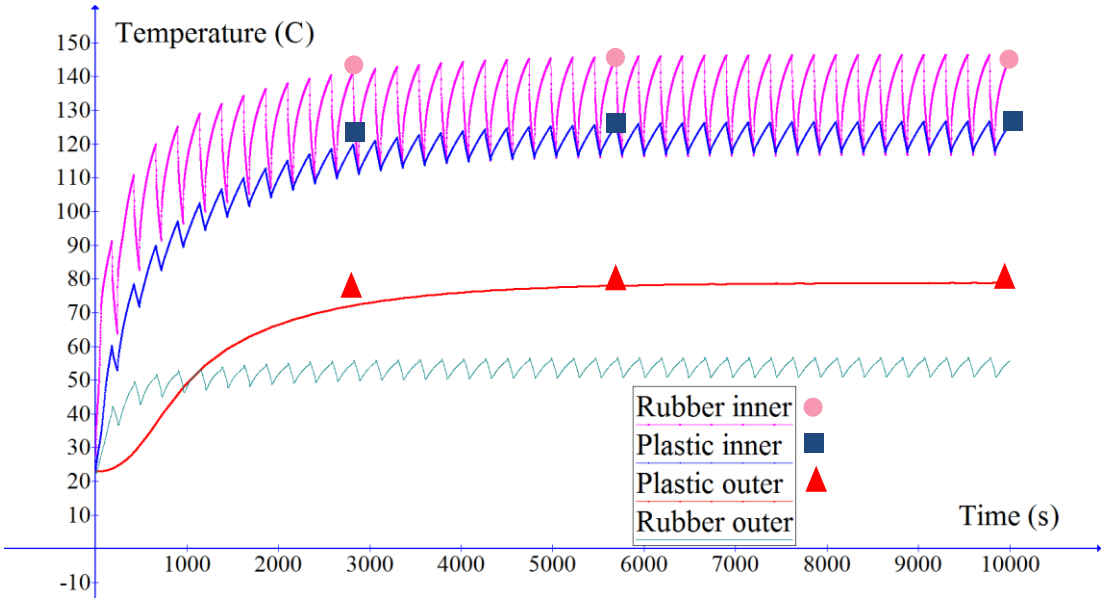

Figure 6.29 : 200 mm 550 kg temperature prediction setup

Temperature Comparison

It was observed from actual dynamic test wheel continued on test up to 5700 seconds only. To pass the dynamic test wheel has to run until 11310 seconds.

Actual temperature recorded until 2820 seconds was plotted to validate the temperature prediction.

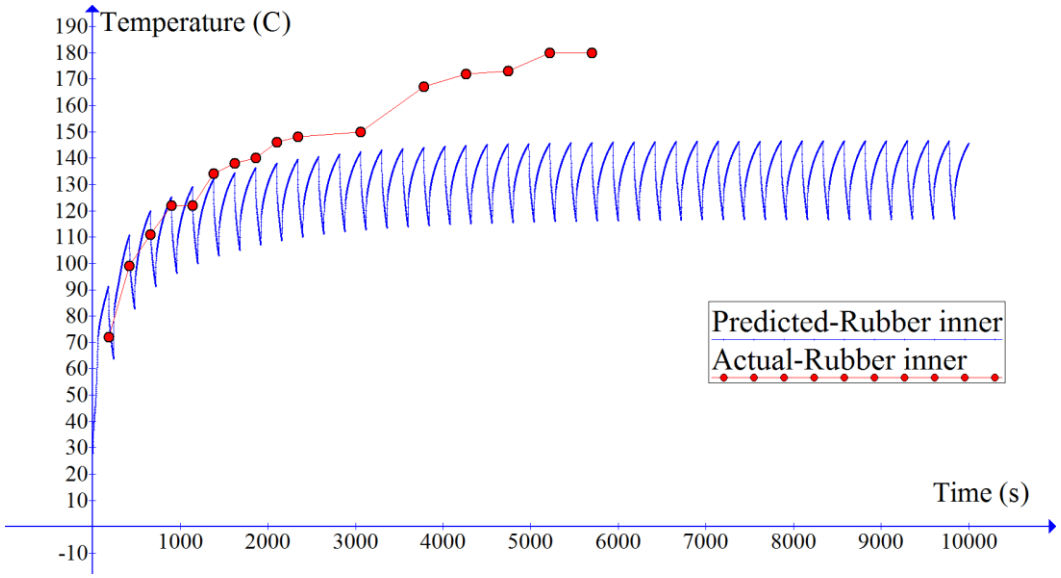

Figure 6.30 : Rubber inner temperature comparison, 200 mm 550 kg

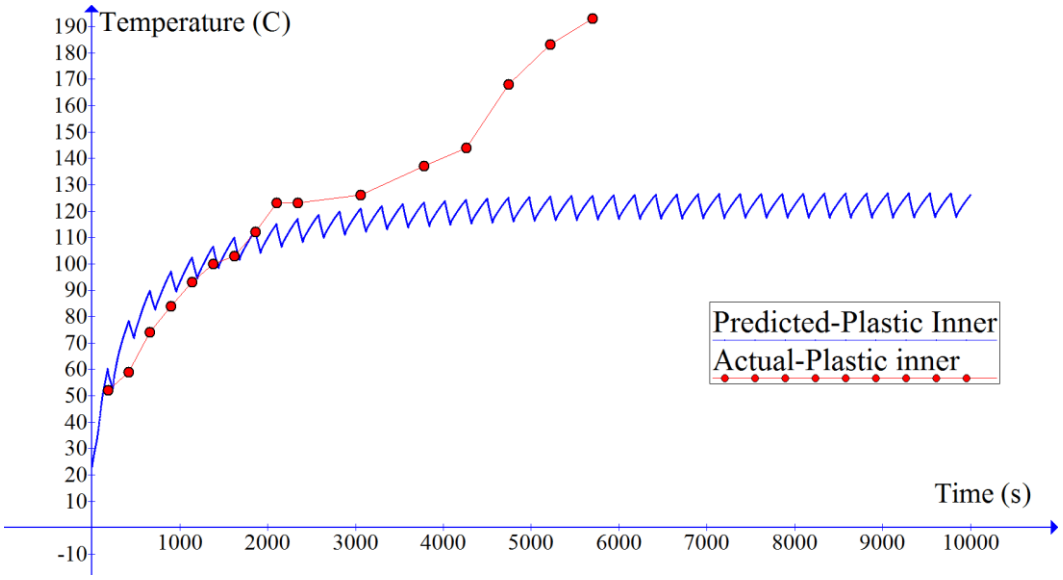

Figure 6.31 : Plastic inner temperature comparison. 200 mm 550 kg

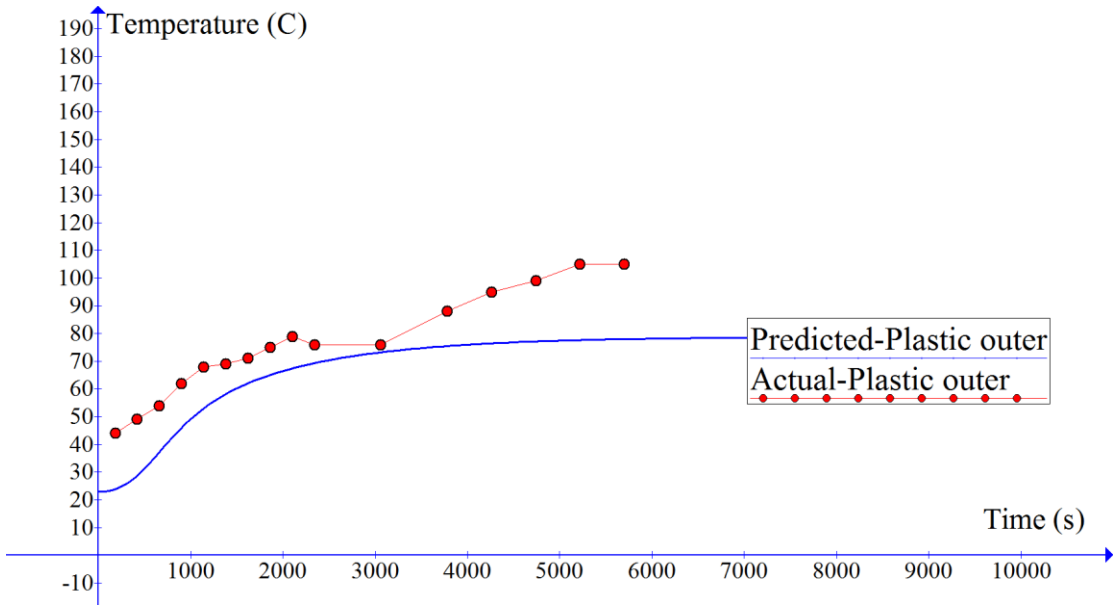

Figure 6.32 : Plastic outer temperature comparison, 200 mm 550 kg

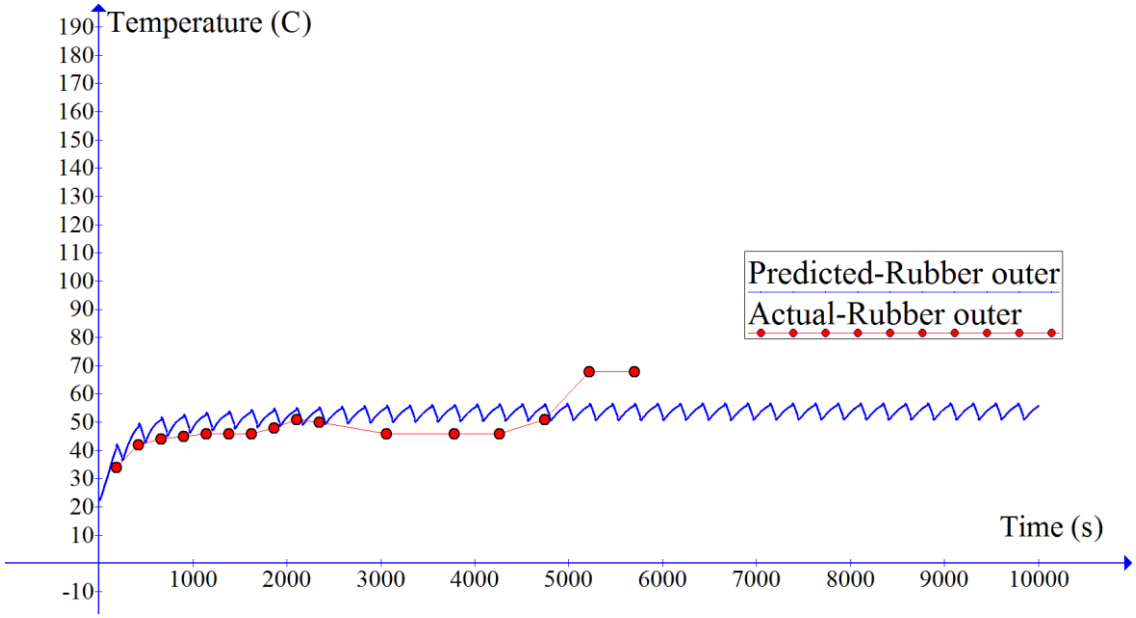

Figure 6.33 : Rubber outer temperature comparison, 200 mm 550 kg

It was observed from actual rubber inner and actual plastic inner graph, wheel continued temperature development even after predicted steady state level. No prominent steady state level was observed from those temperatures also. Castor wheel failure was evaluated to check weather wheel was yielded before entering steady state level which would lead to observed type performance.

Failure Analysis

From initial static load analysis plastic center was stressed up to 26.4 MPa. From 2D axisymmetric static loading simulation required load was calculated to stress the center to same level. 4515 N was required to be applied on 2D model to stress center up to 26.4 MPa von Mises stress. Temperature data were loaded to the model and failure analysis was carried out to evaluate wheel failure at steady state level.

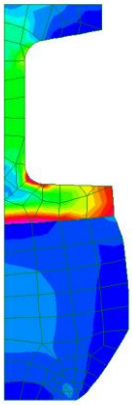

Figure 6.34 : 200 mm 550 kg stress distribution at steady state

Maximum 26.7 MPa von Mises stress was observed in the center part of the wheel at steady state level. Same place was identified as highest temperature of 127 ^{o}C recorded at steady state level. Safety factor analysis was done to evaluate yielding of the wheel at steady state level.

Table 6.9 : 200 mm 550 kg safety factor

	MPa	MPa	
Equivalent load	Stress in nylon centre	Nylon yield stress at 127^{o}C	Safety factor for nylon centre
550 kg	26.7	25.3	0.94

From safety factor analysis, it was observed that plastic was yielded when entering steady state level. Since plastic yields before steady state level in actual test, which cause the continuous increase of actual test temperatures and failing before required run time.

7. Discussion

Castor wheels which are tested in dynamic test procedure goes through several stages which was identified by physical testing and temperature development curves. Initially rapid temperature development phase was observed followed by steady state temperature region. After continuing in steady state level, temperature raised again due to yielding and bounce of the wheel when wheel was close to fail.

Developed temperature prediction model was capable of confidently predicting rapid temperature development phase and steady state phase of the castor wheels in dynamic testing. Simulation model was developed to extract data form static FEA simulations and DMA test data for temperature prediction. Similar models were proposed for pneumatic tyres in previous researches such as [9], [7] .

In this research FEA dynamic loading energy rate was captured by static loading FEA simulation. Then correction factor and wheel rotations were applied to convert captured static energy data to dynamic analysis. Because of this method, developed model can be used with mid-range FEA software also. Steady state FEA analysis with mixed Eulerian/Lagrangian reference frame was used to calculate dynamic energy rate in most literature which is only available with high end expensive FEA software [19] another method was modeling of full tyre and simulating the actual rotation behavior under given load and velocity which consumes lots of computer resources and time [9].

DMA experiment results and calculations obtained in this research was found to be closely matching with literature data and applications for FEA simulation [9]. Castor wheel failure analysis model was developed to predict failures at steady state level. From the model safety factor of the wheel at steady state level was extracted. von Mises failure criterion was used to evaluate this safety factor of the castor wheel. Failure evaluation by von Mises criterion is common practice and from literate also von Mises stress was used to evaluate stress inside rubber tyres [7], [9].

Validation of failure was done for both passed and failed wheel in actual dynamic test and was found to be having close relation with finite element model results. Case study 1 and 2 showed prominent steady state temperature levels matching with actual physical data. In case study 3 and 4 prominent steady state level was not observed in actual temperature records. When analyzed by failure simulation it was observed that these wheels start to yield when wheel comes to steady state level. This observation suggest in actual wheel will continue in temperature development region and fail, which was validated by comparing temperature profiles in case study 3 and 4. From all case studies it was found that when safety factor was below 1 wheel failed in actual test. Passed wheels in dynamic test showed 1.61, 1.12 and 1.41 safety factors at steady state level. So it was decided to keep safety factor above 1.1 for good performing designs.

FEA elements and material models used for rubber and plastic materials were based on literature data and was validated by closely matching results for temperature prediction model in this research. Several literatures were found where developed FEA models were validated by comparing predicted temperature graphs with test data [19], [9], [8].

FEA model was developed analyzing rubber and plastic materials. Developed model can be used with other material castor wheels such as polyurethane, thermoplastic rubber with relevant raw material testing for given materials. But further validation is required to evaluate the accuracy of the model on those areas.

Developed temperature prediction and failure analysis model can be used in castor wheel designs to develop optimized designs and to reduce trial and error costs. Also, it’s recommended to use this model on existing designs to identify potential weaknesses and possible improvements.

Simulation tests were carried out on core i5-4590 3.3 GHz computer with 8 GB ram. Model setup time, manual calculations and static 3D simulation consumed 90% of time while all 2D axisymmetric simulations took only 10% of total simulation time. By incorporating 2D axisymmetric simulations whenever possible in to the model, simulation time of a design kept to a minimum.

8. Conclusions

Developed finite element model was validated to be used with rubber castor wheels made from plastic centers which are tested in dynamic test. Safety factor of 1.1 was selected to be used in design when wheels are loaded at steady state temperature levels. Model can be customized to do dynamic test with different run-stop cycle, test speed and different loads by inputting relevant data to the model.

Model was able to predict temperature development and failure of a given castor wheel design within 8 hrs. With help of the developed model, quick competitive prices can be offered to the customer requests to secure new requests. New wheel development cycle which was 1.5 to 3 months long was reduced to 2 weeks with 70% saving which accounts for Rs.350,000 from trial moulds and testing in general for single wheel development. Rs. 3.5 million can be saved per year if company gets ten new development requirements.

Further opportunities for research was identified in castor wheel failure area to develop a simulation model to predict actual wheel failure start time after wheel achieves steady state level which involves very complex material behaviors, material damage models and practical variations in steady state region.

By using the steps followed its possible to develop simulation models for other rubber tyres such and pneumatic tyres, solid tyres which goes through same type of standard tests with appropriate model parameters and modifications.

Bibliography

[1] "Castors & Wheels | Castors Online | TENTE USA", Tente.com, 2016. [Online]. Available: https://www.tente.com/us-us/.

[2] Export Development Board (EDB), Sri Lanka, "Sri Lankan rubber product sector," Colombo, 2016.

[3] J. K. S. Sankalpa, "Export performance of rubber products manufacturing sector," *Journal of the Rubber Research Institute of Sri Lanka,* vol. 93, pp. 51-61, 2013.

[4] *The ICWM Performance Standard for Casters and Wheels*, ANSI Standard ICWM:2012.

[5] *Castors and wheels. test methods and apparatus*, BS EN Standard 12527:1999.

[6] *Castors and wheels. Castors and wheels for applications up to 1,1 m/s (4 km/h),* BS EN Standard 12532:1999.

[7] N. Korunovi, M. Trajanovi, and M. Stojkovi, “Finite Element Model for Steady-State Rolling Tire Analysis,” *Serbian Soc. Comput. Mech.*, vol. 1, no. 1, pp. 63–79, 2007.

[8] T. Ebbott, "Tire temperature and rolling resistance prediction with finite element," *Tire Science and Technology,* vol. 27, no. 01, pp. 2-21, 1999.

[9] Y. J. Lin and S. J. Hwang, “Temperature prediction of rolling tires by computer simulation,” *Math. Comput. Simul.*, vol. 67, no. 3, pp. 235–249, 2004.

[10] K. Ioi, "Study on Shimmy Vibrations of Wheeled Casters," *International Journal of Materials, Mechanics and Manufacturing,* vol. 03, no. 02, pp. 92-96, 2015.

[11] T. Frank, "Measurement of the turning, rolling and obstacle resistance of wheelchair castor wheels," *Journal of Biomedical Engineering*, vol. 11, no. 6, pp. 462-466, 1989.

[12] I. Evans, "The rolling resistance of a wheel with a solid rubber tyre," *British Journal of Applied Physics*, vol. 5, no. 5.

[13] J. v. Oosten, "Time, tire measurements forces and moments: a new standard for steady state cornering tyre testing," in *EAEC Congress: 'Vehicle systems technology for the next century'*, Barcelona, Spain, 1999.

[14] R. Trivini, "Hubless castor wheel construction". USA Patent US7657969 B2, 10 02 2010.

[15] C. L. Steven Lewis, "Caster wheel having integrated braking means". USA Patent US7712184 B1, 11 05 2010.

[16] M. Shiraishi, "Method for pneumatic tire simulation". USA Patent US20070137290 A1, 21 06 2007.

[17] Y. Nakajima, "Application of Computational Mechanics to Tire Design—Yesterday, Today, and Tomorrow," *Tire Science and Technology*, vol. 34, no. 04, pp. 223-244, 2011.

[18] N. Korunović, "Finite Element Analysis of a Tire Steady Rolling on the Drum," *Journal of Mechanical Engineering*, pp. 888-897, 2011.

[19] R. E. Smith, T. Tang, D. Johnson, E. Ledbury, T. Goddette, and S. D. Felicelli, "Simulation of Thermal Signature of Tires and Tracks," in *Proceedings of the 2012 NDIA ground vehicle systems engineering and technology*, 2012.

[20] U. Suripa, "Finite element stress and strain analysis of a solid tyre," *Journal of Achievements in Materials and Manufacturing Engineering*, vol. 31, no. 02, pp. 576-579, 2008.

[21] M. s. Bani, "Prediction of heat generation in rubber and rubber to metal springs," *Thermal science,* vol. 16, no. 02, pp. 527-539, 2012.

[22] "www.tiniusolsen.com," [Online]. Available: https://www.tiniusolsen.com/list-of-products/model-5-st. [Accessed 05 10 2016].

[23] Kevin P. Menard, Dynamic mechanical analyse: A practical introduction, New York: CRC Press LCC, 1999.

[24] *Dynamic Mechanical Analysis (DMA) Basics and Beyond*,PerkinElmer Inc., 2000.

[25] D. H. ". Qi, "Finite Element Analysis," 2006. [Online]. Available: http://www.colorado.edu/MCEN/MCEN4173/chap_01.pdf. [Accessed 2016].

[26] *Strand 7 Theoretical manual*, 1st ed., Strand 7, Sydney, 2004.

[27] F. Ebrahimi, "http://www.intechopen.com/," 10 2012. [Online]. Available: http://www.intechopen.com/books/finite-element-analysis-applications-in-mechanical-engineering/overview-in-the-application-of-fem-in-mining-and-the-study-of-case-stress-analysis-in-pulleys-of-sta. [Accessed 2016].

[28] C. Aparicio, "MSC Software," 2013. [Online]. Available: http://simulatemore.mscsoftware.com/advanced-contact-modeling-in-fea-marc-video/. [Accessed 04 2016].

[29] www.engineersedge.com, "Engineers Edge," 2016. [Online]. Available: http://www.engineersedge.com/material_science/von_mises.htm. [Accessed 05 2016].

[30] Wolfram Research, Inc, "Wolfram Mathworld," Wolfram Research, Inc, 1999-2016. [Online]. Available: http://mathworld.wolfram.com/RiemannSum.html. [Accessed 06 2016].

[31] Intec, "Physical Properties of Metals vs. Plastics and tempreature effects," 2014. [Online]. Available: http://www.intechpower.com/material-information/effects-of-temperature. [Accessed 07 2016].

[32] T. R. M. R. A. Pavan, "High performance polymer blends," Milan Italy, 2003.

Appendix 1 – Sample wheels dynamic test results summary

Speed : 4 km/h

Tyre	Load (kg)	Time until failure		Standard total run time (Seconds) for 15000 wheel revelutions	Inside		Outside	
		Run Time with out stop cycle (minutes)	Total run time (Seconds)		Center in side C°	Rubber in side C°	Center out side C°	Rubber out side C°
Heavy duty wheels								
125x42 Wheel	375	597	47700	7069	164	158	88	65
	400	66	5220	7069	168	155	77	63
	450	36	2820	7069	169	149	68	47
160x42 Wheel	450	216	17220	9048	168	153	99	64
	500	144	11460	9048	149	137	86	55
	550	45	3540	9048	145	135	82	56
180x42 Wheel	450	231	18420	10179	146	142	85	53
	500	171	13620	10179	148	138	83	51
	550	51	4020	10179	140	130	86	43
200x42 Wheel	450	243	19380	11310	114	141	96	52
	500	198	15780	11310	155	142	98	55
	550	72	5700	11310	193	180	105	68
General application wheels								
125 Common Wheel	100	372	29700	7069	134	108	69	57
	125	105	8340	7069	72	103	63	59
100 Common Wheel	80	363	28980	5655	89	88	63	48
	100	36	2820	5655	118	92	66	47

Appendix 2 – Static loading energy calculation case study 1

	m	N	N	Nm	Nm
Increment	**Displacement**	**Force**	**Forcex4**	**Step Energy**	**Sum of Energy**
1	0.0000	0.00	0.00		
2	0.0001	1.19	4.75	0.0005	
3	0.0002	4.08	16.31	0.0017	
4	0.0003	8.58	34.31	0.0035	
5	0.0004	15.27	61.06	0.0062	
6	0.0005	24.22	96.89	0.0099	
7	0.0006	35.10	140.40	0.0143	
8	0.0007	47.57	190.27	0.0194	
9	0.0008	61.61	246.42	0.0251	
10	0.0009	76.97	307.87	0.0314	
11	0.0010	93.81	375.25	0.0383	
12	0.0011	111.94	447.74	0.0457	
13	0.0012	131.47	525.89	0.0537	
14	0.0013	152.54	610.15	0.0623	
15	0.0014	175.10	700.41	0.0715	
16	0.0015	199.04	796.15	0.0812	
17	0.0016	224.06	896.23	0.0915	
18	0.0017	250.59	1002.35	0.1023	
19	0.0018	278.34	1113.37	0.1136	
20	0.0019	307.61	1230.46	0.1256	
21	0.0020	338.24	1352.97	0.1381	
22	0.0021	370.21	1480.83	0.1511	
23	0.0022	403.35	1613.40	0.1646	
24	0.0023	437.93	1751.73	0.1787	
25	0.0024	473.74	1894.97	0.1934	
26	0.0026	511.11	2044.45	0.2086	
27	0.0027	550.26	2201.05	0.2246	
28	0.0028	590.80	2363.20	0.2411	
29	0.0029	632.54	2530.18	0.2582	
30	0.0030	675.68	2702.72	0.2758	
31	0.0031	720.04	2880.15	0.2939	
32	0.0032	765.89	3063.56	0.3126	
33	0.0033	812.98	3251.93	0.3318	
34	0.0034	861.44	3445.77	0.3516	
35	0.0035	911.83	3647.32	0.3722	
36	0.0036	963.51	3854.05	0.3933	
37	0.0037	1016.51	4066.06	0.4149	

38	0.0038	1070.76	4283.06	0.4370	
39	0.0039	1126.46	4505.83	0.4598	6.30
40	0.0040	1183.48	4733.90	0.4830	
41	0.0041	1241.88	4967.51	0.5069	7.29
42	0.0042	1301.61	5206.44	0.5313	
43	0.0043	1362.75	5450.99	0.5562	8.38
44	0.0044	1425.27	5701.07	0.5818	
45	0.0045	1489.68	5958.72	0.6080	
46	0.0046	1555.68	6222.72	0.6350	
47	0.0047	1623.12	6492.47	0.6625	
48	0.0048	1691.83	6767.32	0.6905	
49	0.0049	1762.00	7048.01	0.7192	
50	0.0050	1833.63	7334.53	0.7484	

Appendix 3 – Total energy rate calculation case study 1

	J/mm3	mm3	J		J/s
Element ID	**Energy density**	**Element Volume**	**Element energy**		**Distributed total energy rate**
136	0.000535	27.2	0.014541	7.02%	4.269
121	0.000561	25.1	0.014073	6.80%	4.131
586	0.000432	23.52	0.010157	4.91%	2.982
676	0.000475	20.91	0.009924	4.79%	2.914
106	0.000432	21.17	0.009146	4.42%	2.685
151	0.000357	24.82	0.008864	4.28%	2.602
391	0.000508	16.3	0.008273	4.00%	2.429
601	0.000366	20.86	0.007631	3.69%	2.240
376	0.000386	17.82	0.006878	3.32%	2.019
406	0.000307	20.99	0.006452	3.12%	1.894
616	0.000225	28.02	0.006303	3.04%	1.850
46	0.000181	34.87	0.006300	3.04%	1.850
421	0.000312	18.38	0.005734	2.77%	1.683
706	0.000307	18.52	0.005686	2.75%	1.669
451	0.000447	12.33	0.005510	2.66%	1.618
571	0.000463	11.88	0.005499	2.66%	1.614
61	0.000195	26.53	0.005186	2.51%	1.522
646	0.000333	14.29	0.004761	2.30%	1.398
556	0.000436	10.66	0.004644	2.24%	1.363
241	0.000450	9.68	0.004354	2.10%	1.278
31	0.000158	26.67	0.004210	2.03%	1.236
76	0.000187	21.48	0.004009	1.94%	
166	0.000147	25.46	0.003745	1.81%	
631	0.000341	10.92	0.003727	1.80%	
91	0.000181	20.57	0.003725	1.80%	
436	0.000358	9.46	0.003387	1.64%	
226	0.000509	6.39	0.003251	1.57%	
181	0.000150	20.54	0.003086	1.49%	
196	0.000200	14.41	0.002882	1.39%	
661	0.000514	5.2	0.002671	1.29%	
511	0.000105	23.38	0.002457	1.19%	
496	0.000143	17.15	0.002446	1.18%	
16	0.000140	17.25	0.002420	1.17%	
481	0.000186	12.83	0.002389	1.15%	

211	0.000286	7.15	0.002046	0.99%	
1	0.000110	16.3	0.001790	0.86%	
691	0.000392	4.39	0.001722	0.83%	
526	0.000078	19.96	0.001564	0.76%	
466	0.000221	6.66	0.001472	0.71%	
256	0.000160	6.15	0.000985	0.48%	
541	0.000069	9.83	0.000680	0.33%	
301	0.000033	15.15	0.000503	0.24%	
316	0.000031	16.16	0.000501	0.24%	
331	0.000026	13.72	0.000362	0.17%	
286	0.000033	10.85	0.000361	0.17%	
361	0.000033	9.2	0.000308	0.15%	
271	0.000032	6.13	0.000196	0.09%	
346	0.000022	8.84	0.000191	0.09%	

Appendix 4 – Material property data

Material thermal properties

Material	Mass Density	Specific Heat capacity	Heat conductivity	Forced Convection-Air	Rubber to floor conduction
	kg/mm3	W/kg/k	W/mm/c	$W/mm^2/c^\circ$	$W/mm^2/c^\circ$
PP	0.00000091	1800	0.00018	0.0000060	
Nylon	0.00000125	1700	0.00026	0.0000060	
NR-1	0.0000012	1700	0.000239	0.0000060	0.0001
NR-2	0.0000012	1700	0.000239	0.0000060	0.0001

Nylon

Temperature (°C)	Modulus(MPa)	Yield (MPa)
23	821.2	68.4
140	614.0	19.9

Polypropylene

Temperature (°C)	Modulus(MPa)	Yield (MPa)
23	194.5	24.6
120	152.0	9.2

Appendix 5 – Static load energy calculation case study 2

	m	N	N	Nm	Nm
Increment	**Displacement**	**Force**	**Forcex4**	**Step Energy**	**Sum of Energy**
1	0.00010	0	0.00		
2	0.00020	1.257258	5.03	0.0005	
3	0.00030	3.84284	15.37	0.0015	
4	0.00040	7.206436	28.83	0.0029	
5	0.00050	11.40075	45.60	0.0046	
6	0.00060	16.24889	65.00	0.0065	
7	0.00070	21.98813	87.95	0.0088	
8	0.00080	28.48838	113.95	0.0114	
9	0.00090	35.47014	141.88	0.0142	
10	0.00100	43.02067	172.08	0.0172	
11	0.00110	51.48609	205.94	0.0206	
12	0.00120	60.42285	241.69	0.0242	
13	0.00130	69.90346	279.61	0.0280	
14	0.00140	79.80058	319.20	0.0319	
15	0.00150	90.56133	362.25	0.0362	
16	0.00160	101.9456	407.78	0.0408	
17	0.00170	113.855	455.42	0.0455	
18	0.00180	126.2865	505.15	0.0505	
19	0.00190	139.0828	556.33	0.0556	
20	0.00200	152.2478	608.99	0.0609	
21	0.00210	166.0777	664.31	0.0664	
22	0.00220	180.4575	721.83	0.0722	
23	0.00230	195.2797	781.12	0.0781	
24	0.00240	210.6726	842.69	0.0843	
25	0.00250	226.3694	905.48	0.0905	
26	0.00260	242.4892	969.96	0.0970	
27	0.00270	258.9483	1035.79	0.1036	
28	0.00280	275.9915	1103.97	0.1104	
29	0.00290	293.4132	1173.65	0.1174	
30	0.00300	311.2933	1245.17	0.1245	1.41
31	0.00310	329.5096	1318.04	0.1318	
32	0.00320	348.092	1392.37	0.1392	
33	0.00330	367.0028	1468.01	0.1468	
34	0.00340	386.1508	1544.60	0.1545	
35	0.00350	405.5723	1622.29	0.1622	

36	0.00360	425.4024	1701.61	0.1702	
37	0.00370	445.7278	1782.91	0.1783	
38	0.00380	466.2945	1865.18	0.1865	
39	0.00390	487.0827	1948.33	0.1948	
40	0.00400	508.1855	2032.74	0.2033	
41	0.00410	529.505	2118.02	0.2118	
42	0.00420	550.992	2203.97	0.2204	
43	0.00430	572.9177	2291.67	0.2292	
44	0.00440	595.0815	2380.33	0.2380	
45	0.00450	617.4105	2469.64	0.2470	
46	0.00460	639.9348	2559.74	0.2560	
47	0.00470	662.8398	2651.36	0.2651	
48	0.00480	685.9876	2743.95	0.2744	
49	0.00490	709.2901	2837.16	0.2837	
50	0.00500	732.814	2931.26	0.2931	

Appendix 6 – Total energy rate calculation case study 2

	j/mm3	mm3	j		j/s
Element ID	Energy density	Element Volume	Element energy		Distributed total energy rate
316	0.000265870	10.6077	0.002820266	8.11%	1.292
331	0.000252908	9.67325	0.002446438	7.04%	1.121
301	0.000203095	11.7425	0.002384842	6.86%	1.093
1006	0.000192424	12.2099	0.002349472	6.76%	1.076
1021	0.000230018	10.1773	0.002340966	6.73%	1.073
991	0.000149435	13.6587	0.002041084	5.87%	0.935
346	0.000204574	9.3742	0.001917716	5.52%	0.879
1036	0.000209048	8.47719	0.001772136	5.10%	0.812
1111	0.000160948	9.9696	0.001604584	4.62%	0.735
361	0.000137740	9.8194	0.001352526	3.89%	0.620
721	0.000166655	8.02756	0.001337835	3.85%	0.613
271	0.000085904	13.5214	0.001161544	3.34%	0.532
286	0.000087106	12.792	0.001114260	3.21%	0.511
496	0.000111334	9.30384	0.001035835	2.98%	0.475
256	0.000070042	13.6411	0.000955448	2.75%	0.438
1051	0.000143685	6.48561	0.000931886	2.68%	0.427
976	0.000062597	12.9214	0.000808836	2.33%	0.371
736	0.000112505	5.41065	0.000608726	1.75%	
376	0.000058295	10.4366	0.000608400	1.75%	
1081	0.000100734	5.55336	0.000559409	1.61%	
391	0.000046323	9.66751	0.000447824	1.29%	
241	0.000034355	12.2522	0.000420926	1.21%	
586	0.000075645	5.45711	0.000412806	1.19%	
1096	0.000062330	5.46608	0.000340701	0.98%	
1066	0.000090956	3.65384	0.000332339	0.96%	
751	0.000069900	3.05763	0.000213727	0.61%	
406	0.000028449	6.67923	0.000190017	0.55%	
871	0.000068980	2.6912	0.000185640	0.53%	
766	0.000050072	2.857	0.000143057	0.41%	
511	0.000039924	3.28712	0.000131234	0.38%	
886	0.000052473	2.47377	0.000129806	0.37%	
226	0.000012054	9.44255	0.000113816	0.33%	
646	0.000052992	2.08619	0.000110551	0.32%	
856	0.000058347	1.66181	0.000096962	0.28%	
901	0.000025591	3.33241	0.000085278	0.25%	
661	0.000041102	2.07454	0.000085267	0.25%	

421	0.000018083	4.28921	0.000077561	0.22%	
841	0.000044893	1.4802	0.000066451	0.19%	
166	0.000010322	6.13154	0.000063293	0.18%	
781	0.000032610	1.88477	0.000061462	0.18%	
826	0.000031427	1.87331	0.000058873	0.17%	
811	0.000036671	1.48722	0.000054538	0.16%	
526	0.000022276	2.3696	0.000052785	0.15%	
961	0.000005143	8.72056	0.000044851	0.13%	
211	0.000007167	5.92793	0.000042485	0.12%	
181	0.000005758	7.18575	0.000041379	0.12%	
151	0.000007802	5.04791	0.000039383	0.11%	
796	0.000021629	1.7508	0.000037869	0.11%	
631	0.000022445	1.63264	0.000036644	0.11%	
76	0.000033536	1.06177	0.000035607	0.10%	
436	0.000012839	2.74106	0.000035192	0.10%	
676	0.000011942	2.70406	0.000032293	0.09%	
601	0.000014803	2.02524	0.000029979	0.09%	
196	0.000005037	5.58552	0.000028134	0.08%	
916	0.000004477	6.26928	0.000028069	0.08%	
91	0.000022565	1.24036	0.000027989	0.08%	
61	0.000026557	1.02183	0.000027136	0.08%	
106	0.000011736	2.04604	0.000024012	0.07%	
931	0.000003762	5.67673	0.000021357	0.06%	
616	0.000015749	1.31141	0.000020653	0.06%	
946	0.000004227	4.79977	0.000020287	0.06%	
121	0.000005494	3.13512	0.000017223	0.05%	
706	0.000003193	4.97009	0.000015870	0.05%	
451	0.000009152	1.65951	0.000015188	0.04%	
1141	0.000011233	1.32921	0.000014932	0.04%	
541	0.000008620	1.70588	0.000014705	0.04%	
136	0.000003133	4.24859	0.000013311	0.04%	
46	0.000017865	0.711695	0.000012715	0.04%	
466	0.000005754	2.19612	0.000012636	0.04%	
1	0.000004916	1.54294	0.000007585	0.02%	
481	0.000004284	1.76682	0.000007570	0.02%	
556	0.000005440	1.23487	0.000006718	0.02%	
691	0.000001495	4.08363	0.000006104	0.02%	
571	0.000004028	1.36092	0.000005482	0.02%	
16	0.000004377	1.21743	0.000005329	0.02%	
31	0.000006565	0.722598	0.000004744	0.01%	
1126	0.000007526	0.457442	0.000003443	0.01%	

Appendix 7 - Static load energy calculation case study 3

	m	N	N	Nm	Nm
Increment	**Displacement**	**Force**	**Forcex4**	**Step Energy**	**Sum of Energy**
1	0.0000	0.00	0.00		
2	0.0001	1.24	4.95	0.0005	
3	0.0002	3.61	14.43	0.0015	
4	0.0003	6.92	27.69	0.0028	
5	0.0004	10.96	43.84	0.0045	
6	0.0005	15.91	63.63	0.0065	
7	0.0006	21.56	86.24	0.0088	
8	0.0007	27.73	110.93	0.0113	
9	0.0008	34.80	139.20	0.0142	
10	0.0009	42.66	170.65	0.0174	
11	0.0010	50.92	203.66	0.0208	
12	0.0011	60.01	240.05	0.0245	
13	0.0012	69.88	279.53	0.0285	
14	0.0013	80.41	321.64	0.0328	
15	0.0014	91.25	364.99	0.0372	
16	0.0015	102.79	411.15	0.0420	
17	0.0016	115.23	460.91	0.0470	
18	0.0017	128.24	512.95	0.0523	
19	0.0018	141.86	567.43	0.0579	
20	0.0019	155.82	623.27	0.0636	
21	0.0020	170.52	682.10	0.0696	
22	0.0021	185.93	743.71	0.0759	
23	0.0022	201.87	807.46	0.0824	
24	0.0023	218.26	873.05	0.0891	
25	0.0024	235.22	940.88	0.0960	
26	0.0025	252.60	1010.40	0.0516	0.9387
27	0.0026	270.47	1081.89	0.1082	
28	0.0027	288.98	1155.92	0.1156	
29	0.0028	308.11	1232.42	0.1232	

Appendix 8 - Total energy rate calculation case study 3

	mm3	j/mm3	j		j/s
Element ID	**Element Volume**	**Energy density**	**Element energy**		**Distributed total energy rate**
316	7.18371	0.00027528	0.0019776	8.28%	1.083
331	6.6234	0.00026892	0.0017811	7.46%	0.976
631	7.50451	0.00023269	0.0017462	7.31%	0.957
301	7.46889	0.00020512	0.0015320	6.41%	0.839
646	6.7869	0.00021239	0.0014415	6.04%	0.790
616	7.33481	0.00018974	0.0013917	5.83%	0.762
346	5.8648	0.00022742	0.0013338	5.58%	0.731
601	6.47454	0.00015446	0.0010000	4.19%	0.548
661	5.47471	0.00017820	0.0009756	4.08%	0.534
1066	5.32881	0.00016825	0.0008966	3.75%	0.491
361	5.30246	0.00016385	0.0008688	3.64%	0.476
286	7.97832	0.00008470	0.0006757	2.83%	0.370
271	7.92035	0.00008106	0.0006420	2.69%	0.352
676	4.88749	0.00013070	0.0006388	2.67%	0.350
586	6.01317	0.00010380	0.0006242	2.61%	0.342
1186	4.617	0.00013388	0.0006181	2.59%	0.339
256	7.55159	0.00007050	0.0005324	2.23%	0.292
1051	4.49976	0.00011087	0.0004989	2.09%	0.273
871	4.50944	0.00010767	0.0004855	2.03%	0.266
376	4.88574	0.00007644	0.0003735	1.56%	
241	7.21567	0.00004904	0.0003539	1.48%	
691	4.26953	0.00007678	0.0003278	1.37%	
1081	3.01122	0.00009651	0.0002906	1.22%	
391	4.56164	0.00006133	0.0002798	1.17%	

Appendix 9 - Static load energy calculation case study 4

	m	N	N	Nm	Nm
Increment	**Displacement**	**Force**	**Forcex4**	**Step Energy**	**Sum of Energy**
1	0.0000	0.0	0.00		
2	0.0002	2.4	9.73	0.0019	
3	0.0004	7.3	29.03	0.0058	
4	0.0006	15.0	60.17	0.0120	
5	0.0008	24.5	98.15	0.0196	
6	0.0010	36.1	144.37	0.0289	
7	0.0012	50.2	201.00	0.0402	
8	0.0014	65.9	263.52	0.0527	
9	0.0016	82.7	330.63	0.0661	
10	0.0018	100.8	403.32	0.0807	
11	0.0020	119.9	479.73	0.0959	
12	0.0022	140.1	560.34	0.1121	
13	0.0024	161.8	647.03	0.1294	
14	0.0026	184.4	737.49	0.1475	
15	0.0028	207.6	830.40	0.1661	
16	0.0030	231.6	926.36	0.1853	
17	0.0032	257.0	1028.10	0.2056	
18	0.0034	283.3	1133.16	0.2266	
19	0.0036	310.4	1241.59	0.2483	
20	0.0038	338.4	1353.44	0.2707	
21	0.0040	367.1	1468.44	0.2937	
22	0.0042	397.1	1588.45	0.3177	
23	0.0044	428.3	1713.25	0.3426	
24	0.0046	460.2	1840.62	0.3681	
25	0.0048	492.7	1970.88	0.3942	
26	0.0050	525.7	2102.99	0.4206	
27	0.0052	560.1	2240.39	0.4481	
28	0.0054	595.8	2383.01	0.4766	
29	0.0056	632.0	2527.91	0.5056	
30	0.0058	669.0	2675.83	0.5352	
31	0.0060	706.7	2826.63	0.5653	
32	0.0062	744.8	2979.35	0.5959	
33	0.0064	784.3	3137.02	0.6274	
34	0.0066	824.4	3297.67	0.6595	
35	0.0068	866.4	3465.58	0.6931	

36	0.0070	909.3	3637.31	0.7275	
37	0.0072	952.8	3811.24	0.7622	
38	0.0074	996.9	3987.54	0.7975	
39	0.0076	1042.1	4168.26	0.8337	
40	0.0078	1088.2	4352.90	0.8706	
41	0.0080	1135.1	4540.34	0.9081	
42	0.0082	1183.6	4734.42	0.9469	
43	0.0084	1233.1	4932.32	0.9865	
44	0.0086	1283.2	5132.90	1.0266	
45	0.0088	1334.0	5336.15	1.0672	
46	0.0090	1385.5	5542.12	1.1084	19.4
47	0.0092	1438.0	5751.94	1.1504	
48	0.0094	1491.3	5965.39	1.1931	
49	0.0096	1545.5	6182.13	1.2364	
50	0.0098	1600.9	6403.74	1.2807	

Appendix 10 - Total energy rate calculation case study 4

	mm3	j/mm3	j		j/s
Element ID	**Element Volume**	**Energy density**	**Element energy**		**Distributed total energy rate**
354	10.78	0.00063315	0.0068226	8.28%	10.763
351	9.94	0.00061851	0.0061449	7.46%	9.694
631	11.26	0.00053519	0.0060245	7.31%	9.504
620	11.20	0.00047179	0.0052856	6.41%	8.338
646	10.18	0.00048851	0.0049732	6.04%	7.845
433	11.00	0.00043641	0.0048015	5.83%	7.575
349	8.80	0.00052307	0.0046015	5.58%	7.259
604	9.71	0.00035525	0.0034501	4.19%	5.443
664	8.21	0.00040985	0.0033657	4.08%	5.310
1069	7.99	0.00038698	0.0030932	3.75%	4.880
364	7.95	0.00037685	0.0029973	3.64%	4.728
289	11.97	0.00019480	0.0023313	2.83%	3.678
274	11.88	0.00018643	0.0022149	2.69%	3.494
679	7.33	0.00030061	0.0022038	2.67%	3.477
589	9.02	0.00023875	0.0021534	2.61%	3.397
1189	6.93	0.00030792	0.0021325	2.59%	3.364
259	11.33	0.00016215	0.0018368	2.23%	2.898
1054	6.75	0.00025501	0.0017212	2.09%	2.715
874	6.76	0.00024765	0.0016751	2.03%	2.643
379	7.33	0.00017582	0.0012885	1.56%	
244	10.82	0.00011280	0.0012209	1.48%	
694	6.40	0.00017660	0.0011310	1.37%	
1084	4.52	0.00022197	0.0010026	1.22%	
394	6.84	0.00014106	0.0009652	1.17%	